ENGINEERING A NEW MATERIAL FOR HOT GAS CLEANUP

FINAL TECHNICAL REPORT

July 1, 1999 – June 30, 2003

T. D. Wheelock, L. K. Doraiswamy, and K. P. Constant
Principal Investigators

Justinus A. Satrio
Research Associate

T. T. Akiti, Jr., and D. J. L. Hasler
Graduate Assistants

Michael Chesnut, Stephen Dak, Brandon Franck, and Tanya Harris
Undergraduate Assistants

Issued: September 2003

DOE Award No. DE-FG26-99FT40587

Chemical Engineering Department,
Materials Science and Engineering Department, and
Center for Sustainable Environmental Technologies
2114 Sweeney Hall
Iowa State University
Ames, IA 50011-2230

DISCLAIMER

This report was prepared as an account of work sponsored by an agency of the United States Government. Neither the United States Government nor any agency thereof, nor any of their employees, makes any warranty, express or implied, or assumes any legal liability or responsibility for the accuracy, completeness, or usefulness of any information, apparatus, product, or process disclosed, or represents that its use would not infringe privately owned rights. Reference herein to any specific commercial product, process, or service by trade name, trademark, manufacturer, or otherwise does not necessarily constitute or imply its endorsement, recommendation, or favoring by the United States Government or any agency thereof. The views and opinions of the authors expressed herein do not necessarily state or reflect those of the United States Government or any agency thereof.

ENGINEERING A NEW MATERIAL FOR HOT GAS CLEANUP

FINAL TECHNICAL REPORT

T. D. Wheelock, L. K. Doraiswamy, and K. P. Constant
Principal Investigators

ABSTRACT

The overall purpose of this project was to develop a superior, regenerable, calcium-based sorbent for desulfurizing hot coal gas with the sorbent being in the form of small pellets made with a layered structure such that each pellet consists of a highly reactive lime core enclosed within a porous protective shell of strong but relatively inert material. The sorbent can be very useful for hot gas cleanup in advanced power generation systems where problems have been encountered with presently available materials.

An economical method of preparing the desired material was demonstrated with a laboratory-scale revolving drum pelletizer. Core-in-shell pellets were produced by first pelletizing powdered limestone or other calcium-bearing material to make the pellet cores, and then the cores were coated with a mixture of powdered alumina and limestone to make the shells. The core-in-shell pellets were subsequently calcined at 1373 K (1100°C) to sinter the shell material and convert $CaCO_3$ to CaO. The resulting product was shown to be highly reactive and a very good sorbent for H_2S at temperatures in the range of 1113 to 1193 K (840 to 920°C) which corresponds well with the outlet temperatures of some coal gasifiers. The product was also shown to be both strong and attrition resistant, and that it can be regenerated by a cyclic oxidation and reduction process.

A preliminary evaluation of the material showed that while it was capable of withstanding repeated sulfidation and regeneration, the reactivity of the sorbent tended to decline

with usage due to CaO sintering. Also it was found that the compressive strength of the shell material depends on the relative proportions of alumina and limestone as well as their particle size distributions. Therefore, an extensive study of formulation and preparation conditions was conducted to improve the performance of both the core and shell materials. It was subsequently determined that MgO tends to stabilize the high-temperature reactivity of CaO. Therefore, a sorbent prepared from dolomite withstands the effects of repeated sulfidation and regeneration better than one prepared from limestone. It was also determined that both the compressive strength and attrition resistance of core-in-shell pellets depend on shell thickness and that the compressive strength can be improved by reducing both the particle size and amount of limestone in the shell preparation mixture.

A semiempirical model was also found which seems to adequately represent the absorption process. This model can be used for analyzing and predicting sorbent performance, and, therefore, it can provide guidance for any additional development which may be required.

In conclusion, the overall objective of developing an economical, reusable, and practical material was largely achieved. The material appears suitable for removing CO_2 from fuel combustion products as well as for desulfurizing hot coal gas.

TABLE OF CONTENTS

LIST OF GRAPHICAL MATERIAL

INTRODUCTION

This research project was directed towards the further development of a regenerable, calcium-based sorbent for desulfurizing hot coal gas because there is a continuing need for such material in advanced power generation systems which employ gas turbines. For maximum thermal efficiency the turbines should be supplied with clean fuel gas at coal gasifier outlet temperatures which typically range from 973 K (700°C) to 1273 K (1000°C) or more. Therefore, the gas should be cleaned at these temperatures without cooling and reheating. Lime (CaO) is one of the few materials which can effectively absorb most of the H_2S and COS from the gas in this temperature range. However, lime is soft and friable so it does not withstand handling well. Also in the past it has proved difficult to regenerate the sulfided sorbent.

These problems were addressed in a previous investigation which showed that a promising sorbent can be made by pelletizing a mixture of pulverized limestone and calcium aluminate cement in two stages so as to produce a layered structure.[1] The basic concept evolved into a core-in-shell pellet structure in which a relatively weak but highly reactive core is encased in a stronger, porous but less reactive shell. A practical method of regenerating the sorbent was also demonstrated which involved treating the sulfided sorbent with an oxidizing gas (e.g., air) and then with a reducing gas (e.g., CO or H_2) and then repeating the cycle.

The present project was undertaken to build on the previous results which, while highly promising, did not provide a complete solution to the problems. Since a type of hydraulic cement had been used in making the pellets, they had to be steam cured to strengthen the shell material, but the hydraulic bond was lost subsequently when the pellets were calcined, resulting in a loss in strength. Furthermore, the reactivity of the sorbent tended to decline as the sorbent was repeatedly sulfided and regenerated.

Overcoming these problems became the focus of the present investigation because when the problems are solved, the way will be clear for producing a superior high temperature sorbent. Overcoming the loss in strength of the shell material was attacked by employing a sinterable powder in place of hydraulic cement so that when the coated pellets were calcined the particles would fuse together forming a strong but porous layer of material. Overcoming the loss in reactivity of the CaO sorbent was attacked by determining the cause of the loss and seeking a way around it. A review of the technical literature indicated that the loss in reactivity was due most likely to sintering of the CaO. This review also indicated that MgO and possibly SrO would inhibit sintering of CaO. Therefore, sources of CaO which are also sources of MgO were investigated, and these included dolomite ($CaCO_3 \cdot MgCO_3$) and a derivative of dolomite known as dolime [$CaMg(OH)_4$]. Also the addition of small amounts of SrO to CaO was investigated as a stabilizer. In addition, since the rate of sintering is a function of the properties of the crystal lattice, plaster of Paris ($CaSO_4 \cdot \frac{1}{2}H_2O$) was investigated as a source of CaO because it could provide a somewhat more open structure than that provided by limestone and therefore reduce the rate of sintering.

Since the future commercial development and application of the core-in-shell pelletized sorbent will depend on both the absorption capacity and the rate of absorption of the material, consideration was given to the factors which control these properties and to the development of a mathematical model which can represent the kinetics of the absorption process. Such a model can provide the means for analyzing and predicting sorbent performance.

To address these issues an extensive program of experimental research was conducted which required preparing and characterizing a large number of different sorbent pellet formulations. Both coated and uncoated sorbent pellets were prepared from different materials

and subsequently tested. The absorption capacity and rate of absorption were determined by thermogravimetric analysis (TGA). The crushing strength, abrasion resistance, apparent porosity, apparent density, and pore volume of selected pellets were measured by appropriate methods. The morphology of selected pellets was also observed by scanning electron microscopy. In addition, selected pellets were subjected to multicycles of absorption and regeneration to observe changes in the reactivity of the sorbent. A detailed description of these methods and the results achieved follow.

EXECUTIVE SUMMARY

The engineering development of an advanced calcium-based sorbent for desulfurizing hot coal gas was conducted on a laboratory scale. The overall objective of developing an economical, reusable, and practical material was largely achieved. The material was shown to operate effectively at temperatures in the range of 1113 to 1193 K (840 to 920°C) which are not greatly different from typical coal gasifier outlet temperatures. Therefore, the material offers a way of cleaning the hot gas directly for application in gas turbines and fuel cells without sacrificing thermal efficiency imposed by lower temperature cleaning methods. Also it was shown that the material can be regenerated by a cyclic oxidation and reduction process and that it is strong and attrition resistant. Furthermore, the material can be regenerated and reused repeatedly, but with some loss in capacity over time. The material can also be employed as a reusable sorbent for carbon dioxide at somewhat lower temperatures and, therefore, it can provide a practical means for separating carbon dioxide from other combustion products.

The new sorbent material is made in the form of small spherical pellets such that each pellet consists of a CaO core surrounded by a strong but porous shell made largely of sintered alumina. This design takes advantage of the high chemical reactivity of CaO for H_2S and COS while at the same time overcoming the poor structural properties of CaO and its tendency to decrepitate.

The core-in-shell pellets are readily produced by a simple two-stage pelletization process which is carried out with a revolving drum pelletizer. The pellet cores are produced in the first stage by pelletizing powdered limestone or other calcium-bearing material, and in the second stage the cores are coated with a mixture of powdered alumina and limestone. Only water or a dilute lignin solution is employed as a binder. The pellets are subsequently calcined at 1373 K (1100°C) to partially sinter the shell material and convert $CaCO_3$ to CaO. Although these steps were carried out one at a time in the laboratory, they readily lend themselves to a low-cost, continuous operation when applied on an industrial scale.

For the present study core-in-shell pellets were prepared with a small pelletizer, calcined, and subjected to a series of measurements and tests to determine the important physical properties and absorption characteristics of the pellets. These included the absorption capacity of the material for H_2S (and in some cases for CO_2) as well as the compressive strength and attrition resistance of the pellets. In some cases the apparent porosity, apparent density and surface area were also measured. The physical structure of the pellets was studied by employing scanning electron microscopy (SEM), and the distribution of sulfur within the pellets was determined by employing the associated energy dispersive spectroscopy (EDS).

Pellets were formulated with a variety of materials in different concentrations and combinations in seeking to produce a product which would have a large absorption capacity, high compressive strength, good attrition resistance, and be capable of withstanding repeated loading and regeneration. Pellet cores were prepared from each of the following materials and tested: pure $CaCO_3$, limestone, plaster of Paris, dolomite, and dolime. While only calcination was required to convert most of the materials to CaO, a cyclic process of reduction and oxidation was required to convert the plaster of Paris into CaO. The CaO derived from any of these materials proved highly reactive and absorptive, but the reactivity also tended to decline with usage due to sintering. The rate of decline was highest for CaO derived from pure $CaCO_3$ and limestone and lowest for CaO derived from dolomite and dolime. While the rate of decline was high initially, it seemed to become very low after several cycles of loading and regeneration so the material tended to approach a stable state. For CaO derived from dolime the rate of decline became negligible after eight cycles of sulfidation and regeneration, whereas for CaO derived from plaster of Paris the rate of decline only became negligible after 20 cycles, but it still left a material with appreciable absorption capacity. The presence of MgO in the sorbents derived from dolime and dolomite seemed to stabilize the reactivity of CaO after it had been reacted and regenerated several times.

Pellet shell materials were prepared for testing with different particle mixtures of alumina and either pure $CaCO_3$, limestone, or kaolin. Preliminary tests showed that a binary mixture composed of 60 wt.% T-64 alumina having a median particle size of 8.65 μm and 40 wt.% A-16 alumina having a median particle size of 0.88 μm produced strong pellets after sintering. Even stronger pellets were produced by adding either $CaCO_3$, limestone or kaolin to the mixture. The maximum compressive strength achieved with the addition of limestone depended upon both the particle size and concentration of the limestone. For -44 μm particles of limestone, maximum compressive strength was achieved with only 5 wt.% in the shell mixture, whereas for limestone particles in the range of 44 to 297 μm, maximum compressive strength was achieved with 20 wt.% in the mixture. In both cases the compressive strength of the resulting calcined core-in-shell pellets was found directly proportional to shell thickness for pellets of the same diameter. However, the compressive strength of pellets made with the finer particles of limestone was greater than that of pellets made with the coarser particles when the shell thickness exceeded 0.35 mm. Substitution of either pure $CaCO_3$ or kaolin particles for the limestone in 20 wt.% concentration produced pellet shells of comparable compressive strength.

The attrition resistance of calcined core-in-shell pellets made with a shell mixture containing 20 wt.% limestone (44 – 210 μm) was also found to be proportional to shell thickness. Furthermore, the attrition resistance was observed to be greater when the shell

ingredients were wet mixed rather than dry mixed either due to better mixing or the presence of a small amount of sodium hexametaphosphate in the aqueous suspension. Also there was less variation in the compressive strength of pellets prepared by wet mixing the shell materials.

A study of the mechanism that controls the rate of absorption or reaction of H_2S with CaO to form CaS showed that for a core-in-shell pellet the mechanism is well represented by a shrinking core model which assumes that the rate is controlled by diffusion of H_2S through both the shell material and the layer of reacted product surrounding the core of unreacted CaO. The model was observed to apply well over a range of 0 to 85% conversion of CaO and should prove useful for analyzing and predicting sorbent performance over a practical range of application.

LITERATURE REVIEW

HOT GAS DESULFURIZATION

An integrated coal gasification combined cycle (IGCC) system is an example of an advanced power generation system which holds great promise for producing electric power efficiently and economically. However, to achieve maximum energy conversion efficiency, such systems need to include hot gas cleanup methods capable of operating close to gasifier outlet temperatures which may range from 1000 K (727°C) to 1600 K (1327°).[1,2] While various sorbent materials have been proposed for desulfurizing hot coal gas, few will withstand or be effective at such temperatures.[3,4,5] At lower temperatures zinc-based sorbents are highly effective, but their use is limited to temperatures below 925-975 K (652-702°C). At higher temperatures calcium-based sorbents may offer the most promise for the least cost because the following reaction is both thermodynamically and kinetically favorable:[3,6]

$$CaO_{(s)} + H_2S_{(g)} = CaS_{(s)} + H_2O_{(g)} \quad (1)$$

Since this reaction is exothermic, the reaction equilibrium becomes somewhat less favorable at very high temperatures, and, of course, the reverse reaction is favored by large steam concentrations. Also if the reaction temperature is not very high, reaction 1 has to compete with the endothermic reaction shown below because of the presence of CO_2 in coal gas.

$$CaO_{(s)} + CO_{2(g)} = CaCO_{3(s)} \quad (2)$$

Reaction 2 becomes less favorable thermodynamically as the temperature is raised. An earlier thermodynamic analysis of this reaction system showed that the gas produced by a typical air- and steam-blown coal gasifier operating at 20 atm could be 95% desulfurized under equilibrium conditions over a temperature range of 1043 to 1673 K (770 to 1400°C).[3] A more recent thermodynamic analysis indicated that the H_2S content of gas produced by a Shell entrained flow gasifier could be reduced to 20 ppmv by contacting the gas under a total pressure of 30 bar with CaO under highly reducing conditions over a temperature range of 1088 to 1118 K (815 to 845°C).[7]

Over the years much consideration has been given to sorbents based on limestone and dolomite because these materials are plentiful and inexpensive.[7,8] However, since these materials are soft and friable, they don't stand up well to handling and repeated use. Also they have proved difficult to regenerate and are subject to a loss in reactivity when regenerated and reused repeatedly.[9] Regeneration is especially difficult because there is a greater thermodynamic tendency for CaS to be converted into $CaSO_4$ than into CaO upon oxidation except at very high temperature.[10]

Voss[11] claimed to overcome the friability problem by pelletizing pulverized limestone and a clay binder. Kampius et al.[12] reported making attrition resistant sorbent pellets by agglomerating limestone particles with unspecified binders. The pellets were said to have an open porous microstructure which was highly favorable for gas absorption.

To improve the physical properties of pelletized limestone, Wheelock et al.[1] utilized a two-step pelletizing process in which pulverized limestone was pelletized in the first step, and the pellets were than coated with a hydraulic cement in a second step. After steam curing, each

pellet consisted of a weak but highly reactive core encased in a relatively strong and porous shell. It was found subsequently that the physical properties of the pellets were improved further by adding hydraulic cement to the pellet core and limestone to the shell.

A promising method of regenerating a sulfided sorbent was demonstrated by Jagtap and Wheelock.[10] This method first treats the spent sorbent with an oxidizing gas (e.g., air) at 1273-1373 K (1000-1100°C) to convert an outer layer of the material from CaS to $CaSO_4$ by the following reaction:

$$CaS + 2\ O_2 = CaSO_4 \qquad (3)$$

Not all of the material reacts because of pore blockage. Therefore, the material is treated next with a reducing gas such as H_2 or CO to convert the $CaSO_4$ layer to CaO as illustrated below.

$$CaSO_4 + H_2 = CaO + SO_2 + H_2O \qquad (4)$$

The oxidation/reduction cycle is repeated until all of the material is converted into CaO. Although the regeneration method has only been demonstrated on a laboratory scale, it lends itself to application in either fixed bed, moving bed, or fluidized bed reactors.[13]

GAS-SOLID REACTION MODELS

In searching for a gas-solid reaction model to represent the kinetics of the reaction between H_2S and a sorbent pellet composed of CaO, consideration was given to a wide range of models which have been proposed to represent such reactions. The results of this search follow.

The first model for describing the behavior of a solid as it undergoes reaction with a gas was proposed over a half-a-century ago by Yagi and Kunii.[14] This is the shrinking core model (SCM), also called the sharp interface model (SIM). Several other models have been proposed since then, such as the expanding core (as an extension of SCM), volume reaction, reaction zone, particle-pellet, crackling core, grain-micrograin, nucleation, computational, and percolation

models. The percolation models are based on the statistical physics of disordered media and include such phenomena as aggregation processes, scaling, network modeling of the pore space, discretization, and random walk representation of diffusion processes. An increasing number of papers are being published on percolation models (see Sahimi et al.[15] for a review), but research on the other models continues because of the practical usefulness of these models (see, e.g., Szekely et al.;[16] Ramachandran and Doraiswamy;[17] Doraiswamy and Sharma;[18] Doraiswamy and Kulkarni,[19] Mazet,[20,21] Bhatia and Gupta[22]). In reactions involving high temperatures, such as the present one, the solid tends to sinter but studies on the analysis of sintering are few.

The simplest of these models are those in which the internal structure of the pellet is not considered and its behavior as a whole is modeled. These are normally called the macroscopic models. In all other models, the behavior of the distinctive elements of a pellet such as the grain, micrograin, or the pore constitutes the central feature of the models. The first such models did not account for pore evolution (through changes in particle size distribution) with progress of reaction. The later models that took this into account, the so-called structural models, can roughly be divided into two categories: grain models and pore models.

A particularly important class of non-structural models is the group of zone models in which a reaction zone is sandwiched between the ash layer and the unreacted core (Bowen and Cheng,[23] Mantri et al.,[24] Bowen et al.,[25] Dudukovic and Lamba[26]). The experimental results of Prasannan and Doraiswamy[27] on the oxidation of zinc sulfide clearly reveal all three stages of the reaction.

The original grain model is based on an explicit recognition of the granular structure of the pellet (Szekely and Evans[28]). The overall behavior of the pellet itself is assumed to be identical

to that of the grain, i.e., shrinking core behavior. Several extensions of the grain model have been proposed and the important ones are considered in the following sections.

Structural changes can be analyzed by considering the changes in the grains due to reaction or by corresponding changes in the pore structure (pore evolution). It is relatively simple to calculate grain size distributions using pore size distribution data obtained from mercury porosimetry measurements. The parent grain model mentioned earlier has been modified in different ways to account for changes in grain size and grain size distribution due to reaction. Alternatively, in the pore models, the pore has directly been considered to be the chief parameter.

In a particularly useful grain model, proposed by Heesink et al.,[29] the original model is made much more acceptable by accounting for grain size distribution, change in grain size with conversion, and pore blocking. Instead of using a continuous distribution of grain size, the grains are divided into groups and the conversion calculated for each group using the SCM. This study is particularly important from the point of view of the present work since the present authors used a similar experimental system for validating the model.

Another, more sophisticated, model is the so-called grain-micrograin model proposed by Dam-Johanson et al.[30] and Prins et al.[31] In this model, the solid (pellet) is assumed to consist of porous grains which in turn are made up of nonporous micrograins that react according to the SCM under product layer diffusion control. When the pores within the micrograin get blocked (resulting in significant reaction rate reduction), the pores between the grains are still open for mass transfer; the grains then react, also according to the SCM (partially reacted).

In contrast to the grain models in which the grains are, in a sense, assumed to be dispersed in a continuous gas phase, in the pore models the solid is regarded as the continuous phase. A

number of pore models have been proposed over the years, the earliest (and perhaps the most fundamental) being that of Ramachandran and Smith.[32] Perhaps the most realistic model is the random pore model of Bhatia and Perlmutter.[33-36] This model assumes that the actual reaction surface of the reacting solid is the result of the random overlapping of a set of cylindrical pores. Equations for calculating the evolving reaction surface have been developed. Several refinements of this model have been proposed (see Bhatia and Gupta[22]), a particularly interesting one being the inclusion of "newly discovered" pores (Delikouras and Permutter[37]).

Choice of Model for the Present Reaction

The experimental results obtained in this study using CaO pellets, and reported later in this report, clearly show a shrinking core. Further, when a pellet core is encased in a shell of stronger material, there is a built-in case for adding an additional resistance to the SCM, thus making this model a prime candidate for describing the sulfidation reaction. It is noteworthy, however, that the grain model has been successfully used for the sulfidation of precalcined limestone with different microstructures (Heesink et al.[29]). The micrograin-grain model has also been successfully used in the sulfidation of calcium oxide (Dam-Johanson et al.[30]). More extensive experimental data involving several physico-chemical property measurements are needed to examine the suitability of these models.

Thus, considering the *a priori* acceptability of the SCM, the emphasis of the present work on pellet development, and the need for a simple (semiempirical) equation for purposes of reactor design, it was considered desirable to confine the modeling to the SCM at this stage.

EXPERIMENTAL

MATERIALS

Several materials were used for the preparation of different core-in-shell pellet formulations (Table 1). One of the principal materials was limestone obtained from a quarry located near Ames, Iowa. The composition of the Iowa limestone based on X-ray fluorescence analysis is reported in Table 2. It can be seen that the material was largely calcite (96.8 wt.%) with a small amount of dolomite (1.8 wt.%) and silica (0.7 wt.%). The material was ground and screened to provide different size fractions of particles. The –297/+44 μm size fraction was used in the pellet shell formulations and in the pellet core formulations prepared in the Initial Development and Characterization study (pages 20-39). However, in later work the -210/+44 μm size fraction was used in pellet shells and the –44 μm fraction was utilized

Table 1. Materials used for the preparation of core-in-shell sorbent pellets.

Material	Supplier
Limestone (Iowa)	Martin Marietta Aggregates Quarry, Ames, IA
Limestone (Kentucky)	Martin Marietta Aggregates, Three Rivers Quarry, Smithland, KY
Dolomite (Ohio)	Graymont Dolime (OH) Inc., Genoa, OH
Dolomitic hydrated lime (Type S)	Graymont Dolime (OH) Inc., Genoa, OH
Plaster of Paris (OK)	U.S. Gypsum Co., Southard, Oklahoma
Plaster of Paris (DAP)	DAP Inc., Baltimore, MD
Kaolin (EPK)	Feldspar Corp., Atlanta, GA
Alumina (T-64)	Alcoa World Chemicals, Leetsdale, PA
Alumina (A-16 SG)	Alcoa World Chemicals, Leetsdale, PA

Table 2. Composition of limestone and plaster of Paris samples obtained from various commercial sources.

Component	Limestone, wt.%		Plaster of Paris, wt.%		
	Iowa	Kentucky[a]	DAP (I)	DAP (II)	U.S. Gypsum
$CaCO_3$	96.8	92.8	19.7	15.2	---
$CaCO_3 \cdot MgCO_3$	1.8	---	3.8	6.1	---
$MgCO_3$	---	5.9	---	---	0.2
$SrCO_3$	0.1	---	0.4	0.4	---
$CaSO_4 \cdot ½H_2O$	---	---	75.6	77.2	98.1
$SrSO_4$	---	---	---	---	0.3
$MgSO_4$	---	---	---	---	0.1
SiO_2	0.7	1.1	0.2	0.6	0.2
Other	0.6	0.2	0.3	0.5	1.1
Total	100.0	100.0	100.0	100.0	100.0

[a]Typical composition according to the suppler.

in the pellet cores. Another limestone used for preparing cores and shells in the Initial Development and Characterization study was obtained from Kentucky. This material had a lower concentration of $CaCO_3$ (92.8 wt.%) and a higher concentration of $MgCO_3$ (5.9 wt.%) than the Iowa limestone. The -297/+44 μm size fraction was used for preparing pellet cores and shells.

Plaster of Paris was also used for making pellet cores. The material was obtained from two different sources. A relatively pure form of plaster of Paris was supplied by U.S. Gypsum Co. which produced and calcined material from a gypsum deposit located near Southard, Oklahoma; it contained over 98 wt.% calcium sulfate hemihydrate (Table 2), and it appeared to

have a particle size distribution similar to that of the -44μm fraction of Iowa limestone. A material of lesser purity containing 76-77 wt.% $CaSO_4 \cdot ½H_2O$ came from DAP Inc. This material contained significant amounts of calcite (15-20 wt.%) and dolomite (4-6 wt.%).

Some pellet cores were made of Ohio dolomite or of dolomitic hydrated lime (dolime) derived from the dolomite. These materials were supplied by Graymont Dolime (OH) Inc. According to this supplier either material had the following composition after being calcined at 1273 K (1000°C): 58 wt.% CaO, 38 wt.% MgO, 0.5 wt.% SiO_2, and 0.5 wt.% other metal oxides. Also according to the supplier, the composition of the freshly produced dolime corresponded to $CaMg(OH)_4$. However, by the time it was utilized in the present project it appeared to be more like $CaCO_3 \cdot Mg(OH)_2$ which indicates that it had absorbed CO_2 from the atmosphere.

The pellet shells were made largely of a mixture of A-16 SG alumina powder and T-64 tabular alumina particles supplied by Alcoa. The first material had a median particle diameter of 0.88 μm and the second a median particle diameter of 8.65 μm. Both materials were high-purity calcined alumina.

Although most batches of core-in-shell pellets were made with shells composed of alumina and limestone, a few batches were made with shells composed of alumina and kaolin. The kaolin was designated as EPK Kaolin by the supplier, the Feldspar Corp., which also indicated that the material was 97% kaolinite ($Al_2O_3 \cdot 2SiO_2 \cdot 2H_2O$) with small amounts of other metal oxides. The supplier also indicated that the material had been water washed through a 44 μm screen.

For pelletizing limestone cores it proved advantageous to employ a dilute lignin solution as a binder. In most cases a solution composed of 5 vol.% Norlig A in deionized water was used.

The Norlig A was supplied by Lignotech and is described as a calcium lignosulfonate solution or suspension having a pH of 3.5 containing 16 wt.% reducing sugars, 6 wt.% total sulfur, 5 wt.% sulfonate sulfur, and 4 wt.% calcium. In a few cases an experimental mixture called "a high temperature binding agent composed of sodium lignosulfonates, sugar acids, and inorganic salts" was utilized. The mixture had a pH ≈ 10.

Other materials required for preparing and testing different sorbent formulations included small amounts of reagent grade fine chemicals and several different gases including H_2S, H_2, CO, CO_2, O_2, and N_2. The individual gases were obtained in high pressure cylinders and most were technical grade. An important exception was nitrogen since a prepurified grade was employed with less than 50 ppm impurities.

SORBENT PREPARATION

Core-in-shell sorbent pellets were prepared in two stages using a small bench-scale drum pelletizer which had a maximum diameter of 25 cm and could be operated at various speeds up to 120 rpm. Generally it was operated in the range of 40 to 80 rpm for pelletization. The pellet cores were prepared first by placing a measured amount (e.g., 50 g) of the appropriate powdered material in the drum, and as the drum revolved at a preselected speed, the powder was sprayed at frequent intervals with water or a dilute lignin solution until pellets formed. Water was used for pelletizing plaster of Paris, whereas a lignin solution was used for pelletizing limestone. The small pellets were grown into larger pellets by gradually adding more material and sometimes gradually increasing the drum speed. When the pellets reached the desired size range, they were separated by screening, and the smaller pellets were returned to the drum for additional growth. When these pellets had grown to the desired size, the drum was emptied, and the pellets were rescreened. All of the pellets of the desired size were then returned to the drum for hardening

and to improve their sphericity and uniformity. For hardening a constant drum speed of 60 to 70 rpm was often used, but in later work the drum speed was increased gradually during the treatment. The hardening process was continued for 60 min. for limestone pellet cores but only for 20 min. for plaster of Paris cores. During this time the surface of the pellets was kept moist by spraying the pellets occasionally.

If the hardened pellet cores were uniform in size, they were returned directly to the drum for coating. Otherwise they were first separated by hand screening, and only cores of the desired size were returned for coating with a specific coating material. After the pellets were placed in the drum, they were moistened, and the pelletizer was turned on. While the drum speed was kept in the range of 30 to 40 rpm, a measured amount of powdered coating material was added gradually as the pellets were sprayed with water or a dilute lignin solution. Once the pellets were fully coated, the drum was cleaned of any excess material, and the pellets were allowed to tumble for 60 to 120 min. to consolidate the coating. During this time the pellets were sprayed at approximately 5 min. intervals with water or a dilute lignin solution, and the drum speed was increased gradually to 100-120 rpm. The coated pellets were subsequently removed and screened.

Coated pellets of the desired size were then calcined to sinter the shell material. The heat treatment was conducted in a Lindberg box furnace, and it subjected the pellets to gradually increasing temperature so that after 3 hr. they were at 1373 K (1100°C). The pellets were held at this temperature for 2 hr, and then the furnace was allowed to cool slowly back to room temperature over 4 hr.

SORBENT CHARACTERIZATION

Several methods were used to test and characterize the finished core-in-shell sorbent pellets as well as pellet cores and shell material. These methods are described in the following paragraphs.

Sorbent Capacity

The absorption characteristics of a sorbent pellet were determined by employing a thermogravimetric analysis (TGA) system to measure changes in the weight, usually of a single pellet, over time as it was treated with an appropriate gas mixture at a selected temperature. In this system the pellet was suspended in a quartz basket from a Cahn model 2000 electrobalance so that it could be weighed continuously as it was treated with a flowing gas in a vertical tubular reactor made of 25 mm diameter quartz tubing. The reactor had an overall length of 61 cm and a heated length of 30.5 cm. A gas mixture of known composition was supplied to the reactor at a flow rate of 500 cm^3/min. measured at room temperature and pressure. The system temperature was determined with a thermocouple protected by a quartz thermowell located just below the suspended basket. The temperature was maintained by an electric furnace surrounding the reactor. The effluent from the reactor was passed through a caustic solution to remove any toxic or corrosive gases. During the later stages of the research project, the electrobalance and the thermocouple were both connected to a personal computer for data acquisition.

To measure the absorption characteristics of a core-in-shell pellet with a core derived from limestone, the pellet was placed in the basket and suspended in the reactor, and as it was heated to the temperature selected for the absorption measurement, it was surrounded by a stream of nitrogen. In most cases the pellet was precalcined to sinter the shell material, and this treatment also converted the limestone to CaO. But if the pellet had not been precalcined, the

limestone was converted to CaO as its temperature was raised to the temperature selected for absorbing H_2S. Once this temperature was reached and the system stabilized, the composition of the gas flowing through the reactor was adjusted to include H_2S in an appropriate and known concentration which usually fell in the range of 0.5 to 3.0 vol.%. In some cases H_2 was also added to the gas mixture. As the treatment continued, a constant system temperature was maintained, and the weight of the pellet was recorded. The treatment was discontinued when the weight of the pellet became constant or after a predetermined absorption time had passed.

If the pellet core had been derived from plaster of Paris, it was largely in the form of $CaSO_4$ after the pellet had been precalcined. To convert the $CaSO_4$ to CaO, the pellet was heated to 1323 K (1050°C) in the TGA system and subjected to a cycle of reduction with CO (30 vol.%) or H_2 (9 vol.%) and then oxidation with O_2 (13 or 20 vol.%). The cycle was repeated several times to achieve complete conversion of the $CaSO_4$ to CaO. The absorption characteristics of the pellet were then determined as described above.

In some cases a sorbent pellet was subjected to a multicycle test of absorption and regeneration by employing the TGA system. The absorption phase of each cycle was conducted as described above except that the time allowed for absorbing H_2S was usually limited to 20 or 30 min. At the end of this phase the temperature had to be raised to a higher level, usually 1323 K (1050°C), for regeneration. As the temperature was being raised pure N_2 was passed through the system. When the regeneration temperature was reached, the sorbent was subjected to several cycles of oxidation with 13 vol.% O_2 and reduction with 9 vol.% H_2 in nitrogen. The process of regeneration was continued until the pellet approached a constant weight. Then while passing only N_2 through the system, the temperature was lowered to the level used for absorption and the whole cycle of absorption and regeneration was repeated.

Compressive Strength

The compressive strength of core-in-shell pellets was determined by measuring the force required to fracture a single pellet when it was placed between two flat plates of an Accuforce EZ 250 test stand and the upper plate was lowered at a rate of 10 mm/min. The maximum force required to crack a pellet was recorded. The determination was repeated several times for each batch of pellets to determine the average compressive strength. For spherical pellets, the compressive strength was usually reported as the ratio of the breaking force to pellet diameter. A ratio of 8.9 N/mm is regarded as adequate for fixed-bed applications.[38] Therefore, this value was taken to be the minimum requirement for the present development effort. In some cases the compressive strength was reported as the ratio of the breaking force to the maximum cross-sectional area of the pellet.

Attrition and Abrasion Resistance

The attrition resistance of core-in-shell pellets was determined by employing an ASTM[39] standard test for measuring the attrition resistance of catalysts and catalyst carriers. The method utilizes a cylindrical drum having an inside diameter of 25.4 cm (10 in.) and a length of 15.2 cm (6 in.) with a single 5.1 cm (2 in.) high baffle extending the length of the cylinder. To conduct a test the drum is charged with approximately 100 g of dried pellets, and the drum is placed on a set of rollers and rotated at a rate of 60 rpm for 30 min. The contents of the drum are then poured onto a No. 20 (850 μm) ASTM sieve, and the sieve is shaken gently to pass the fines which have been created. The attrition loss is calculated as follows:

$$\text{Attrition loss (\%)} = \left[\frac{W_i - W_f}{W_i}\right]100 \qquad (5)$$

where W_i is the initial weight of pellets and W_f is the final weight.

The method was modified for the present work by excluding chipped pellets and fragments which did not pass through the sieve from the final weight of pellets. Therefore, the reported results are more conservative than those provided by the standard method.

Surface Area Analysis

The classical method for surface area analysis was used to determine the surface area of sorbent pellets. The technique was developed for multi-layer gas adsorption by Brunnauer, Emmett and Teller (BET). The measurements were conducted with a Micromeretics 2000 surface area analyzer by adsorbing N_2 gas at 77 K (-196°C). Prior to measurement the pellet samples were degassed at 383 K (110°C) under vacuum to remove any moisture which might have been adsorbed by the samples. The method not only provided a measure of the surface area, it also provided a measure of the specific volume and size distribution of the open pores smaller than 780 Å.

Density and Porosity Measurements

The density and porosity of sorbent pellets were determined by applying Archimedes principle. The method requires measuring the dry weight W_D of a specimen, the weight of the specimen saturated with liquid W_S, and the weight of the saturated specimen suspended in the same liquid W_{SS}. The liquid used for the present work was n-decane. After these measurements had been carried out on a sample of sorbent pellets, the bulk density ρ_b, apparent density ρ_L, and apparent porosity P_a of the pellets were calculated by employing the following formulas:

$$\rho_b = \frac{W_D \cdot \rho_L}{W_S - W_{SS}} \tag{6}$$

$$\rho_a = \frac{W_D \cdot \rho_L}{W_D - W_{SS}} \tag{7}$$

$$P_a = \frac{W_S - W_D}{W_S - W_{SS}} \quad (8)$$

The apparent porosity is the fraction of the total pellet volume which is occupied by open pores, and is often expressed as a percent.

Chemical Composition and Structure

Several different techniques were employed to determine the chemical composition and structure of core-in-shell sorbent pellets. These techniques included X-ray diffraction (XRD), X-ray fluorescence (XRF), scanning electron microscopy (SEM), and energy dispersive spectrometry (EDS). XRD was used to identify crystalline phases present, and XRF was used for bulk chemical analysis. A Siemens D500 instrument was used for XRD analysis, and a Philips PW 2404 instrument for XRF analysis.

A JEOL 6100 scanning electron microscope with a tungsten filament was used for examining the structure of core-in-shell pellets. This instrument was also used for elemental analysis by EDS which showed how individual elements were distributed throughout a pellet.

RESULTS AND DISCUSSION

INITIAL DEVELOPMENT AND CHARACTERIZATION

It had been shown previously that a promising sorbent for desulfurizing hot coal gas can be made in the form of small pellets such that each pellet has a core made largely of limestone encased in a strong, porous shell made largely of calcium aluminate cement.[1] However, at projected gas desulfurization temperatures of 1073 – 1173 K (800 - 900°C) the hydraulic cement became dehydrated, and its strength suffered. Therefore, the present investigation turned at once to a more promising method of making a strong, porous shell. This method makes use of a sinterable powder which can be applied as a coating to the limestone pellet cores. The coated

pellets are calcined subsequently at a temperature which is sufficiently high to sinter the coating but not so high as to cause sintering of the limestone cores. Although various sinterable powders were considered, the one which seemed to best fit the present requirements was a mixture of alumina particles of different sizes. Even though the sintering temperature of larger particles of pure alumina would be too high, it was possible that the sintering temperature of ultrafine-size particles would be in the right range. Furthermore, the sintering temperature could be reduced further by adding a second component such as powdered limestone which might also enhance the porosity of the shell. This indeed proved to be the case.

During the initial stage of development which is described below, an attractive shell material was formulated, tested, and utilized in the preparation of core-in-shell sorbent pellets. Also plaster of Paris was investigated as an alternative to limestone for making the pellet cores. Numerous batches of core-in-shell pellets were made from these materials and subsequently characterized to determine the absorption capacity of the pellets for H_2S and the effects of shell thickness, temperature, and H_2S concentration on the rate of absorption of H_2S.

Shell Formulation

To show that a strong shell material can be made by combining different sizes of alumina particles and limestone particles in optimum proportions followed by calcination to sinter the material, numerous batches of tablets were prepared and tested. The batches were formulated by combining A-16 SG alumina powder having a median particle diameter of 0.88 μm with T-64 tabular alumina particles having a median particle diameter of 8.65 μm with Iowa limestone particles which ranged from 44 to 297 μm in size. These materials were mixed with water to form a very thick slurry which was poured into a mold to form cylindrical tables having a diameter of 14.2 mm and thickness of 5.3 mm. The molded tablets were air-dried for 24 hr and

then calcined at 1373 K (1100°C) for 2 hr to sinter the material. The tablets were subsequently tested to determine the force required to break a tablet when a single sample was placed on edge between the two flat plates of an Accuforce EZ 250 test stand, and the upper plate was lowered at a rate of 10 mm/min. The determination was repeated with five different tablets selected at random from each batch of tablets.

Initially several different batches of tablets were formulated by combining only A-16 SG alumina and T-64 alumina in different proportions. After the tablets had been calcined, the force required to break the tablets was measured and the results are presented in Figure 1. Each point represents an average of five determinations of the crushing force for a given composition. It can be seen that the strength of the material was a maximum when the material contained about 60% T-64 alumina or, in other words, when the ratio of T-64 alumina to A-16 SG alumina was 3:2.

Several additional batches of tablets were prepared to study the effect of adding either pure calcium carbonate or Iowa limestone to the 3:2 mixture of T-64 alumina and A-16 SG alumina. The tablets were prepared and tested as described above, and the results with Iowa limestone are presented in Figure 2. Although the results obtained with pure calcium carbonate are not shown, they were very similar to those obtained with limestone. It is apparent that the crushing strength of the material was a maximum when 20% limestone was incorporated in the formulation. For this formulation the force required to break a tablet was more than twice that of the formulation which did not contain limestone. However, when the limestone content was increased beyond the optimum level, the required crushing force decreased rapidly. The results suggest that with the optimum level of limestone a calcium aluminate compound formed upon sintering which served as a particle bonding agent. However, when excess limestone was

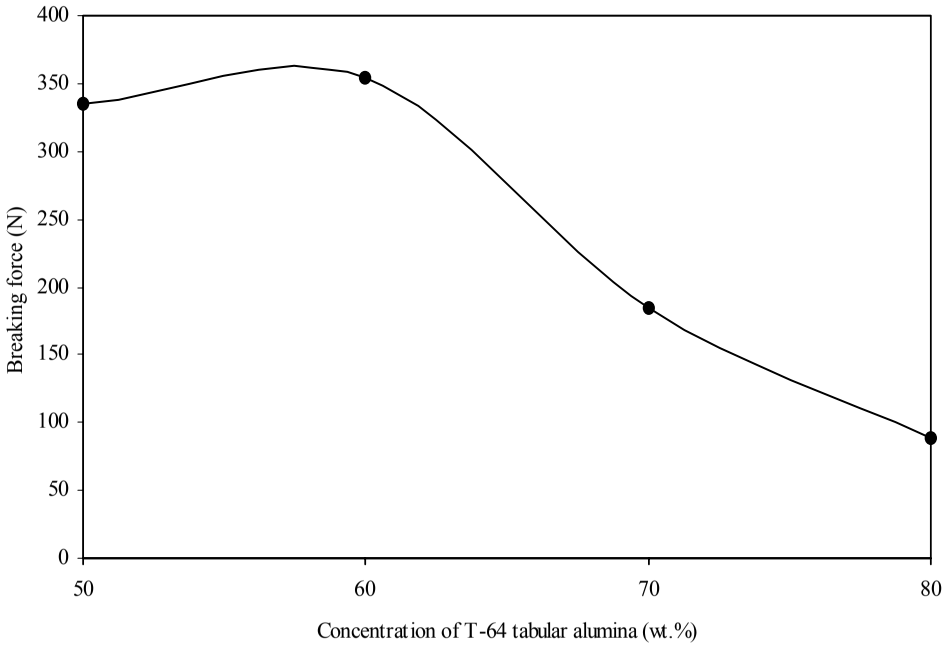

Figure 1. Effect of composition on the force required to break the calcined tablets made with a mixture of T-64 alumina and A-16 SG alumina powders

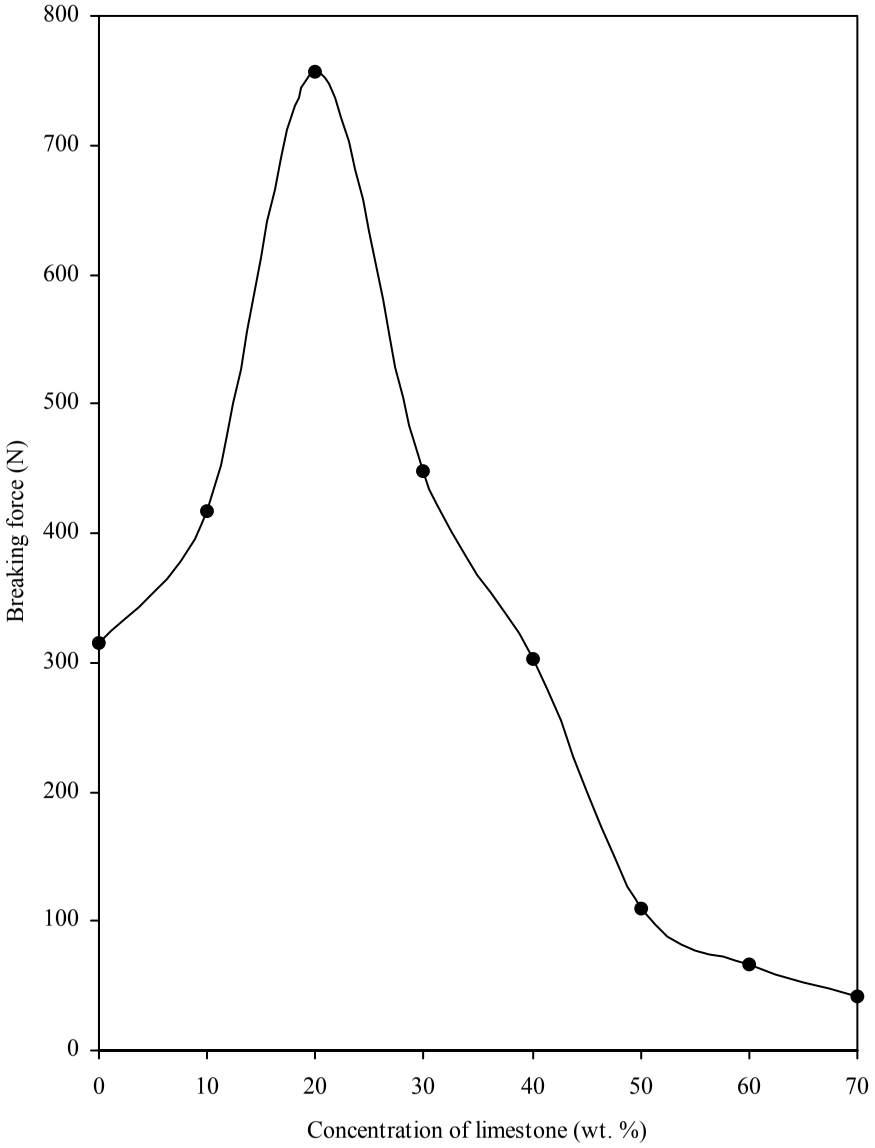

Figure 2. Effect of limestone concentration on the force required to break the calcined tablets made with 3:2 ratio of T-64 alumina to A-16 SG alumina

incorporated in the formulation, free CaO may have been present which weakened the calcined material.

Core-in-Shell Pellets

To demonstrate the applicability of the new shell material for core-in-shell pellets, several batches of core-in-shell pellets were prepared by the two-stage pelletization process whereby pellet cores were prepared by pelletizing pulverized limestone (-297/+44 μm) in the first stage and subsequently coating selected cores with the optimum mixture of alumina and limestone particles in the second stage. Since previous work had shown that the compressive strength of core-in-shell pellets could be increased by adding some A-16 SG alumina to the core material, the concentration of alumina in the cores was varied among batches. In addition, the shell thickness was varied among batches to see what affect the thickness would have on pellet strength. The thickness was determined only approximately from the nominal diameter of the cores and nominal diameter of the finished pellets. These diameters were determined by comparing the cores and pellets to standard screen openings. During pelletization of both the cores and shells, the material in the pelletizing drum was sprayed intermittently with a dilute lignin solution. The pellet cores and also the coated pellets were separated by screening. Coated pellets of the desired size were calcined at 1373 K (1100°C) for 2 hr. The force required to break a calcined pellet was determined for several pellets within each batch, and then the absorption characteristics of several different pellets were determined by measuring the gain in weight of one pellet at a time exposed to a stream of gas containing 1.1 vol.% H_2S at 1153 K (880°C) for 1.0 hr.

Table 3. Absorption capacity and crushing strength of core-in-shell sorbents made with Iowa limestone.

Sorbent	Limestone[a] conc., wt.%	Nominal dia., mm		Shell thick., mm	Ave. breaking force, N/mm	Absorption[b] cap., wt.%
		Core	Pellet			
I	80	3.35	3.96	0.30	7.57 ±1.35	6.99 ±0.24
II	90	3.35	3.96	0.30	8.94 ± 1.39	7.20 ± 0.94
III	100	3.35	3.96	0.30	3.39 ± 0.79	12.26 ± 2.33
IV	80	3.96	4.76	0.40	9.64 ± 1.76	4.80 ± 2.10
V	90	3.96	4.76	0.40	4.03 ± 0.33	8.14 ± 1.44
VI	100	3.96	4.76	0.40	3.15 ± 0.74	12.80 ± 1.06

[a]Limestone concentration in pellet core.
[b]Gain in weight of sorbent treated with 1.1 vol.% H_2S at 1153 K (880°C) for 1 hr.

The results were quite encouraging inasmuch as reasonably strong core-in-shell pellets with a moderately high absorption capacity were prepared in some cases (Table 3). The compressive strength is reported as the ratio of the breaking force to the pellet diameter and the reported value is an average for two or more batches of pellet and for several pellets within each batch. The reported adsorption capacity is based on several pellets within a single batch for each case. The 95% confidence limits for the mean adsorption capacity and breaking force are also indicated. For both sizes of pellets, the crushing strength was improved by having 10% A-16 SG in the core, but increasing the alumina content of the core to 20% produced mixed results. It is clear that the adsorption capacity of the pellets increased as the limestone content of the core formulation increased. On the other hand, neither the crushing strength nor the absorption capacity of the pellets was affected by a small difference in shell thickness. In the end only sorbents II and IV appeared to have sufficient strength for fixed-bed applications since it has been suggested that the minimum breaking force for such applications is 8.9 N/mm.[38]

Properties of Core-in-Shell Pellets

Numerous batches of core-in-shell pellets were prepared to investigate the effects of shell thickness and different core formulations on the physical properties of the sorbent pellets. All of the pellets were made with the optimum shell composition, i.e., 48% T-64 tabular alumina, 32% A-16 SG alumina powder, and 20% Iowa limestone. The cores were made either of limestone or a DAP plaster of Paris. Most of the limestone cores were made of Iowa limestone and most contained 10% A-16 SG alumina. After the pellets had been calcined, various physical properties were determined including compressive strength, bulk density, and apparent density. Typical results are presented in Table 4 for several different sorbent formulations. The examples represent pellets made with different core materials and made with shells of different thickness. The pellet dimensions were determined more accurately than before by measuring the overall diameter and shell thickness of a number of pellets with hand held calipers and averaging the results. The pellet core diameter was kept within the range of 3.2 to 3.4 mm. The property values listed for each sorbent represent the mean of three batches of pellets. Since the crushing strength was measured on five pellets selected at random from each batch, each value of compressive strength is based on the breakage of 15 different pellets. The crushing strength correlated extremely well with shell thickness. The following relationship between compressive strength S (N/mm) and shell thickness t (mm) was developed by applying linear regression to the experimental data:

$$S = 19.5\ t + 0.65 \tag{9}$$

Since the correlation coefficient r had a value of 0.993, this equation seemed to account for most of the variation in the compressive strength so core composition had little effect. According to

Table 4. Physical properties of core-in-shell sorbent pellets after calcination at 1373 K (1100°C) for 2 h.

Sorbent designation	A	B	C	D	E
Initial core composition	90% Ames limestone + 10% A-16SG Alumina	90% Kentucky limestone + 10% A-16SG Alumina	90% Ames limestone + 10% A-16SG Alumina	100% Plaster of Paris	100% Plaster of Paris
Pellet diameter (mm)	4.20 ± 0.06	4.23 ± 0.13	4.80 ± 0.20	4.54 ± 0.14	5.14 ± 0.17
Shell thickness (mm)	0.40 ± 0.04	0.42 ± 0.05	0.78 ± 0.03	0.62 ± 0.12	0.91 ± 0.15
Fractional shell volume	0.47 ± 0.03	0.48 ± 0.03	0.69 ± 0.02	0.64 ± 0.01	0.73 ± 0.07
Compressive strength (N/mm)	8.94 ± 1.39	8.57 ± 1.79	16.44 ± 0.48	12.10 ± 3.16	18.28 ± 3.09
Apparent density (g/cm^3)	3.40 ± 0.05	3.30 ± 0.03	3.46 ± 0.04	3.39 ± 0.02	3.49 ± 0.11
Bulk density (g/cm^3)	1.60 ± 0.09	2.03 ± 0.15	1.95 ± 0.02	1.48 ± 0.06	1.86 ± 0.03
Apparent porosity (%)	52.7 ± 3.8	38.4 ± 4.8	43.8 ± 0.0	56.4 ± 2.2	46.7 ± 2.7

equation 9, a shell thickness of 0.43 mm would withstand a crushing force approaching 8.9 N/mm which is considered adequate for fixed bed applications.[38]

The data in Table 4 indicate only a small variation in the apparent density of pellets made with different formulations and a much larger variation in the bulk density. The bulk density and the apparent porosity reflect the fractional pellet volume occupied by open pores. Therefore, formulation D had the largest volume of accessible pores and formulation B the lowest. Since the apparent porosity decreased as the shell thickness increased and made up a larger share of the total pellet volume for a given core material, the porosity of the shells must have been smaller than the porosity of the cores. Because the porosity of sorbent C was less than that of either sorbents D or E with comparable fractional shell volumes, it is apparent that the porosity of the plaster-based pellets was larger than that of the limestone-based pellets.

Core-in-Shell Pellet Structure

In order to examine the actual structure of the core-in-shell pellets, several pellets were cross-sectioned and viewed with a scanning electron microscope. The pellets were made with Iowa limestone cores and the optimum shell composition. The cores also contained 10% A-16 SG alumina. The structure of an uncalcined pellet is revealed in Figure 3. The core and shell are clearly delineated by the difference in texture of the two regions. The shell had a much coarser texture due to the presence of relatively large tabular alumina particles intermixed with much finer but discrete alumina and limestone particles. Also the shell appeared to be slightly darker than the core, and the shell had fewer and smaller voids or holes than the core. Calcination produced a change in the structure which is revealed in Figure 4. The texture of the calcined shell material was much finer than before due to particle sintering. Consequently it became more difficult to distinguish the shell from the core.

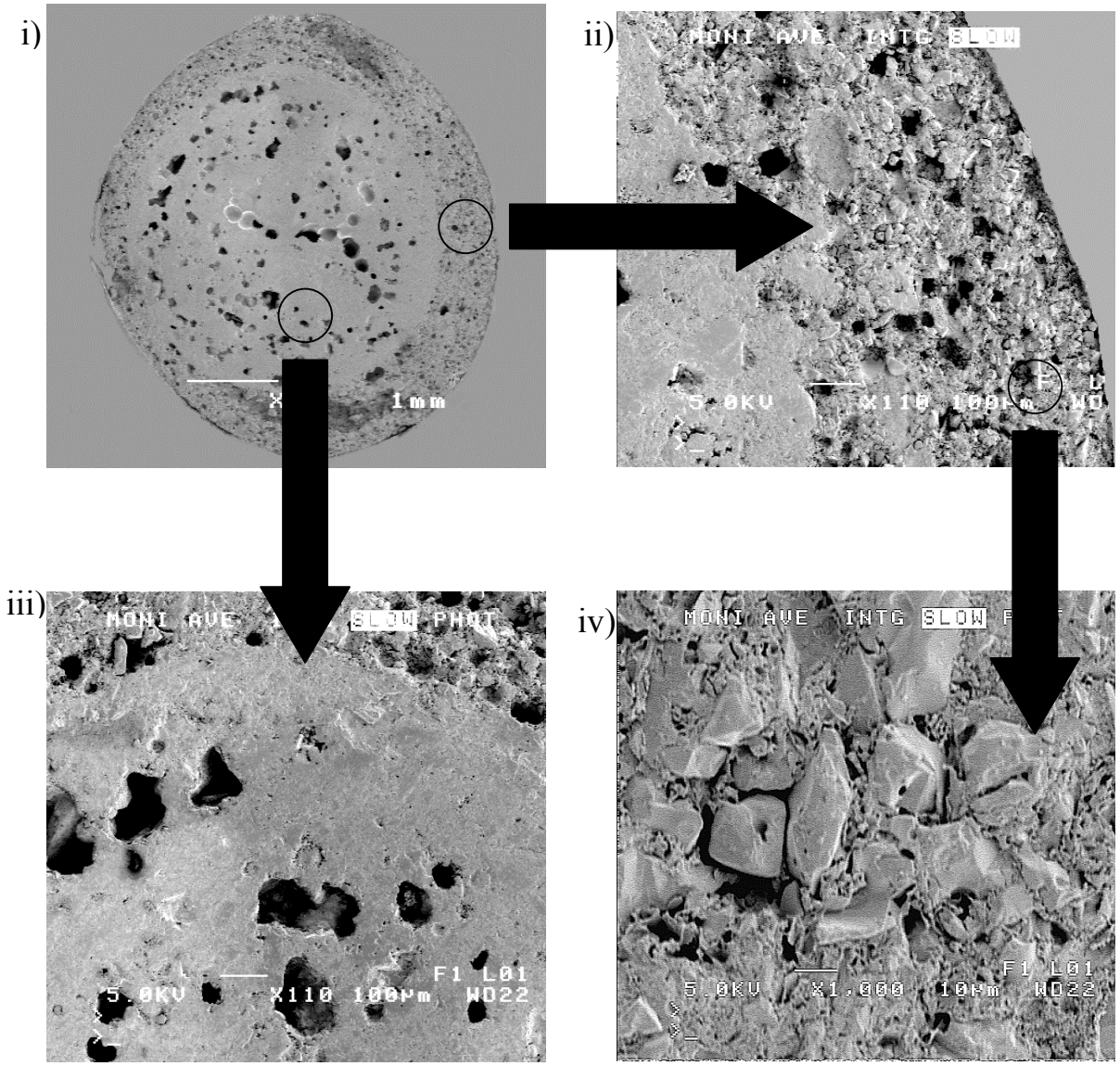

Figure 3. Micrographs of a freshly made limestone-based pellet; i) section of an entire pellet at ×17, ii) the shell at ×110, iii) the core at ×110, and iv) the shell at ×1000.

Conversion of $CaSO_4$ to CaO in Plaster-based Cores

Since calcination alone did not convert pellets made with calcium sulfate cores into a calcium oxide-based sorbent, the pellets had to be subjected to the cyclic process of reduction and oxidation which had been developed previously.[40,41] However, for the present application one pellet at a time was treated in the TGA apparatus. The results of treating several different

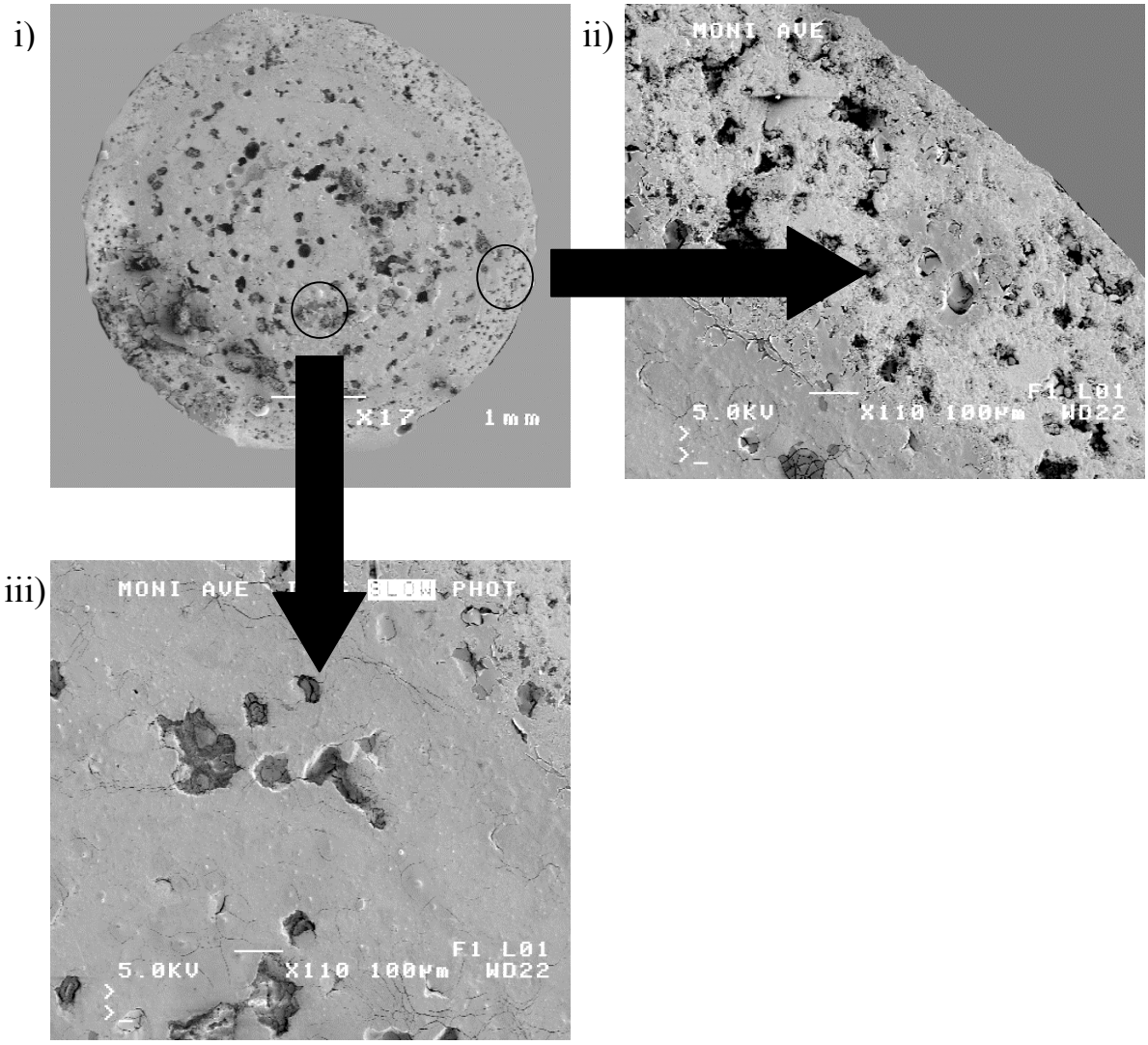

Figure 4. Micrographs of a fired limestone-based pellet; i) section of an entire pellet at ×17, ii) the shell at × 110, iii) the core at ×110.

pellets made of DAP plaster of Paris are shown in Figure 5. The treatment was applied at 1343 K (1070°C) using a nitrogen gas mixture containing 30% CO for reduction and 20% O_2 for oxidation. The cyclic treatment was continued until the pellets reached a constant weight. One of the pellets was a bare core without a shell which had only been heated to 1343 K (1070°C) before applying the treatment while two of the pellets had shells which were 0.42 and 0.83 mm thick, respectively, and had been calcined at 1373 K (1100°C). It can be seen that during each

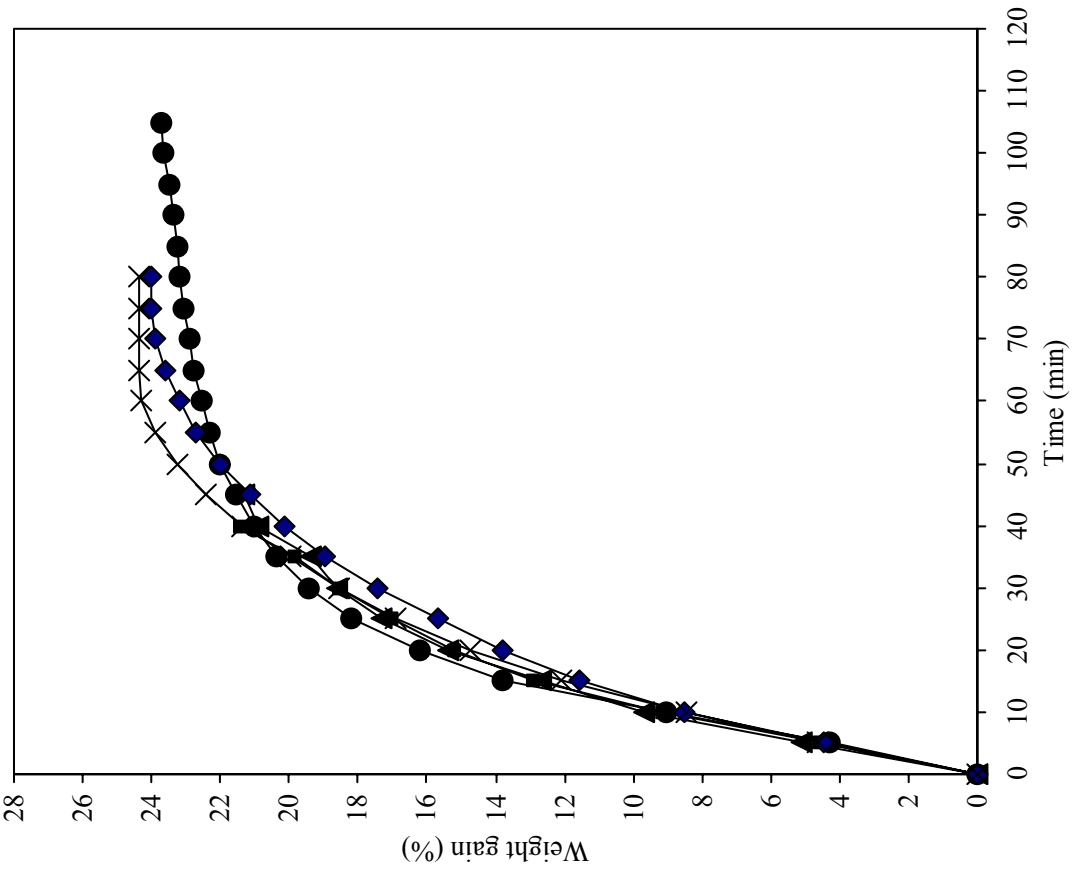

Figure 6. Replicate runs with pellet cores made of either DAP plaster of Paris or limestone. Absorption was conducted with 1.1%H_2S at 1153 K (880°C).

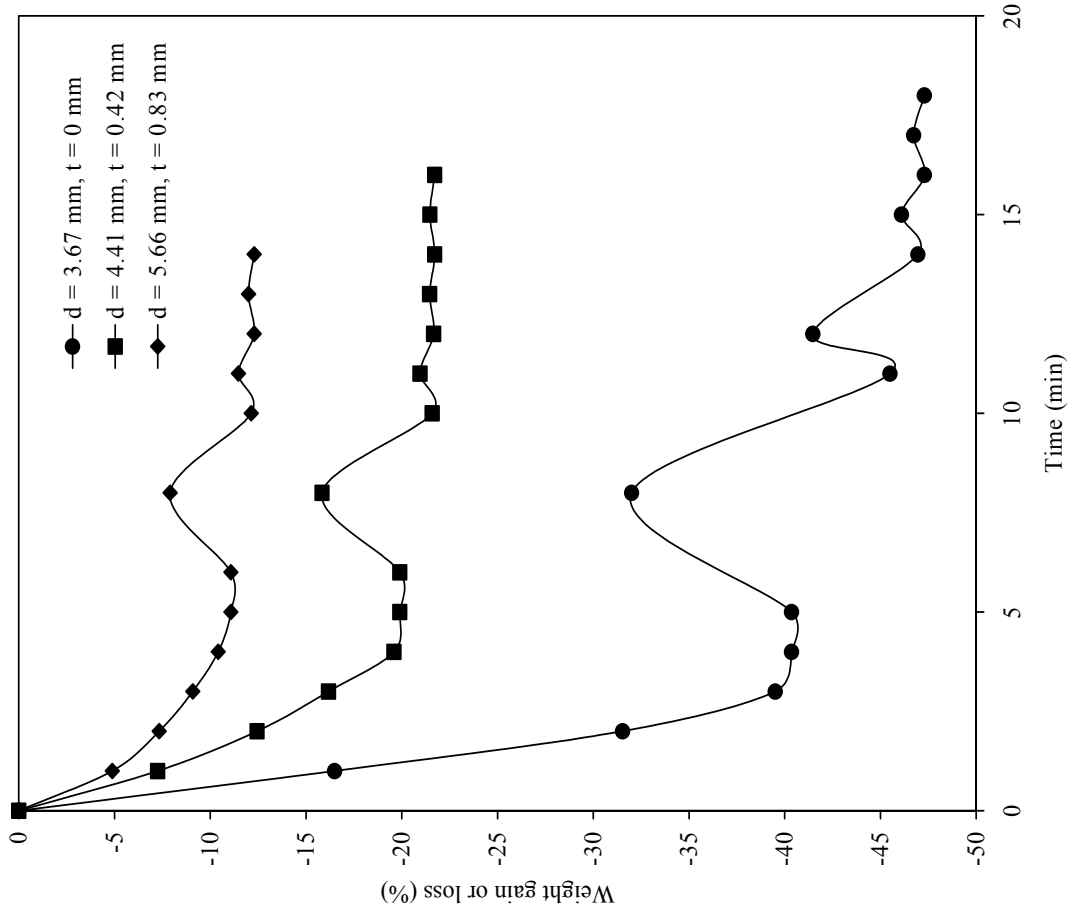

Figure 5. Decomposition of $CaSO_4$ in various pellets by a cyclic oxidation and reduction process conducted at 1343 K (1070°C).

reduction step the pellets lost weight as $CaSO_4$ was converted into a mixture of CaO and CaS. Then during the following oxidation step the pellets gained weight as CaS was converted into a mixture of CaO and $CaSO_4$. Of course, the amount of weight gained or lost decreased with each cycle because of the SO_2 produced. It is also apparent that the ultimate loss in weight on a percentage basis declined with increasing shell thickness because the core mass became a smaller fraction of the total pellet mass. For the bare pellet core the ultimate loss in weight of 47% was close to the theoretical maximum loss in weight of 50% if all of the $CaSO_4$ in the impure material were converted to CaO.

Sorbent Characteristics

The absorption characteristics of pellets made from Iowa limestone or from DAP plaster of Paris were determined after the $CaCO_3$ or $CaSO_4$ had been converted to CaO. Pellets made with limestone cores always included 10% A-16 SG alumina in the core preparation mixture. Pellet shells were made with the optimum shell composition which included 20 wt.% Iowa limestone having a particle size which ranged from 44 to 297 μm.

The absorption characteristics of several pellet cores were determined first to establish a base line. Although the cores had not been precalcined at 1373 K (1100°C), they had been preheated sufficiently to convert the starting materials to CaO. The absorption tests were conducted at 1153 K (880°C) with 1.1% H_2S in a nitrogen mixture. While some of the H_2S could have decomposed at this temperature, other work[42] suggests that the extent of decomposition would probably not have exceeded 7-10%. The results presented in Figure 6 indicate good agreement between repeated tests and virtually no difference in the absorption characteristics of pellets made from the different starting materials. The observed maximum gain in weight for either material was approximately 24% which corresponded closely to the

theoretical gain in weight of the limestone-based pellets if all the CaO were converted to CaS. However, it was 10% less than the theoretical gain in weight of the plaster-based pellets if all the calcium compounds had first been converted to CaO and all of the CaO had then been converted to CaS.

Several absorption tests were conducted with precalcined core-in-shell pellets to study the effect of increasing shell thickness. Again the tests were conducted at 880° C with 1.1% H_2S in a nitrogen mixture. Results obtained with limestone-based pellets are shown in Figure 7 and results with plaster-based pellets in Figure 8. In both cases it is apparent that the ultimate gain in weight due to absorption decreased as shell thickness increased. Also the ultimate gain in weight of limestone-based pellets was greater than that of plaster-based pellets. These effects are the result of expressing the gain in weight as a percentage of the initial pellet mass. As the shell thickness increased, the reactive core mass became a smaller fraction of the total pellet mass since all of the pellets had approximately the same initial core diameter, 3.5 mm. Furthermore, the pellet cores derived from limestone had more CaO than those derived from plaster because the molar volume of the $CaCO_3$ particles was less than the molar volume of the $CaSO_4 \cdot 2H_2O$ particles.

While it is apparent from Figures 7 and 8 that the rate of weight gain decreased with increasing shell thickness, it is not so apparent that the rate of conversion of CaO to CaS was generally not greatly affected by shell thickness. This can be seen by comparing the conversion of the different pellets at a particular time assuming that the conversion was proportional to the fractional change in pellet weight based on the ultimate gain in weight at steady state. For example, after 20 min. of absorption most of the plaster-based pellets registered a conversion of 68 to 69%. Only the pellet with the thickest shell registered a slightly higher conversion (71%).

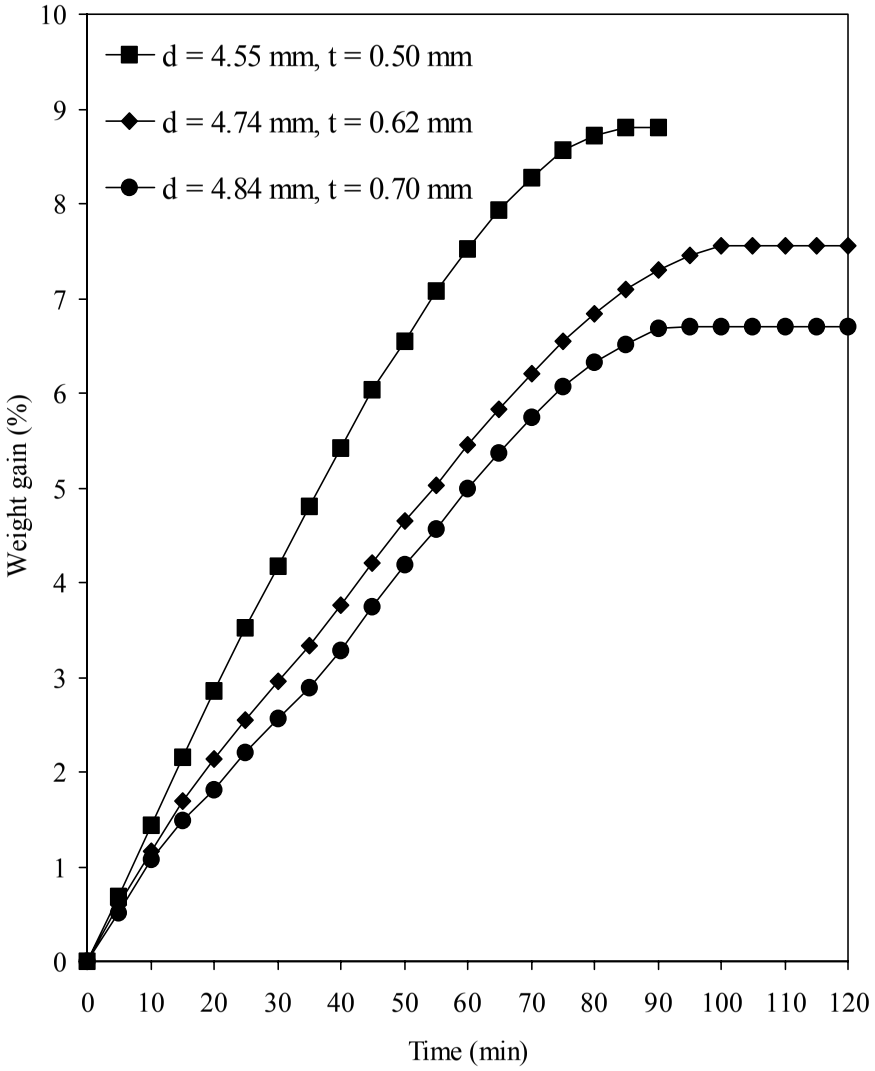

Figure 7. Effect of shell thickness t on the absorption capacity of limestone-based, core-in-shell pellets. Absorption was conducted with 1.1% H_2S at 1153 K (880°C).

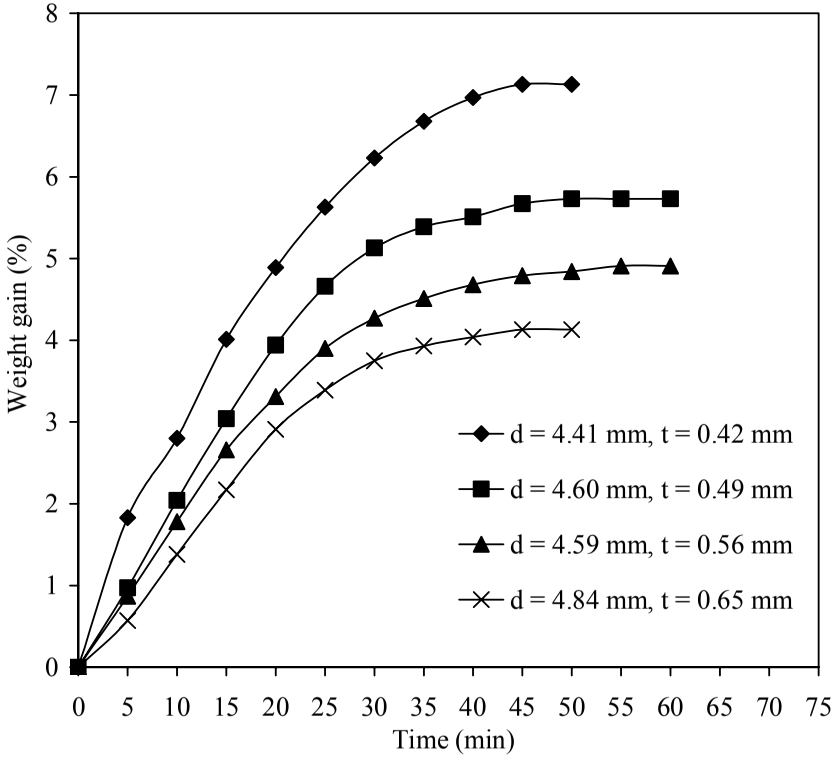

Figure 8. Effect of shell thickness t on absorption capacity of plaster-based, core-in-shell pellets. Absorption was conducted with 1.1% H_2S at 1153 (880°C).

The difference is not considered significant. For the limestone-based pellets the results suggest that shell thickness had some effect. After 50 min. of absorption the pellet with the thinnest shell registered a conversion of 74% while the other two pellets having thicker shells registered conversions of 62 and 63%, respectively. Since the plaster-based pellets in 20 min. registered a conversion which was equal to or greater than that registered by the limestone-based pellets in 50 min. with a comparable shell thickness, it is apparent that the plaster-based pellets reacted more rapidly.

The difference in reactivity of the two types of core-in-shell pellets may seem surprising since the uncalcined pellet cores made of the different materials appeared to react equally rapidly with H_2S (Figure 6). However, the limestone-based cores initially contained 10% A-16 SG alumina which probably reacted with part of the lime when the core-in-shell pellets were calcined at 1373 K (1100°C), thereby changing the properties of the material.

Other absorption tests were conducted with precalcined core-in-shell pellets to investigate the effect of H_2S concentration on the rate of absorption while holding pellet dimensions and other system parameters constant. The results obtained with limestone-based pellets are presented in Figure 9 and those obtained with plaster-based pellets in Figure 10. Although the average outside diameter of both types of pellets was nearly the same (4.9 and 4.8 mm), the average core diameters differed and were 4.0 and 3.5 mm, respectively. Consequently, the average shell thickness was 0.45 mm for the limestone-based pellets and 0.64 mm for the plaster-based. For a given sorbent material the ultimate gain in weight of the sorbent appeared to be independent of H_2S concentration with the exception of the result shown for a limestone-based pellet treated with 3% H_2S (Figure 9). In this case the decline in ultimate capacity of the sorbent may have been due to pore closure.

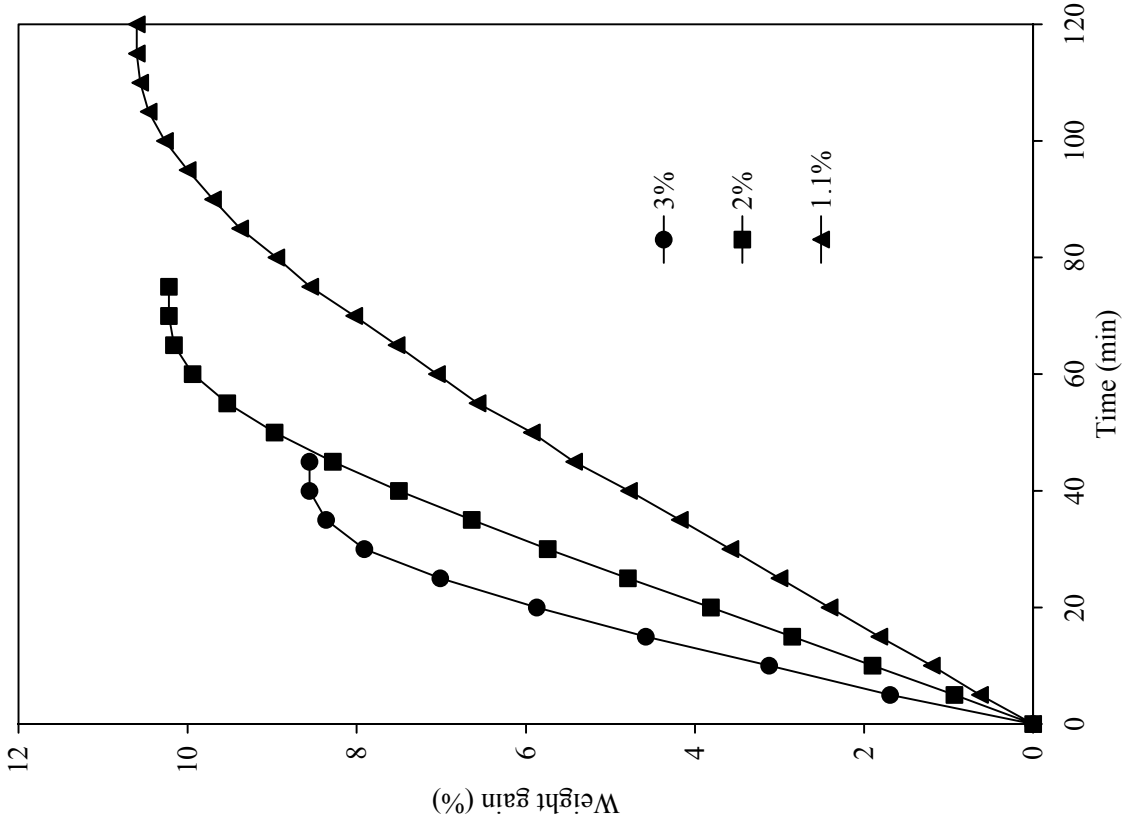

Figure 9. Effect of H_2S concentration on absorption rate of limestone-based, core-in-shell pellets. Runs were conducted at 1153 K (880°C).

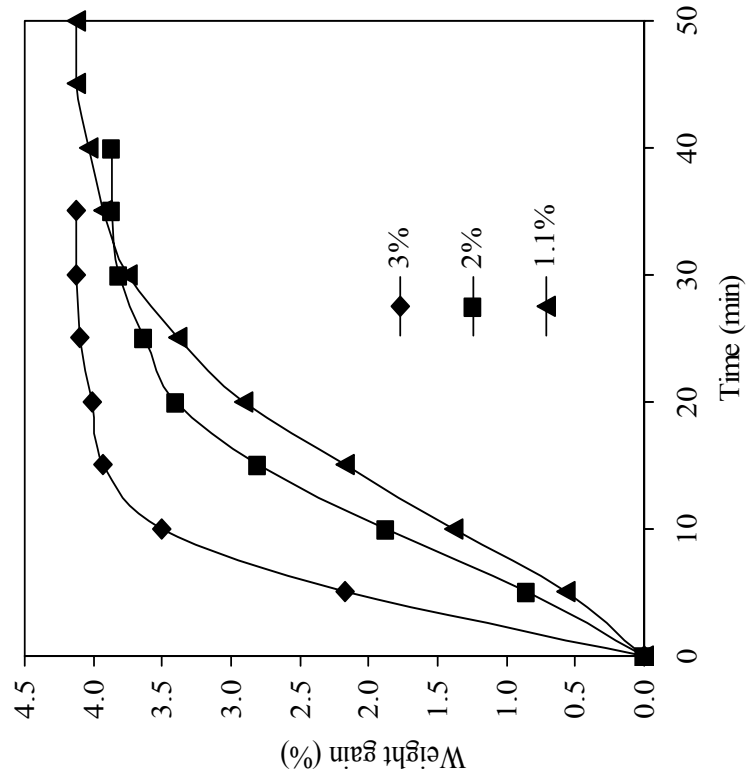

Figure 10. Effect of H_2S on concentration on absorption rate of plaster-based, core-in-shell pellets. Runs were conducted at 1153 K (880°C).

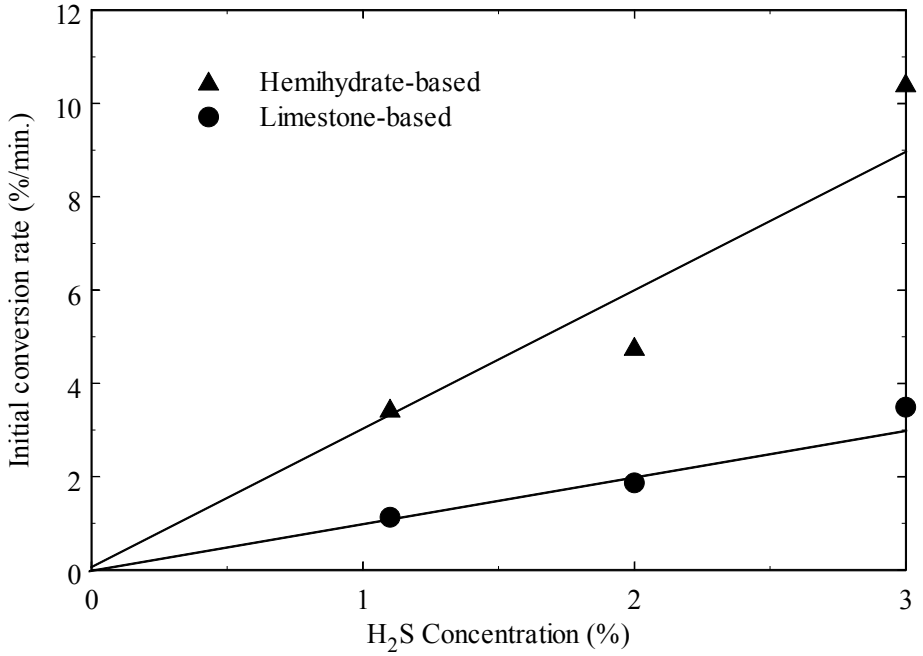

Figure 11. Effect of H_2S concentration on initial global conversion rate for different types of core-in-shell pellets at 1153 K (880°C).

For both sorbent materials the initial rate of absorption was greatly affected by H_2S concentration. In Figure 11 it can be seen that the initial global rate of conversion of CaO to CaS was directly proportional to H_2S concentration which suggests that the process is governed at least initially by first order kinetics. Furthermore, since the global rate of reaction was larger for the plaster-based pellets which also had the thickest shells, the results indicate that the plaster-based cores reacted more rapidly than the limestone-based cores.

Additional absorption tests were conducted with precalcined pellets to study the effect of temperature on the rate of absorption of H_2S. The results are shown in Figures 12 and 13, respectively, for the two types of pellets. For some of these tests, limestone-based pellets having an average overall diameter of 4.88 mm and a shell thickness of 0.48 - 0.55 mm were employed. Figure 12 indicates very little difference in the rate of absorption over the temperature range from 1113 to 1193 K (840 to 920°C). The small differences in the final weight gain of the

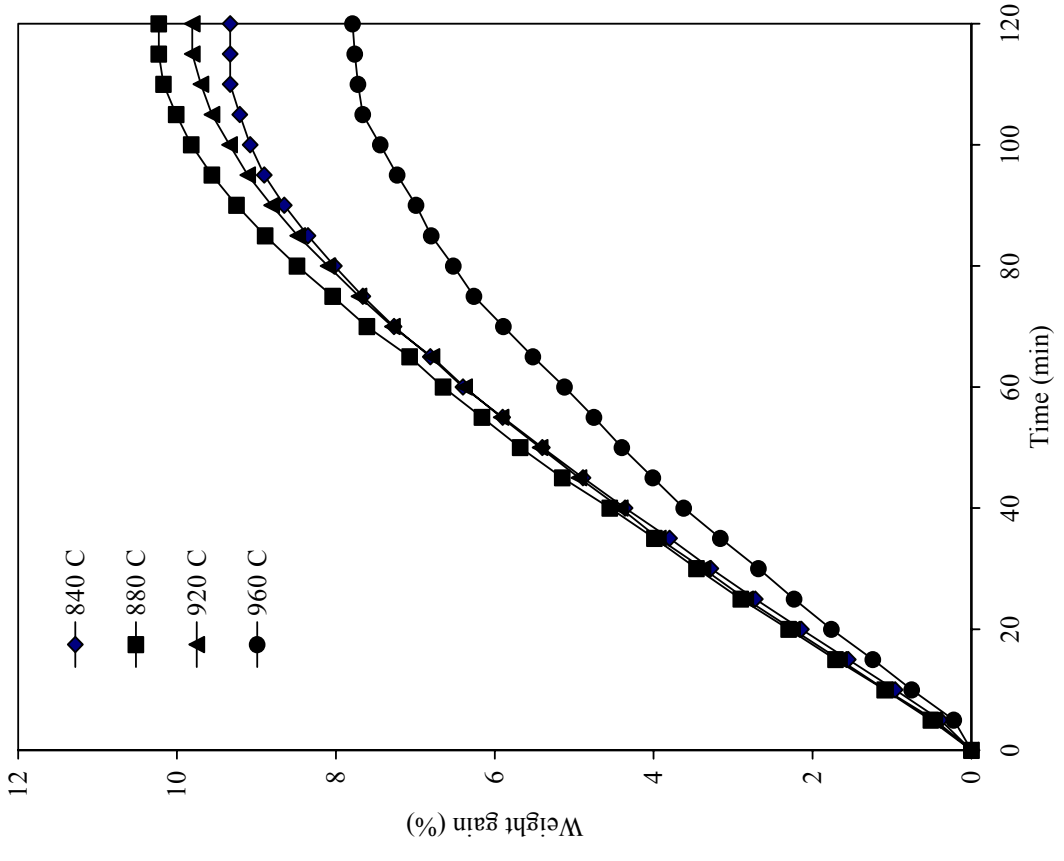

Figure 12. Effect of temperature on absorption rate of limestone-based, core-in-shell pellets. Runs were conducted with 1.1% H_2S in nitrogen.

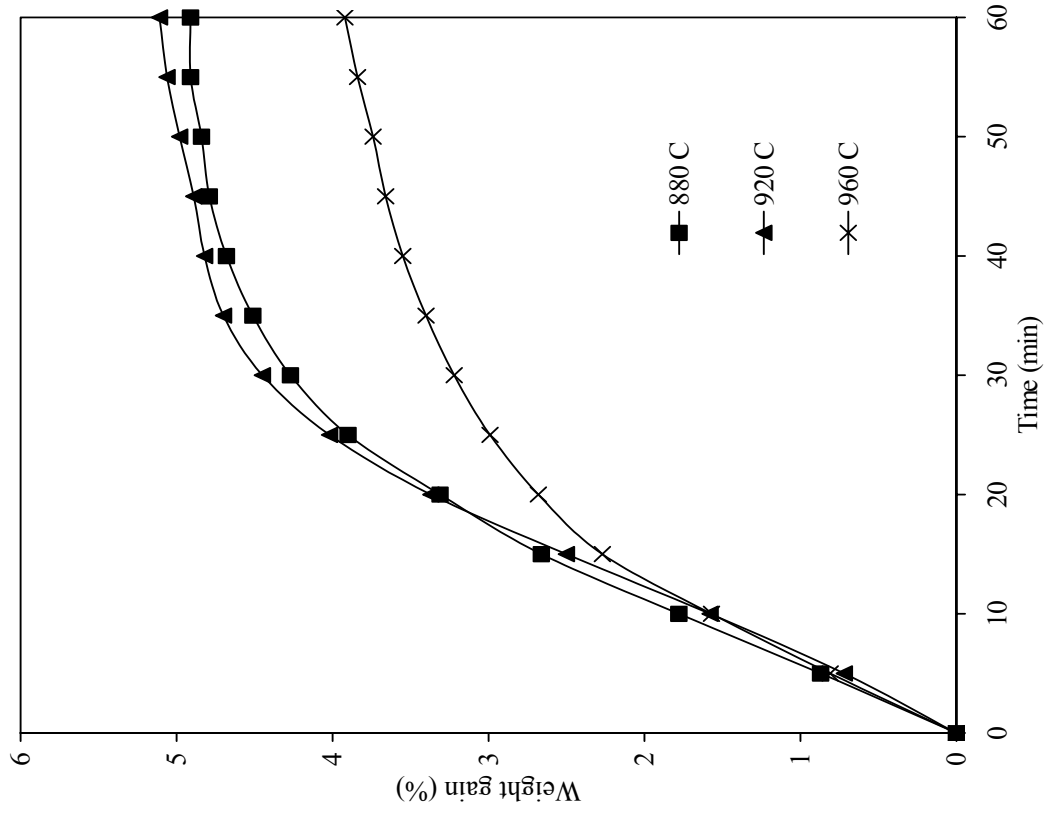

Figure 13. Effect of temperature on absorption rate of plaster-based, core-in-shell pellets. Runs were conducted with 1.1% H_2S in nitrogen.

different pellets were probably due to differences in sorbent mass. However, the lower rate of absorption observed at 1233 K (960°C) was clearly due to the increase in temperature. Similar results were observed with the plaster-based pellets which had an average overall diameter of 4.56 mm and average shell thickness of 0.53 mm (Figure 13). Again the small difference in rate of absorption observed between 1153 K and 1193 K (880°C and 920°C) was not significant, whereas the lower absorption rate observed at 1233 K (960°C) was significant. Considering that for the two cases the rate of absorption didn't seem to be affected significantly by temperatures below 1193 K (920°C), the overall rate did not appear limited by chemical reaction. Therefore, the rate controlling mechanism remained elusive. The marked decrease in absorption rate above 1193 K (920°C) may have been caused by incipient sintering of the material with corresponding pore closure or it may have been caused by greater decomposition of the H_2S with a corresponding decrease in the concentration of the reactant.

SORBENT DEVELOPMENT

The preceding initial results showed that a promising sorbent for desulfurizing hot coal gas can be made in the form of spherical pellets such that each pellet consists of a CaO core surrounded by a strong, porous shell made largely of alumina. However, the effects of subjecting the sorbent to repeated sulfidation and regeneration were not considered nor was the possibility that the results may have been affected by the thermal decomposition of H_2S. Therefore, additional tests were conducted to investigate these potential effects. As the following results will show the reactivity of the sorbent does decline with repeated sulfidation and regeneration, and the results can be affected by H_2S decomposition unless H_2 is present to inhibit the decomposition. To overcome the decline in reactivity, consideration was given to the possible cause and prevention of the decline. Since the decline appeared due to sintering of CaO,

consideration was also given to the possibility that the CaO derived from different sources might not experience the same level of sintering and that the addition of certain substances might inhibit sintering.

Effect of H_2S Decomposition on Testing

The results of a typical multicycle sulfidation and regeneration test of a calcium-based sorbent are shown in Figure 14. These results were obtained with a single core-in-shell pellet that had a core made of DAP plaster of Paris and a shell composed of alumina and Iowa limestone in optimum proportions (i.e., 80 wt.% alumina and 20 wt.% limestone). The pellet core diameter was 5.59 mm and shell thickness was 0.49 mm. The pellet was weighed continuously as it was treated at different temperatures and with different gas mixtures in the TGA system. Initially the pellet was calcined at 1373 K (1100°C) for 2 hr to partially sinter the shell material. Then the pellet was treated at 1323 K (1050°C) by the cyclic reduction and oxidation process to convert $CaSO_4$ to CaO. This treatment accounted for the cyclic changes in pellet weight recorded in Figure 14 during the first 30 min. Approximately 30 min. later after the temperature of the pellet had been reduced to 1153 K 1153 K (880°C), the pellet was treated with a gas mixture containing 1.6 vol.% H_2S and 98.4 vol.% N_2 which caused the pellet to gain weight as CaO was converted to CaS. The treatment was extended until the pellet approached a constant weight. At this point H_2S was no longer supplied and with only N_2 flowing through the system, the temperature was raised to 1323 K (1050°C), and as the temperature was being raised, the weight of the pellet decreased inexplicably. After the weight became constant, the pellet was regenerated by the cyclic oxidation and reduction process which caused the fluctuations in pellet weight starting at 215 min. from time zero. The pellet was subsequently subjected to two additional cycles of sulfidation and regeneration.

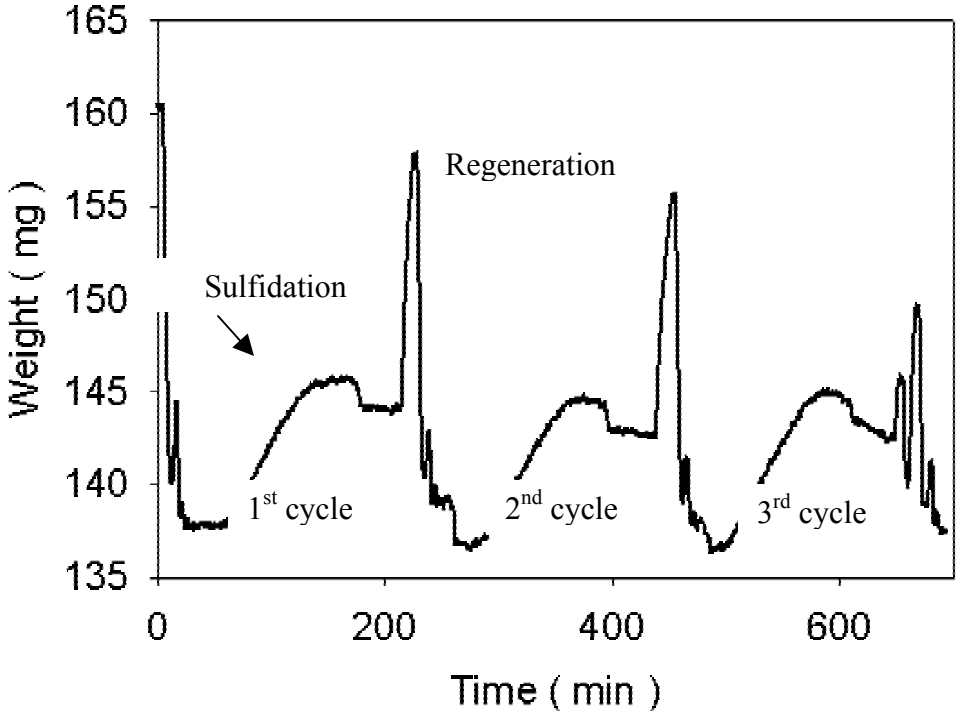

Figure 14. Results of a typical multicycle sulfidation and regeneration test of a core-in-shell pellet using 1.6 vol.% H_2S and 98.4 vol.% N_2 for sulfidation.

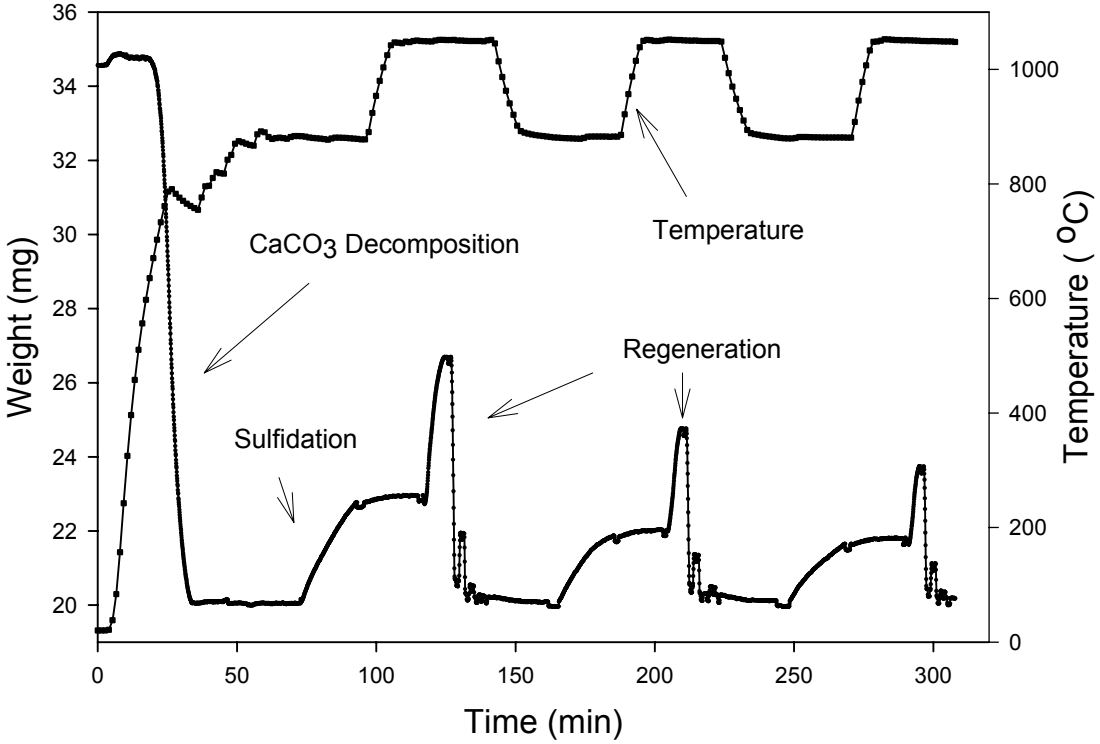

Figure 15. Results of a multicycle sulfidation and regeneration test of a limestone pellet core using 1.0 vol.% H_2S, 24.0 vol.% H_2, and 75.0 vol.% N_2 for sulfidation.

During this test the pellet gained essentially the same amount of weight during the sulfidation phase of each cycle, i.e., 5.8% of the regenerated pellet weight. Furthermore, the slope of the curve was essentially the same for the sulfidation phase of each cycle which indicated no change in the reactivity of the CaO. The only troubling feature of the results was the unexplained drop in pellet weight when the flow of H_2S was discontinued and the temperature raised. This feature was characteristic of the results of many other sulfidation tests conducted with other core-in-shell pellets and also with pellet cores made of limestone or with higher purity plaster of Paris.

It was also observed that during the sulfidation tests some elemental sulfur was deposited on the upper, cooler end of the quartz wire which supported the basket containing the sorbent pellet. Sulfur was also deposited on the lower, inner surface of the tubular reactor which projected out of the bottom of the enclosing furnace. This observation indicated that some H_2S was being decomposed to elemental sulfur. At first it was thought that the amount of H_2S decomposition would be slight and unlikely to affect the CaO sulfidation results. This view was supported by a previous experimental study of H_2S decomposition kinetics which reported only slight decomposition when 1.0 mole % H_2S in nitrogen was passed through a quartz tube at 1153 K (880°C).[42] However, other work[43] indicated that trace amounts of oxygen can accelerate H_2S decomposition. Since the nitrogen generally employed for the present tests could have contained up to 50 ppm O_2, it was possible that the decomposition of H_2S was accelerated by traces of oxygen. Later this was shown to be highly unlikely.

To avoid the H_2S decomposition problem while sulfidizing CaO, Abbasian[8] added hydrogen to the gas mixture to maintain a 3:1 ratio of H_2 to H_2S. To investigate this possible solution of the problem, a series of runs was carried out in which hydrogen was added in

increasing amounts to an H_2S/N_2 mixture that was passed through the heated tubular reactor. For this series of runs an empty quartz basket was suspended inside the reactor heated to 1153 K (880°C). A gas mixture containing 1.6 vol.% H_2S and various concentrations of H_2 and N_2 was passed through the reactor. Any change in weight of the basket and its supporting wire due to sulfur deposition over a period of 25 min. was noted and recorded. Following each run the supporting wire was examined and cleaned. The results are summarized below.

Run No.	H_2 Conc., vol. %	Wt. gain, mg	S deposited
1	0	0.5	Yes
2	6	0.3	Yes
3	12	0.2	Yes
4	18	0	Yes
5	24	0	No.

It was apparent that sulfur was deposited on the upper part of the supporting wire in most runs but the quantity decreased as the hydrogen concentration was raised. While the quantity of sulfur deposited at the lowest hydrogen concentrations could affect the results of the CaO sulfidation tests, it appeared unlikely that the amount deposited at the higher hydrogen concentrations would have much effect.

To see whether the deposition of elemental sulfur on the basket supporting wire and its subsequent removal could account for the loss in weight when a sulfidized pellet was subsequently raised to a higher temperature in nitrogen, several additional multicycle sulfidation and regeneration tests were conducted in which hydrogen was added to the sulfidizing gas. The results of such a test are shown in Figure 15. For this test a single pellet core made entirely of Iowa limestone (-44 μm) was subjected to three cycles of sulfidation and regeneration. As the pellet was heated initially, it lost a large amount of weight as $CaCO_3$ was converted to CaO. Then as it was treated subsequently with a gas mixture containing 1.0 vol.% H_2S, 24 vol.% H_2

and 75 vol.% N_2 it gained weight as CaO was converted to CaS. Before the pellet was completely sulfided, the gas mixture was replaced by pure N_2, and the flow of nitrogen was continued while the temperature was increased to 1323 K (1050°C) for regeneration. During this time the weight remained constant instead of declining as in runs made without hydrogen. Therefore, the deposition of sulfur on the basket supporting wire did seem to account for a certain amount of weight increase in runs made without hydrogen. To avoid this problem all further sulfidation tests were conducted with hydrogen present.

Unlike the results shown in Figure 14 the results shown in Figure 15 indicated a decline in the reactivity of the sorbent between the first and second cycles of sulfidation. Since the two tests had been conducted with CaO derived from different materials, other multicycle sulfidation and regeneration tests were conducted to study the possible effects of the CaO source materials.

Effects of Different CaO Sources

To investigate the effects of different calcium sources, pellet cores were prepared from the following materials and then tested: (1) pure $CaCO_3$, (2) Iowa limestone, (3) OK plaster of Paris, (4) DAP plaster of Paris, (5) dolime, and (6) dolomite. Most of the materials were pelletized as received from the suppliers. One exception was the limestone which had been prescreened and only the material passing a 325 mesh screen (-44 μm) was pelletized. Another exception was the dolomite which had to be dried first since it was too damp for pelletization when received. The two types of plaster of Paris were pelletized with deionized water while the other materials were pelletized with 5 vol.% Norlig A lignin in deionized water. Single pellets of these materials were subsequently treated in the TGA system to prepare the CaO which was then subjected to three cycles of sulfidation and regeneration. Sulfidation was carried out for 20 min. at 1153 K (880°C) with 1.0 vol.% H_2S, 24 vol.% H_2 and 75 vol.% N_2. This was followed by

regeneration involving 3 to 4 cycles of oxidation with 13 vol.% O_2 and reduction with 9 vol.% H_2 over a period of 15 min. The specific absorption capacity which is defined below was used as a measure of performance for comparing the different sorbent materials.

$$\text{Specific Capacity}\,(\%) = \frac{W_2 - W_1}{W_1} \times 100 \qquad (10)$$

In this formulation W_2 is the final weight of the sorbent after sulfidation and W_1 the initial weight. Observed values of the capacity are shown in Figure 16 and 17 for the different materials. These values represent an average of two determinations with pellets prepared from pure $CaCO_3$ and an average of three determinations with pellets prepared from limestone. The other values represent the results of a single determination with each material.

The results of these tests show considerable variation in the absorption capacity among the different materials and also in the rate of decline of absorption capacity from one cycle of sulfidation to the next. However, the observed values represent an apparent absorption capacity which is dependent on the time provided for sulfidation as well as other reaction conditions. Therefore, the differences in observed absorption capacity reflect differences in the rate of absorption as well as differences in the absolute absorption capacity of the materials.

To provide an indication of the absolute absorption capacity of the different materials, the theoretical maximum absorption capacity of each material was calculated based on the complete conversion of the CaO present in the material to CaS. The calculated values are presented in Table 5 together with the values observed during the first and third cycles of sulfidation. It is apparent that for most materials the theoretical maximum capacity was in the range of 27 to 28%. The theoretical capacity of the sorbent derived from $CaCO_3$ was slightly higher than that of the other materials because of the purity of the $CaCO_3$. For all of these materials the difference in observed absorption capacity must have been due to differences in the rate of

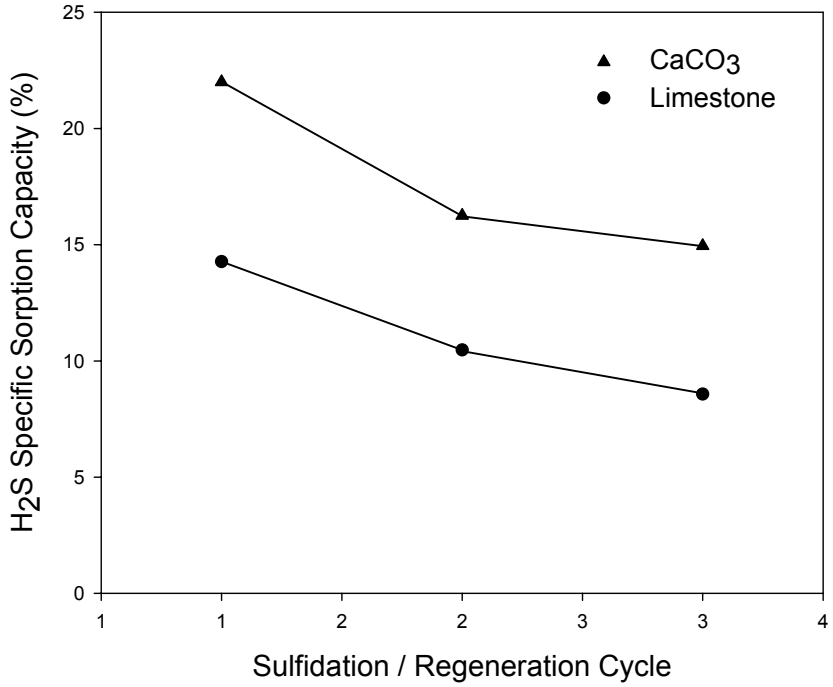

Figure 16. Specific absorption capacity of pure $CaCO_3$ and limestone pellet cores sulfided with 1.0 vol.% H_2S, 24 vol.% H_2, and 75 vol.% N_2 at 1153 K (880°C).

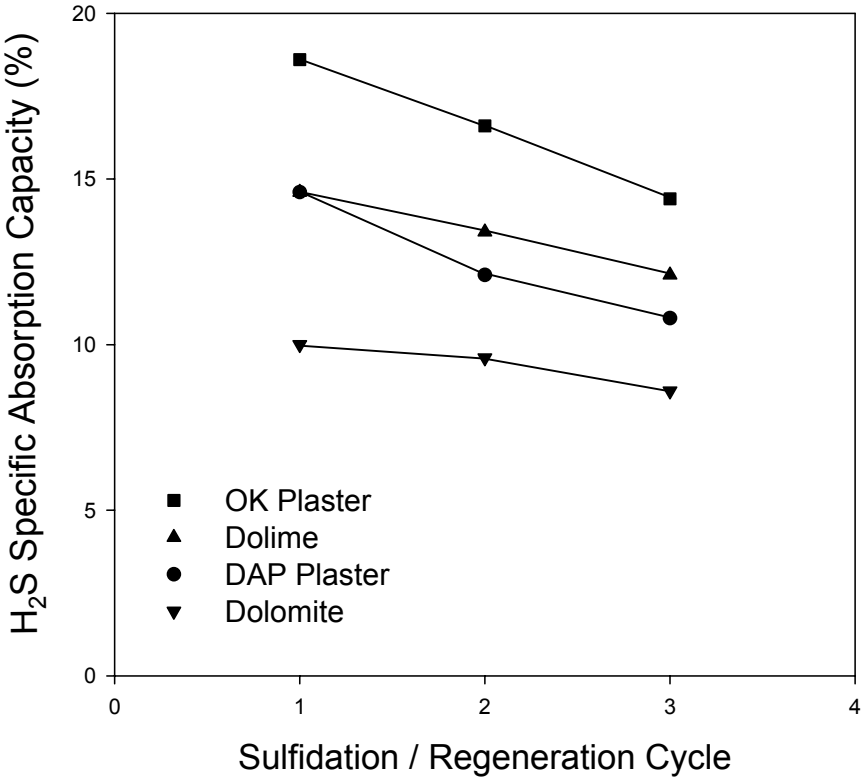

Figure 17. Specific absorption capacity of pellet cores derived from different materials and sulfided with 1.0 vol.% H_2S, 24 vol.% H_2 and 75 vol.% N_2 at 1153 K (880°C).

Table 5. The theoretical maximum specific absorption capacity of different materials and the observed capacity after one or three cycles of sulfidation.

Material	Specific absorption capacity, %		
	Maximum	1st Cycle	3rd Cycle
Pure $CaCO_3$	28.6	22.0	15.0
Iowa limestone	27.1	14.3	8.6
OK plaster of Paris	27.4	18.6	14.4
DAP plaster of Paris	27.1	14.6	10.8
Dolime	16.6	14.6	12.1
Dolomite	16.6	10.0	8.6

absorption which probably depends on particle size, surface area, porosity, pore size distribution, etc. Only in the case of the sorbents derived from dolime or dolomite did the theoretical absorption capacity differ greatly from the others, and this difference was due to the presence of a high concentration of MgO which did not react with H_2S. Of particular interest was the difference in the observed absorption capacity of dolime and dolomite since the dolime had been derived from the dolomite. It is apparent that the conversion of the dolomite to dolime by the supplier had improved the observed absorption capacity of the material, probably because of changes in the physical properties of the material.

Also of special interest was the rate of decline in the observed absorption capacity from cycle to cycle which varied among the different materials (Figures 16 and 17). The sorbents derived from pure $CaCO_3$ or limestone exhibited the highest rate of decline while the sorbents derived from dolime or dolomite exhibited the lowest. The sorbents derived from either form of plaster of Paris displayed an intermediate rate of decline.

Changes in Physical Properties During Multicycle Testing

To see whether the differences in absorption capacity and the rate of decline in capacity with usage could be related to certain physical properties of the sorbent materials, larger batches of pellets were prepared for measurement of surface area, apparent porosity, apparent density, and open pore volume. Only two materials, Iowa limestone and OK plaster of Paris, were chosen for this effort. Pellet cores prepared from these materials and having a diameter of 3.33 to 3.96 mm were dried, calcined and/or treated to convert the materials to CaO, and then subjected to three cycles of sulfidation and regeneration. Since approximately 40 pellets were required for some of the property measurements, 20 pellets at a time were treated in the vertical tubular reactor with the appropriate gas. For sulfidation the pellets were treated for 30 min. at 1153 K (880°C) with a gas mixture containing 1.0 vol.% H_2S, 24 vol.% H_2, and 75 vol.% N_2. For regeneration the pellets were subjected to several cycles of oxidation and reduction at 1323 K (1050°C) over a period of 20 min. Oxidation was conducted with 13 vol.% O_2 in N_2 and reduction with 9 vol.% H_2 in N_2. The physical properties of interest were determined after the following stages:

Stage	Description
1	Green pellets which had been dried over Drierite in a desiccator at room temperature and pressure
2	Green pellets which had been dried at 383 K (110°C) under vacuum for surface area analysis but not calcined
3	Calcined pellets which had been converted to CaO
4	Pellets which had undergone one cycle of sulfidation and regeneration
5	Pellets which had undergone two cycles of sulfidation and regeneration
6	Pellets which had undergone three cycles of sulfidation and regeneration

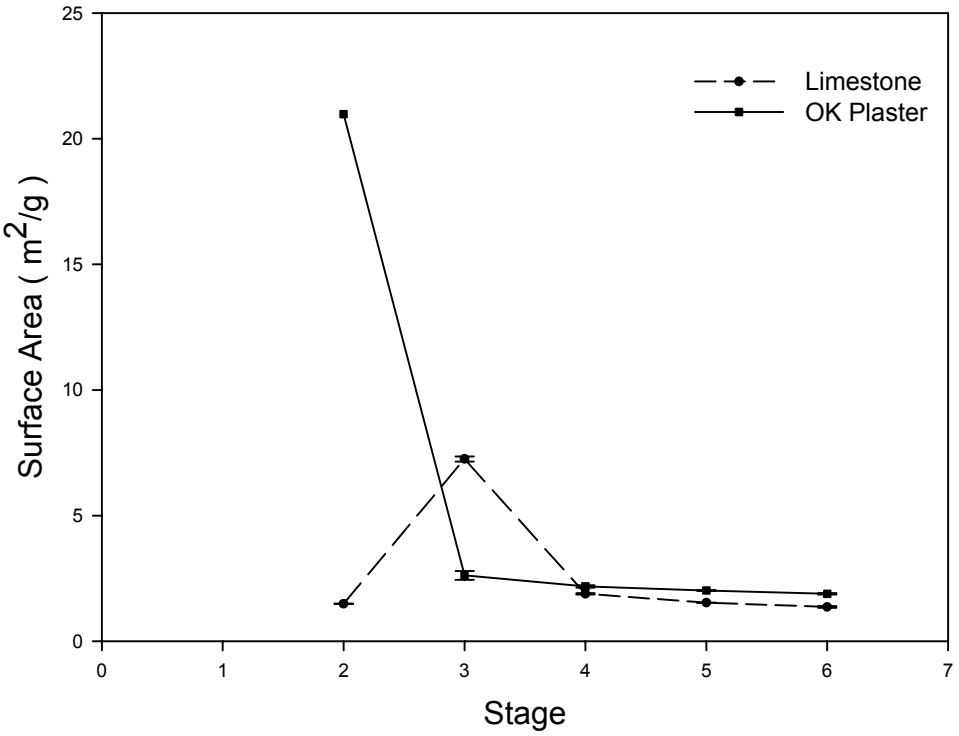

Figure 18. Specific surface area of two different types of pellet cores at different stages of preparation and usage.

The surface area and pore size distribution of the materials were determined by the BET method involving the adsorption of N_2 at 77 K (-196°C). The apparent density and porosity of the materials were determined by application of Achimedes' principle.

The specific surface area of each material at each stage is indicated in Figure 18 and also in Table 6. Most of the indicated values represent an average of two determinations. The surface area of the pellets was first determined after they had been vacuum dried at 383 K (110°C). At this stage the surface area of the plaster-based pellets was much greater than that of the limestone-based pellets because the former had absorbed water of crystallization in accordance with the following reaction, whereas the limestone-based pellets had not undergone such a reaction:

$$CaSO_4 \bullet \tfrac{1}{2}H_2O + \tfrac{3}{2}H_2O \rightarrow CaSO_4 \bullet 2H_2O \qquad (11)$$

Table 6. Specific surface area and open pore volume of sorbents at different stages of preparation and testing

Stage	Plaster-based[a]			Limestone-based[a]		
	Area, m^2/g	$20 < D < 780$ Vol., m^3/g	$D > 780$ Vol., m^3/g	Area, m^2/g	$20 < D < 780$ Vol., m^3/g	$D > 780$ Vol., m^3/g
2	21.0	0.0423	0.463	1.49	0.0036	0.269
3	2.6	0.0042	1.059	7.30	0.0136	0.711
4	2.18	0.0037	1.042	1.89	0.0032	0.701
5	2.02	0.0034	1.054	1.53	0.0026	0.611
6	1.89	0.0032	1.015	1.36	0.0023	0.599

[a]D = diameter of pores in angstroms (Å) which contributed to open pore volume in the indicated size range.

Consequently when the pellets were vacuum dried and the water of crystallization was removed, the plaster-based pellets were left with a more porous structure than the limestone-based pellets. However, after the pellets had been converted to CaO (Stage 3), the surface area of the limestone-based pellets exceeded that of the plaster-based pellets. Calcination of the limestone-based pellets at 1153 K (880°C) to convert $CaCO_3$ to CaO by eliminating CO_2 apparently created new micropores and increased the surface area of the material from 1.5 to 7.3 m^2/g. In contrast when the plaster-based pellets were treated 1323 K (1050°C) to convert $CaSO_4$ to CaO by a cyclic reduction and oxidation process, the surface area dropped from 21 m^2/g to 2.6 m^2/g which indicated a structural rearrangement of the material most likely due to sintering. Through sintering, micropores are consolidated into larger pores with a corresponding reduction in pore surface area.

During Stage 4 the surface area of both materials decreased probably because of additional sintering, especially at the regeneration temperature of 1323 K (1050°C). The plaster-

based material experienced the smallest reduction in surface area since it had already been treated at 1323 K (1050°C) during Stage 3 and, therefore, was likely to have undergone some sintering. Interestingly, following Stage 4 the surface area of both materials was approximately 2 m^2/g, although the surface area of the plaster-based material was slightly greater than that of the limestone-based (Figure 18). Both materials experienced slight decreases in surface area during Stages 5 and 6 probably as a result of additional sintering.

Could these small differences in surface area have been responsible for the much larger differences between the absorption capacities of the two materials indicated by Figure 16 and 17 or for the much larger decrease in the absorption capacity of each material from one sulfidation cycle to the next? Because of the differences in absorption capacity were so much greater than the differences in surface area, it seems highly unlikely that surface area alone accounted for the difference in results. As will be shown in a later section of this report, the kinetics of sulfidation are complex and, therefore, dependent on more than one physical property.

Furthermore, the other physical properties which were measured at this time did not appear at least individually to account for the differences in the performance of the sorbent materials. However, the property measurements did provide an additional record of the physical changes taking place from one stage to the next, and thereby provided additional insight.

The specific volume of the open pores recorded in Table 6 differed noticeably for the two materials. The specific volume of the larger pores (D > 780 Å) was consistently greater for the plaster-based pellets than for the limestone-based. On the other hand, for both materials most of the open pore volume was associated with the larger pores rather than with the micropores, and in both cases the pore volume of the larger pores more than doubled between Stage 2 and Stage 3 and then was not greatly affected over the next three stages. The variation in the open pore

volume of the micropores was more complex since the volume seemed to vary between materials and between stages in much the same way as the specific surface area varied.

Closely associated with the open pore volume is the apparent porosity of the material since it is simply the ratio of the open pore volume to the bulk volume of the material. The apparent porosity for the two materials of interest is indicated in Figure 19 for each of the six stages. It can be seen that the porosity of the plaster-based material was slightly greater than that of the limestone-based over the entire six stages, and this would have made the plaster-based material somewhat more accessible for reaction. Also it is apparent that vacuum drying of the materials at 383 K (110°C) in Stage 2 produced a significant increase in the porosity of the plaster-based material while having little effect on the porosity of the limestone-based material. On the other hand, the conversion of the materials to CaO in Stage 3 produced a greater increase in the porosity of the limestone-based material than in the plaster-based material. Finally, the three sulfidation cycles (Stages 4-6) produced a slight decrease in the porosity of the limestone-based pellets while having little effect on the plaster-based.

Also associated with the open pore volume (V_{op}) is the apparent density of the material (ρ_a) since it corresponds to the ratio of the dry weight of the material (W_D) to the apparent volume (V_a) which in turn is equal to the difference between the bulk volume (V_b) and the open pore volume. These relationships are summarized below.

$$\rho_a = \frac{W_D}{V_a} = \frac{W_D}{V_b - V_{op}} \tag{12}$$

The variation in the apparent density of the two materials from stage to stage is shown in Figure 20. The largest change in apparent density occurred in Stage 3 when the materials lost weight but also experienced a large increase in open pore volume. Although there was

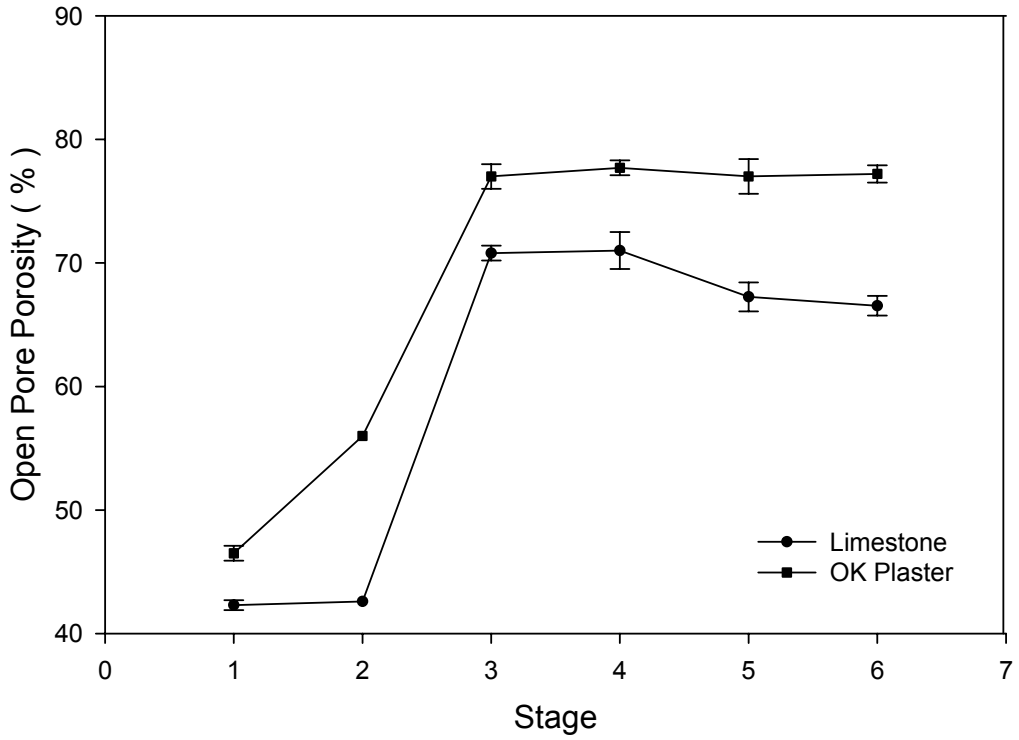

Figure 19. Apparent porosity of two different types of pellet cores at different stages of preparation and usage.

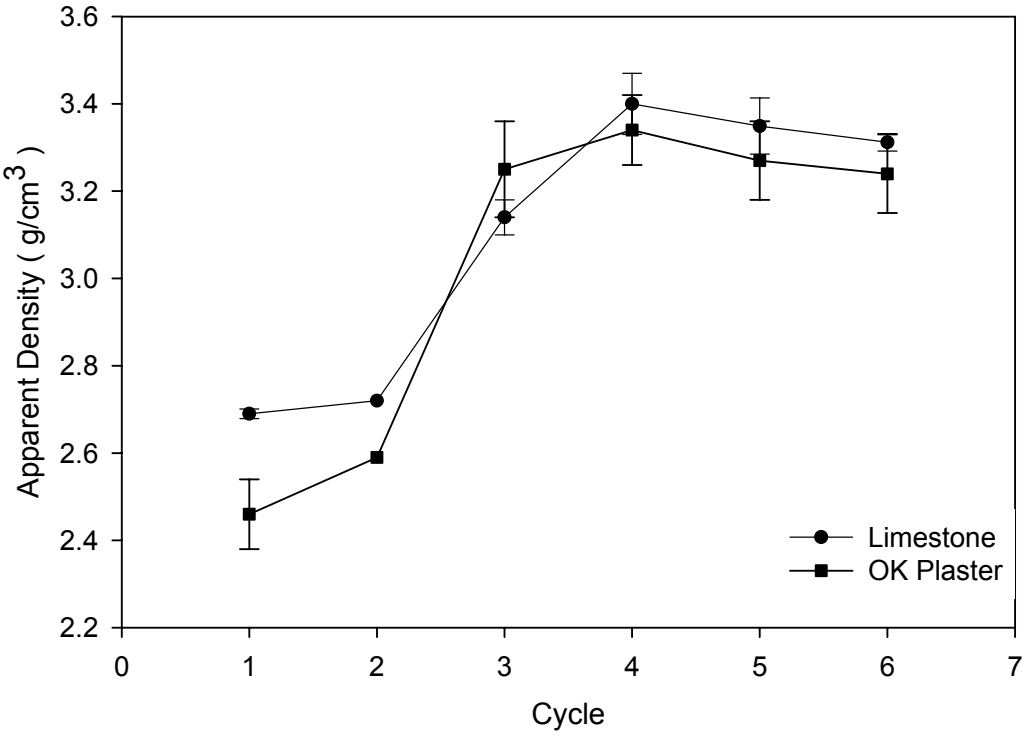

Figure 20. Apparent density of two different types of pellet cores at different stages of preparation and usage.

considerable variation in the apparent density from stage to stage, there was little difference between the densities of the two materials in any given stage.

Extended Multicycle Sulfidation and Regeneration Tests

Several extended multicycle sulfidation and regeneration tests were conducted with pellet cores made of either plaster of Paris or dolime. The purpose of these tests was to see whether the sorbents would eventually approach a stable state of reactivity. The materials selected for these tests were OK plaster of Paris and dolime since they were among the best materials from the standpoint of specific absorption capacity (see Figures 16 and 17).

The multicycle tests were conducted with the TGA system as before. A single pellet prepared from OK plaster or dolime was first converted to CaO and then subjected to eight cycles of sulfidation and regeneration. Each sulfidation was conducted for 20 min. at 1153 K (880°C) with 1.0 vol.% H_2S, 24 vol.% H_2 and 75 vol.% N_2. This was followed by regeneration involving 3 to 4 cycles of oxidation with 13 vol.% O_2 and reduction with 9 vol.% H_2 over a period of 15 min. The variation in specific absorption capacity from one sulfidation cycle to the next is indicated for each material in Figure 21. It can be seen that initially the specific capacity of the plaster-based sorbent was significantly higher than that of the dolime-based sorbent. However, at the end of eight cycles there was little difference in the specific capacity of the two materials because the specific capacity of the plaster-based material declined more rapidly than that of the dolime-based material from cycle to cycle. In fact by the eighth cycle the capacity of the dolime-based sorbent seemed almost unchanged from that of the previous cycle, whereas the capacity of the plaster-based sorbent was noticeably lower than that of the previous cycle. These differences are also apparent in Figure 22 which shows how the relative absorption capacity of the materials declined from cycle to cycle. The relatively capacity is taken to be the ratio of the

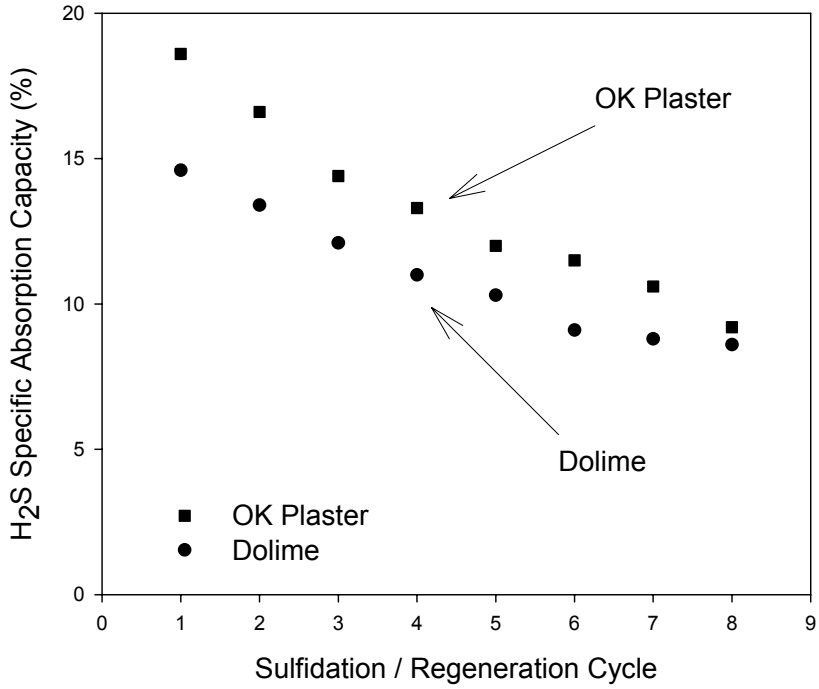

Figure 21. Specific absorption capacity of different pellet cores repeatedly sulfided and regenerated using 1.0 vol.% H_2S, 24 vol.% H_2, and 75 vol.% N_2 for sulfidation at 1153 K (880°C) and using 13 vol.% O_2/9 vol.% H_2 for regeneration at 1323 K (1050°C).

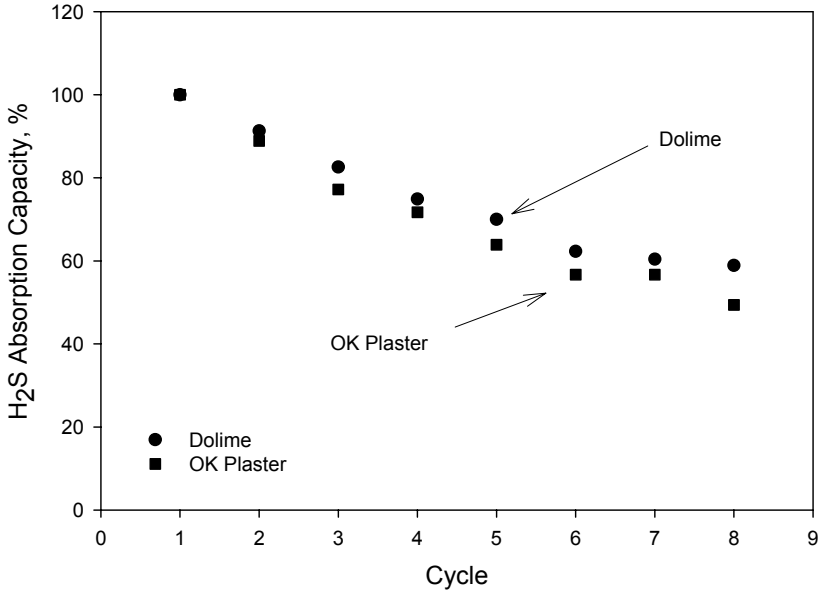

Figure 22. Relative absorption capacity of different pellet cores repeatedly sulfided and regenerated using 1.0 vol.% H_2S, 24 vol.% H_2 and 75 vol.% N_2 for sulfidation at 1153 K (880°C) and using 13 vol.% O_2/9 vol.% H_2 for regeneration at 1323 K (1050°C).

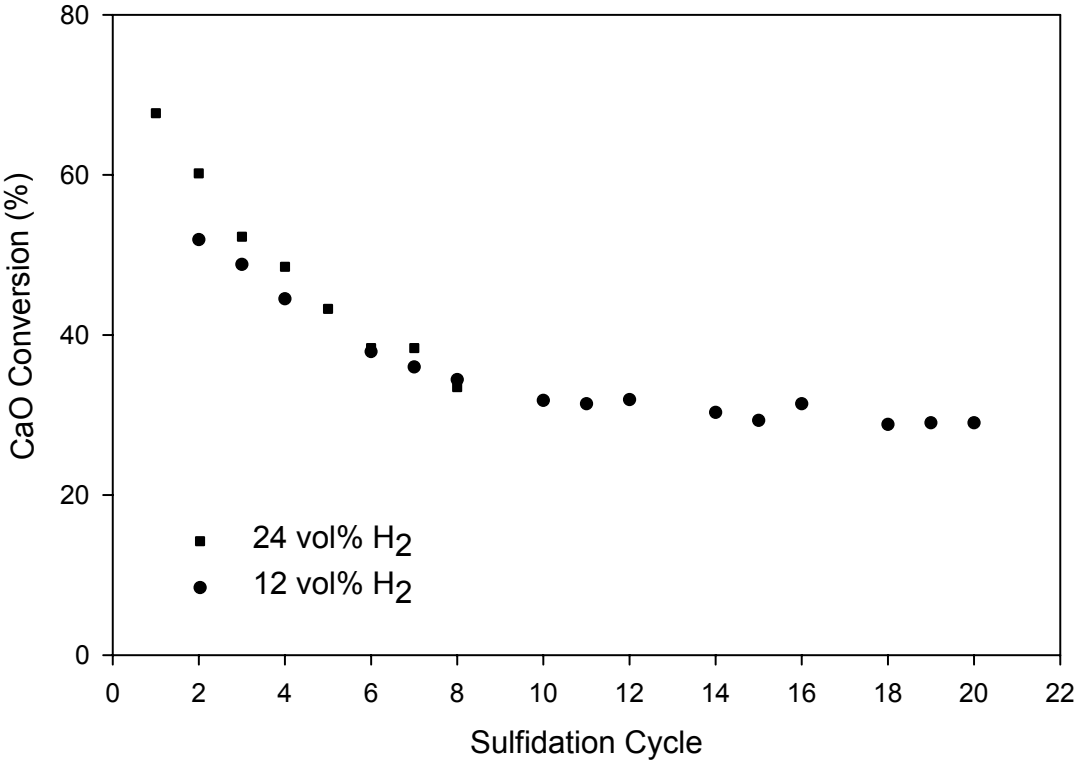

Figure 23. Specific absorption capacity of two different pellet cores repeatedly sulfided at 1153 K (880°) and regenerated at 1323 K (1050°C).

gain in weight of a particular sorbent during a given absorption cycle to the gain in weight of the sorbent during the first cycle. It is readily apparent that by the eighth cycle the capacity of the dolime-based material was approaching a constant value while the capacity of the plaster-based material was still in a downward trend. Therefore, it appeared that the dolime-based sorbent had reached a stable state of reactivity or nearly so by the eighth cycle, whereas the plaster-based pellet had not.

Since the preceding experiment indicated that more than eight cycles of sulfidation and regeneration would be required before the reactivity of the plaster-based sorbent stabilized, another multicycle test was conducted in which a plaster-based pellet was subjected to 20 cycles of sulfidation and regeneration. The conditions were the same as before except that for sulfidation the H_2 concentration was reduced to 12 vol.% and the N_2 concentration was increased

to 87 vol.%; the results are shown in Figure 23. For comparison the results of the preceding eight cycle test with a pellet made of the same material are also shown. Although initially the CaO conversion of the two materials differed slightly, by the eighth cycle there was little difference in the conversion of the two materials. The results also indicated that by the 18th cycle the reactivity of the one pellet had stabilized.

High Temperature Stability of Sorbent Materials

The preceding results showed that the absorption capacity of the calcium-based sorbent materials declined with repeated sulfidation and regeneration, but eventually the capacity of a given material approached a constant value unique for that material. Since the absorption capacity must be directly related to the chemical reactivity of the material, it appeared that the microstructure of the material changed with usage overtime to a more stable form. Such changes are believed caused by sintering at high temperature. Therefore, to preserve the high temperature reactivity of the sorbent, consideration was given to methods which conceivably could inhibit sintering. A method which has been used in the past to stabilize CaO at high temperature is to introduce an inert component such as MgO.

Bandi et al.[44] found that the absorption capacity of CaO for CO_2 at high temperature was stabilized by the presence of MgO in sizeable amounts such as would be present in a sorbent derived from dolomite ($CaCO_3 \cdot MgCO_3$) or huntite ($CaCO_3 \cdot 3MgCO_3$). It seemed that the high temperature stability of CaO increased in direct proportion to the quantity of MgO present. Unfortunately, MgO is not a sorbent for either CO_2 or H_2S at high temperature so it dilutes the active sorbent material.

In searching for other materials which could affect the sintering tendency of CaO, the work of Brown[45] was noteworthy because he had observed that small amounts of SrO inhibit sintering of CaO at high temperature. His work suggested that the life cycle performance of a calcium-based sorbent might be improved by adding a small amount of SrO. If this proved to be the case, a small amount of SrO might be as effective as a large amount of MgO for stabilizing the sorbent.

In order to test this possibility, a number of sorbent pellets were prepared either from physical mixtures of Iowa limestone and strontium carbonate or from coprecipitated calcium carbonate and strontium carbonate. The physical mixtures were prepared by suspending the powders in a 1.0 wt.% sodium hexametaphosphate solution to form a concentrated slurry which then was mixed for 30 min. either with an agitator designed for mixing paint or by ballmilling. Both methods produced homogeneous mixtures which were oven dried, and then the dry cake was ground with mortar and pestle. The coprecipitated material was prepared by adding excess ammonium carbonate to a solution containing a mixture of calcium and magnesium chlorides. The precipitate was filtered, dried and ground.

A series of pellet cores with different compositions, which are shown in Table 7, was prepared for multicycle absorption tests. The pellets designated as type A-mix were prepared by mixing the ingredients in a ball mill, whereas the pellets designated as type B-mix were prepared by mixing the ingredients with a special agitator. Pellets made entirely of Iowa limestone or of dolime were also included for comparison.

To expedite the multicycle absorption tests, they were conducted with CO_2 at 1023 K (750°C) rather than with H_2S because regeneration was much simpler with CO_2 and less time consuming. The tests were conducted by observing the change in weight of a single pellet as it

Table 7. Composition and specific absorption capacity of pellets used for multicycle absorption tests.

Pellet type	Composition, wt.%	Spec. Absorp. Cap., %		Remarks
		1st cycle	8th cycle	
limestone	97% $CaCO_3$	61	44	
A-mix	98% limestone, 2% $SrCO_3$	46	17	ballmilled
B-mix	98% limestone, 2% $SrCO_3$	54	20	stirred
C-mix	90% $CaCO_3$, 10% $SrCO_3$	52	19	coprecipitated
dolime	$CaCO_3$, $Mg(OH)_2$	41	37	

gained weight during the absorption phase or lost weight during the regeneration phase of each cycle. The TGA system was employed for this purpose, and during the absorption phase it was supplied with a mixture of CO_2 (40 vol.%) and N_2 (60 vol.%). For regeneration pure N_2 was passed through the system. The same temperature was used for regeneration as for absorption.

The results of a typical multicycle absorption test with an Iowa limestone pellet are presented in Figure 24. After the pellet was inserted into the tubular reactor, it was heated rapidly to 1023 K (750°C) in a stream of nitrogen which produced the initial loss in weight as the material was converted from $CaCO_3$ to CaO. After the pellet weight remained constant for 18 min., CO_2 was introduced at a level of 40 vol.%, and the weight of the pellet increased rapidly as CO_2 was absorbed. Most of the weight increase took place in the first 2-3 min.; thereafter, the weight increased slowly indicating a change in the rate controlling mechanism most likely due to pore plugging. At the end of 20 min. of absorption, the flow of CO_2 was discontinued, and with only N_2 flowing the weight of the pellet dropped rapidly as CO_2 was desorbed until the weight reached the level observed before the start of the absorption/desorption cycle. The cycle was repeated seven more times, and it can be seen that there was a gradual decrease in the quantity of

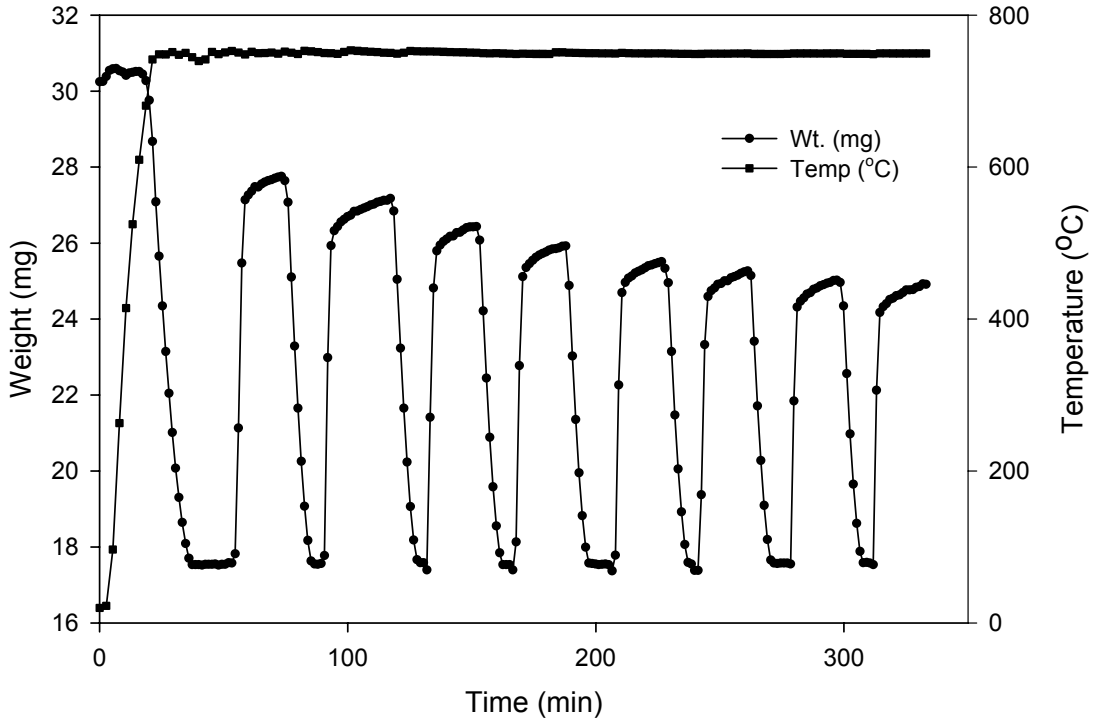

Figure 24. Results of a multicycle CO_2 absorption test with an Iowa limestone pellet.

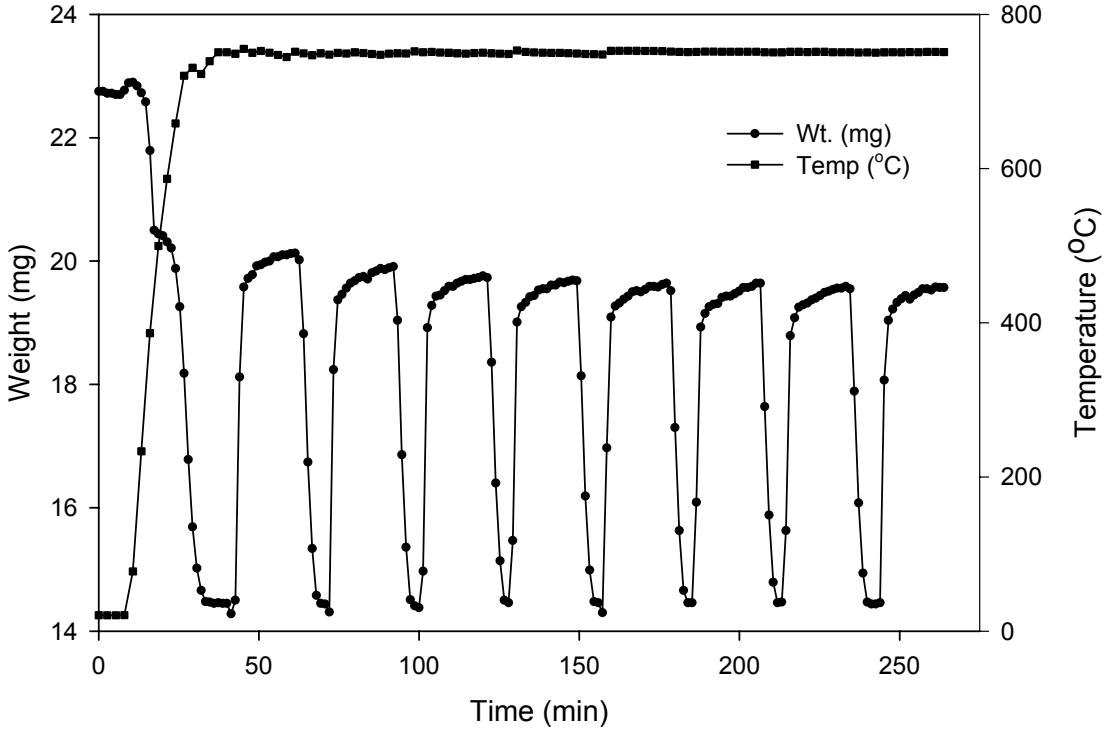

Figure 25. Results of a multicycle CO_2 absorption test with a dolime pellet.

CO_2 absorbed from cycle to cycle indicating a gradual loss in the reactivity of the sorbent due to sintering.

For comparison with the preceding results, Figure 25 shows the results of a similar test conducted with a dolime pellet. In this case the initial loss in weight of the pellet as it was heated to 1023 K (750°) appeared to occur in two steps with the first step corresponding to the loss of H_2O as $Mg(OH)_2$ was converted to MgO and the second step corresponding to the loss of CO_2 as $CaCO_3$ was converted to CaO. The nature of the second step was confirmed by the nearly equal gain in weight of the pellet during the first CO_2 absorption cycle. Compared to the results observed with a limestone pellet, there was very little decline in the quantity of CO_2 absorbed from cycle to cycle by the dolime pellet which indicated that the dolime pellet was much more stable at high temperature.

In contrast to the preceding results, pellets made with mixtures containing $SrCO_3$ appeared to be much less stable than the others. This can be deduced from Figure 26 which shows a rapid decline from cycle to cycle in the quantity of CO_2 absorbed by a pellet made from coprecipitated calcium and strontium carbonates (C-mix). Similar results were observed with pellets made from mixtures of limestone and $SrCO_3$.

Duplicate multicycle CO_2 absorption tests were carried out with each of the pellet types listed in Table 5. Since the reproducibility of these tests was excellent, only the average results of duplicate tests are presented in Table 5 and plotted in Figures 27 and 28 to compare the performance of different sorbent materials. The results show that for the first absorption cycle the limestone pellets had the highest specific absorption capacity and the dolime pellets the lowest while the capacity of the strontium-containing pellets fell in between. However, by the eighth absorption cycle, the specific capacity of the limestone pellets was approaching that of the

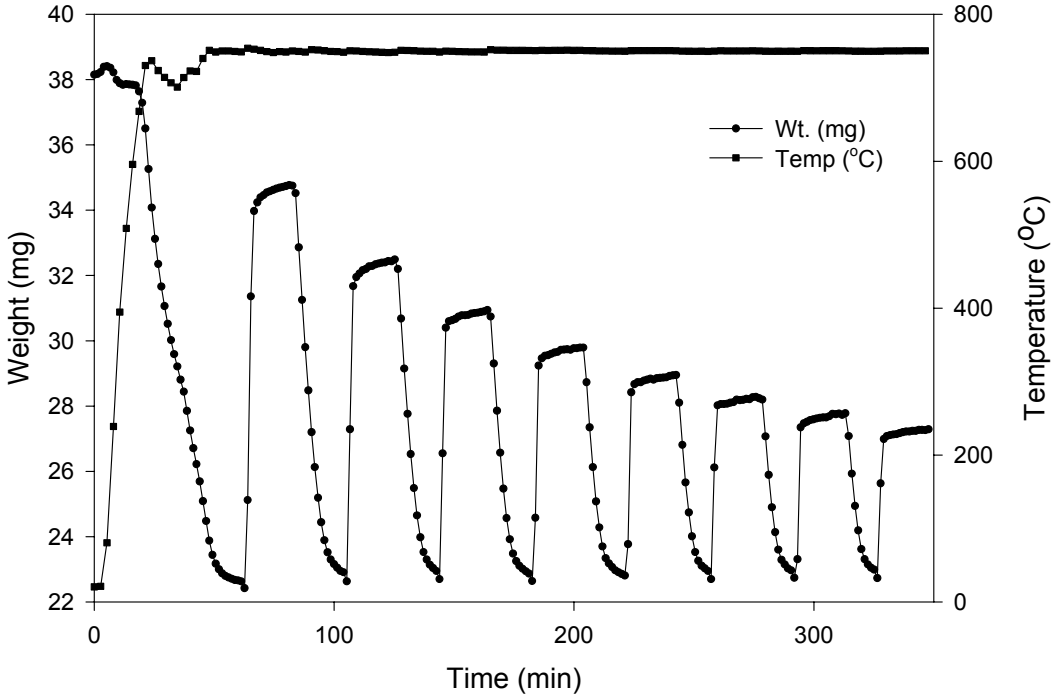

Figure 26. Results of a multicycle absorption test with a pellet made from coprecipitated $CaCO_3$ (90%) and $SrCO_3$ (10%).

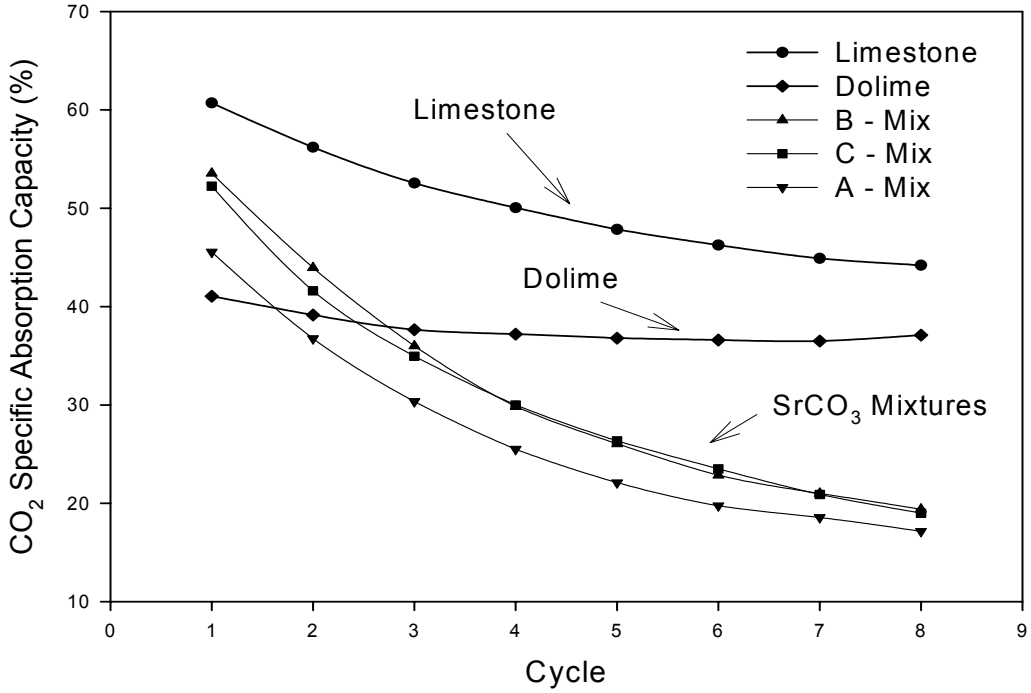

Figure 27. The specific absorption capacity of different materials for CO_2 at 1023 K (750°C).

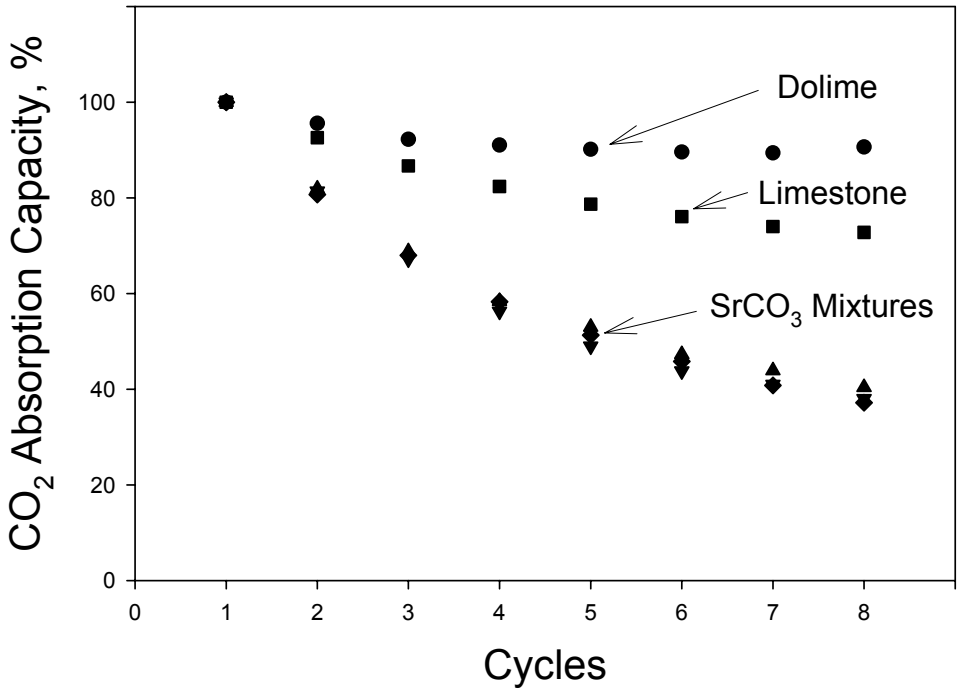

Figure 28. The relative CO_2 absorption capacity of pellets prepared from different materials at 1023 K (750°).

dolime pellets while that of the strontium-containing pellets had fallen far below that of all others. If these trends continued, the specific absorption capacity of the limestone pellets would fall below that of the dolime pellets. Consequently the more stable sorbent would have a clear advantage.

The relative CO_2 absorption capacity shown in Figure 28 is, as noted before, the ratio of the gain in weight of a particular sorbent during a given absorption cycle to the gain in weight of the sorbent during the first cycle. Although the relative absorption capacity of all the materials declined from cycle to cycle, the rate of decline was much lower for dolime than for the other materials and became negligible after the fifth cycle. The rate of decline of the limestone pellets was somewhat larger than that of the dolime pellets but not nearly as great as that of the mixtures

containing strontium. Interestingly, all of the strontium-containing pellets exhibited a similar rate of decline regardless of preparation method and strontium content.

These results with dolime agreed with the results reported by Bandi et al.[44] However, the results achieved with the strontium-containing pellets did not support Brown's[45] conclusion that strontium inhibits CaO sintering.

To provide further evidence that the decline in absorption capacity of the various materials was due to sintering, several pellets were cross-sectioned after the eighth absorption cycle and examined with a scanning electron microscope. The results presented in Figures 29 to 32 show clearly that the degree of sintering varied among the different sorbents in a manner consistent with the rate of decline of absorption capacity of the materials. The sorbent pellet cross section pictured in Figure 29 shows the particles derived from limestone which made up the sorbent pellet, and their appearance suggests that some sintering had taken place. The edges of the larger particles are rounded and clusters of smaller particles appear fused together. The pellet sections portrayed by Figures 30 and 31 are for sorbents containing strontium and they indicate a high degree of sintering which is consistent with the rapid decline in absorption capacity of the materials. Figure 32 showing the sorbent derived from dolime suggests that some sintering had taken place because the very small particles appear fused together. The dolime particles were unusually small which probably accounted for the sintering and yet the sintering was not to the degree which greatly inhibited the diffusion of CO_2 into the material.

The results of this study showed that incorporating MgO in a CaO sorbent improved the stability and life cycle performance of the sorbent, whereas incorporating SrO in the sorbent had the opposite effect. These opposing effects were probably due to the inhibition of CaO sintering by MgO and the promotion of CaO sintering by SrO.

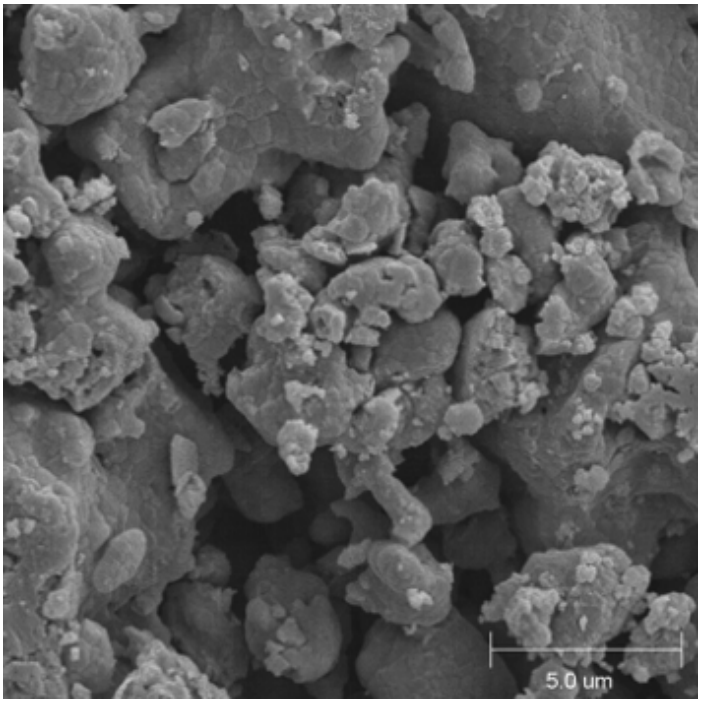

Figure 29. The limestone derived sorbent after eight cycles of absorption at 750°C.

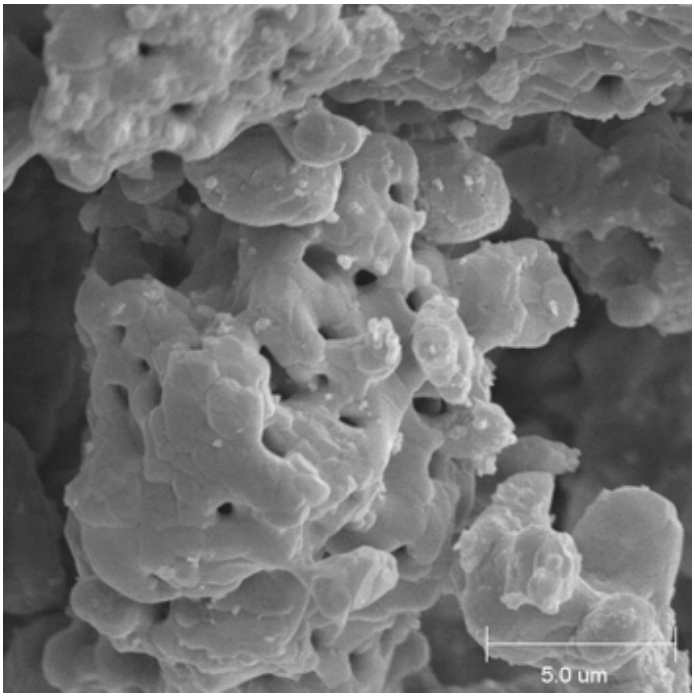

Figure 30. The sorbent derived from the B-mix of limestone (98%)and $SrCO_3$ (2%) after eight absorption cycles at 750°C.

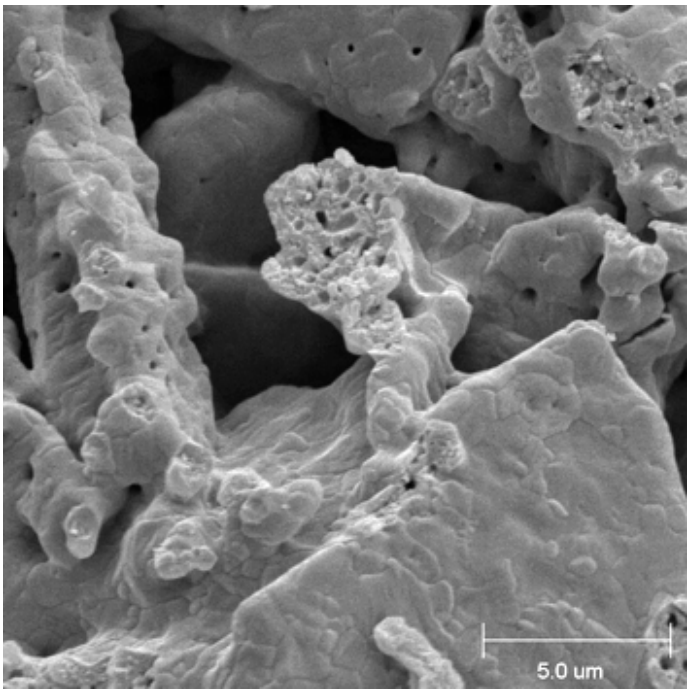

Figure 31. The sorbent derived from the coprecipitated mixture of $CaCO_3$ (90%) and $SrCO_3$ (10%) after eight absorption cycles at 750°C.

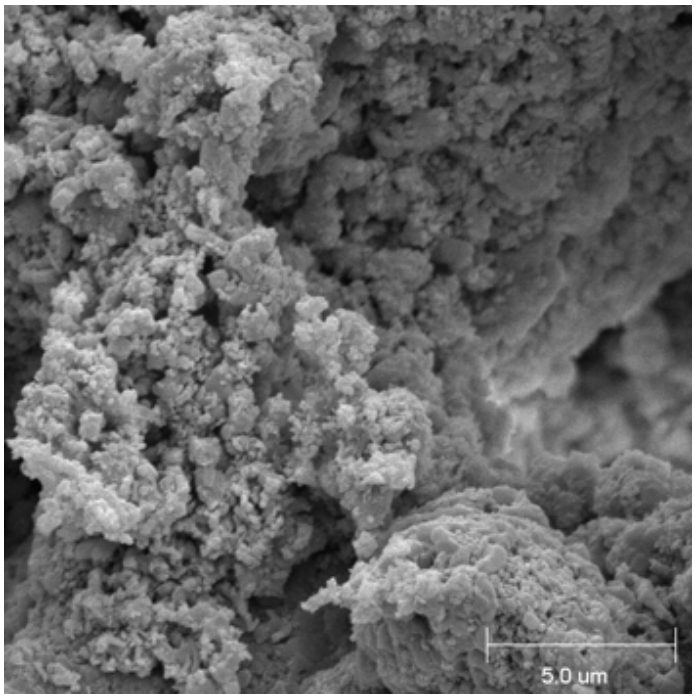

Figure 32. The sorbent derived from dolime after eight absorption cycles at 750°C.

SHELL DEVELOPMENT

During the initial stage of this core-in-shell pellet development project, a shell formulation was found which after sintering provided a material with adequate compressive strength while at the same time the material was sufficiently porous not to interfere excessively with gas diffusion. The formulation was composed of 48 wt.% T-64 tabular alumina, 32 wt.% A-16 SG alumina powder, and 20 wt.% limestone (-297/+44 μm). Later the shell formulation was altered slightly by substituting –210/+44 μm limestone. This particular mixture with Iowa limestone is referred to below as the "standard" mixture. The shell materials were mixed in the dry state and then applied as a coating to selected pellet cores as they were treated in the revolving drum pelletizer to an intermittent spray of a dilute lignin solution. The resulting core-in-shell pellets were subsequently calcined in air at 1373 K (1100°C) to sinter the shell material. Such pellets with a nominal diameter of 5 mm and a shell thickness of 0.42 mm or greater generally met an established minimum compressive strength requirement of F/D = 8.9 N/mm. However, in any given batch of pellets there were numerous pellets which either exceeded or failed to meet this requirement. Also the compressive strength did not provide a good indication of how well the pellets would withstand attrition and abrasion while being handled or being treated in a moving bed reactor. Furthermore, it was not known whether the strength of the shell material would be affected by repeatedly loading and regenerating the sorbent, or if the properties of the shell could be improved further by specific changes in the formulation. Therefore, the following study was undertaken to address these issues.

From the results of the initial shell development work it appeared that at least part of the alumina and lime reacted to form calcium aluminates while the material was being sintered. For experimental verification of this possibility, two types of pellets were prepared and subsequently

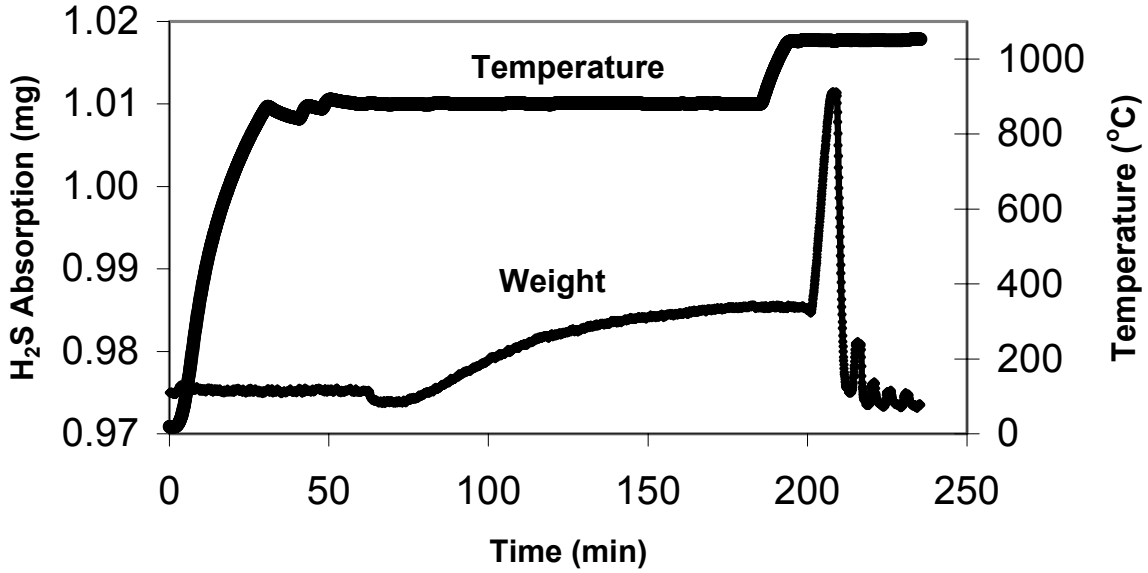

Figure 33. Response of pelletized shell material to sulfidation and regeneration.

analyzed. Both types were prepared entirely of the standard mixture described above. However, one type was prepared by casting a wet-mixture of the components using an appropriate form while the other type was prepared by pelletizing a mixture of the dry components with a revolving drum. Both types of pellets were calcined in air at 1373 K (1100°C) for 2 hr. The cast pellets were then analyzed by X-ray diffraction which showed that the major phases present were CaO and Al_2O_3 with a trace of calcium aluminate present. Before analyzing the pelletized material it was first sulfided and regenerated. These operations were carried out with the TGA system using 1.0 vol.% H_2S, 24 vol.% H_2, and 75 vol.% N_2 for sulfidation at 1153 K (880°C) and alternating between 13 vol.% O_2 in N_2 and 9 vol.% H_2 in N_2 for regeneration at 1323 K (1050°C). Two batches of pellets were treated by this method. Each batch consisted of 10 to 20 spherical pellets which had a diameter of approximately 2 mm. The changes in temperature and pellet weight which took place are indicated in Figure 33 for the first batch of pellets. It can be seen that during the treatment the pellets were held at 880°C for approximately 155 min. before

and during sulfidation and then at 1050°C for about 40 min. while being regenerated. After the treatment the pellets were analyzed by X-ray diffraction which revealed a significant amount of calcium aluminate present in addition to Al_2O_3 and CaO. The presence of more calcium aluminates than found in the preceding case where the pellets had only been calcined suggests that the cycle of sulfidation and regeneration had somehow increased the conversion of CaO and Al_2O_3 to calcium aluminate. A possible cause of the increased conversion was the prolonged exposure of the material to the higher temperatures required for sulfidation and regeneration.

Also of interest is the significant increase in weight of the pellets during sulfidation which is displayed in Figure 33. The increase is equivalent to a 35% conversion of all the CaO present in the shell material irrespective of the amount converted to calcium aluminates. In other words, there had to have been a considerable amount of free CaO present in the calcined shell material which was available for reaction with H_2S or other gases. Similar results were achieved when a second batch of pellets was treated by the same process.

The preceding results indicate that some but not all of the CaO present in the calcined shell material reacted with Al_2O_3 to form calcium aluminates. The extent of this reaction increased when the material was subsequently subjected to the sulfidizing and regenerating conditions employed in the application of the core-in-shell pelletized sorbent. The effect of this increase on the strength of the shell material will be discussed below.

But first to evaluate the abrasion resistance of core-in-shell pellets, six batches of pellets were prepared with limestone cores of similar size and with shells made of the standard mixture of alumina and Iowa limestone. Three of the batches consisted of pellets with relatively thin shells (<0.8 mm thick) and three of pellets with relatively thick shells (0.8 to 1.7 mm thick). The pellets were made by the usual pelletization procedure which included mixing the dry shell

ingredients before applying them in the coating stage. The finished pellets were calcined at 1373 K (1100°C) for 2 hr to sinter the shell material. The abrasion resistance of each calcined batch was determined by using a modified form of the ASTM[39] method to measure the quantity of dust and broken pellets produced in a specified revolving drum in 30 min. The results presented in Table 8 indicated that while the attrition loss was significant, it did not seem excessive for pellets with the thicker shells, especially considering the severity of the test. The results were also reasonably consistent because there was not a large variation in the attrition loss among batches of similar pellets while there was a significant difference in the attrition loss between batches representing different shell thickness. Therefore, it can be concluded that the abrasion resistance of core-in-shell pellets depends on shell thickness, and that it is proportional to this thickness. Consequently, the dependency of abrasion resistance on shell thickness is similar to that of compressive strength on shell thickness.

Table 8. Abrasion resistance of calcined core-in-shell pellets before application as an H_2S sorbent.

Batch No.	Pellet diameter, mm	Shell thickness, mm	Attrition loss, wt.%
1	3.96 < D < 4.76	<0.8	14.9
2	3.96 < D < 4.76	<0.8	16.8
3	3.96 < D < 4.76	<0.8	12.4
4	4.76 < D < 5.66	0.80 – 1.70	5.3
5	4.76 < D < 5.66	0.80 – 1.70	4.6
6	4.76 < D < 5.66	0.80 – 1.70	2.5
7[a]	4.76 < D < 5.66	0.80 – 1.70	2.0

[a]Shell ingredients were wet-mixed.

Since considerable variation in the properties of core-in-shell pellets had been observed among the pellets in any given batch, some consideration was given to the probable causes of this variation and a possible means for reducing it. One possible source of the variation was inadequate mixing of the shell-forming material because the pellets had always been prepared by dry-mixing the shell-forming ingredients, and dry powders are notoriously difficult to mix in order to achieve a homogeneous mixture. Therefore, to overcome this possible source of variation, a batch of core-in-shell pellets was prepared by the usual procedure except that the shell forming ingredients were first suspended in an aqueous solution containing 1.0 wt.% sodium hexametaphosphate and then mixed thoroughly. The water was subsequently evaporated and the remaining solids were dried in an oven at 383 K (110°C). The resulting caked material was repulverized with a mortar and pestle.

The repulverized shell material was used in the preparation of a seventh batch of core-in-shell pellets for abrasion testing. The composition and size of the pellet cores were the same as in the previous six batches. The pellets were calcined at 1373 K (1100°C) for 2 hr and then subjected to the abrasion resistance test. The results which are included in Table 8 show that the material suffered an attrition loss of only 2.0 wt.% which was the lowest of all the batches tested. Therefore, the attrition resistance of the shell material did seem to be improved by the wet mixing operation. The improvement could have resulted from an increase in the homogeneity of the alumina and limestone particle mixture, but it could also have been due to the presence of a small amount of sodium hexametaphosphate.

Several batches of core-in-shell pellets prepared for the abrasion test were also tested for compressive strength. These included the first three batches as well as the seventh batch listed in Table 8. Approximately 10 pellets were selected at random from each of the first three batches

and five pellets from the seventh batch for testing. The results of the compression tests are presented in Table 9. Considerable variation in compressive strength can be seen among the first three batches which were prepared under similar conditions. However, the average compressive strength of each batch of pellets exceeded the minimum requirement of 8.9 N/mm. The compressive strength of the seventh batch (14.1 N/mm) also exceeded the minimum requirement, and it seemed to be in line with the compressive strength of the first three batches. Therefore, wet mixing of the shell material did not seem to have a large effect on the average compressive strength of a pellet batch. However, wet mixing did reduce the variation in the compressive strength among the pellets within a single batch which can be seen by comparing the standard deviation of the compressive strength from batch to batch. For the seventh batch the standard deviation in compressive strength was only 1.4 N/mm while for the first three batches it ranged from 3 to 7 N/mm. A similar trend is also reflected by the standard deviation of the pellet breaking force which was 8 N for the seventh batch and ranged from 20 to 40 N for the other batches.

Another interesting comparison can be drawn from the pellet failure rate which is the percent of pellets selected from a given batch for testing that failed the minimum compressive strength requirement. As the results in Table 9 indicate, the minimum failure rate for the pellets prepared with wet-mixed shell material was 0% (batch 7), whereas it ranged from 20 to 40% for the pellets prepared with dry-mixed shell material (batches 1 to 3).

All of these results show that the wet mixing process produces a more uniform shell material than is produced by dry mixing.

Table 9. Average compressive strength of core-in-shell pellets which had been calcined or calcined and then sulfated and regenerated several times.

Pellet batch no.	1	2	3	7	8	9A	9B
Shell material	alumina & limestone	alumina & limestone	alumina & limestone	alumina & limestone	alumina & limestone	alumina & limestone	alumina & limestone
Shell mixing method	dry	dry	dry	wet	wet	dry	dry
Core material	limestone	limestone	limestone	limestone	limestone	limestone	limestone
No. pellets tested	10	10	10	5	6	4	4
Final state	calcined	calcined	calcined	calcined	regenerated[a]	calcined	regenerated[b]
Pellet diameter (mm)	5.9 ± 0.5	5.5 ± 0.2	5.6 ± 0.4	6.0 ± 0.2	5.5 ± 0.2	4.37 ± 0.22	4.64 ± 0.29
Shell thickness (mm)	0.95 ± 0.20	0.65 ± 0.08	0.66 ± 0.14	1.06 ± 0.11	0.98 ± 0.09	0.45 ± 0.01	0.451 ± 0.10
Breaking force (N)	72 ± 25	54 ± 20	101 ± 40	84 ± 8	91 ± 8	39.0 ± 3.7	41.7 ± 14.2
Comp. strength (N/mm)	12.3 ± 3	9.8 ± 4	18.0 ± 7	14.1 ± 1.4	16.7 ± 1.7	8.92 ± 0.70	8.89 ± 2.52
Failure rate (%)[c]	20	50	20	0	0	---	---

[a]After 4 cycles of sulfidation and regeneration.
[b]After 6 cycles of sulfidation and regeneration.
[c]Percentage of pellets from a batch with F/D < 8.9 N/mm

Another concern which was addressed is the possible effect of repeated sulfidation and regeneration of the sorbent on the compressive strength of the shell material. As already noted, additional calcium aluminates seemed to be produced when calcined pellets of shell material were subjected to a cycle of sulfidation and regeneration. To see whether this type of treatment would produce stronger pellets, a batch of core-in-shell pellets was prepared with Iowa limestone cores and with shells composed of the standard mixture which had been wet-mixed. The pellets were calcined at 1373 K (1100°C) for 2 hr and then six of the pellets were subjected to four cycles of sulfidation and regeneration. All six pellets were treated simultaneously in the TGA system. Each sulfidation was conducted for 30 min. at 1153 K (880°C) using 1.0 vol.% H_2S, 24 vol.% H_2 and 75 vol.% N_2. Regeneration was carried out at 1323 K (1050°C) by treating the material alternately with 13 vol.% O_2 and then with 9 vol.% H_2 in N_2. The changes in the system temperature and in the weight of the pellets during the course of the treatment are recorded in Figure 34. The treated pellets were subsequently tested for compressive strength and the results are identified as batch 8 in Table 9. Since these results were achieved with a batch of pellets which had been prepared the same way as the previous batch had been made, a direct comparison of the results of batches 7 and 8 is justified. Furthermore, the average shell thickness was nearly the same for both batches, and the standard deviation in compressive strength was low and not greatly different for the two cases. Therefore, the average compressive strength of 16.7 N/mm reported for the sulfided and regenerated pellets seemed to be significantly greater than the corresponding value of 14.1 N/mm reported for the pellets which had only been calcined.

The absorption characteristics displayed in Figure 34 suggest that the properties of the pellets remained unchanged from cycle to cycle. However, this indication can be deceptive

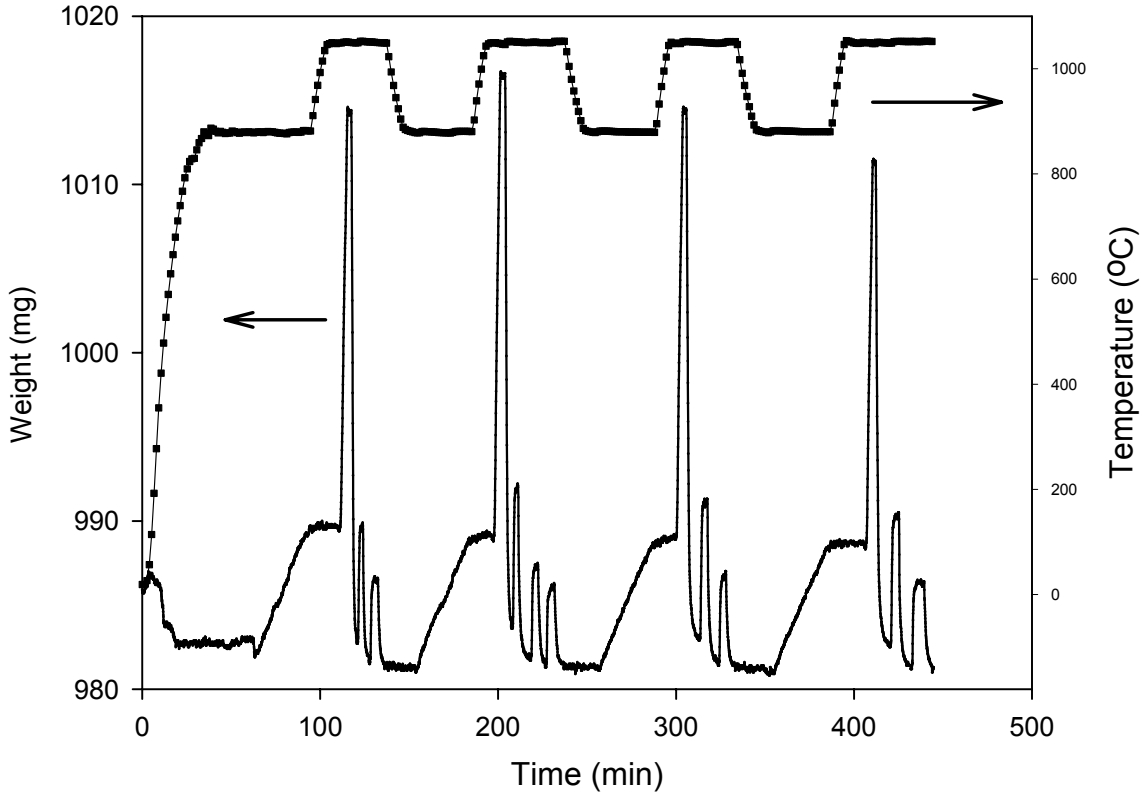

Figure 34. Results of a multicycle sulfidation and regeneration test with six core-in-shell pellets from batch 8.

because the rate of absorption could have been controlled by the rate of diffusion of H_2S through the gas surrounding the pellets. This was a likely possibility because the TGA pellet holder did not allow gas to diffuse as freely around six pellets as around a single pellet. If the overall rate of absorption was controlled by gas phase diffusion, the rate would appear constant throughout each cycle and from cycle to cycle.

A similar experiment was conducted with another batch of core-in-shell pellets which were also prepared with Iowa limestone cores but with shells made by dry mixing the standard mixture of alumina and limestone particles. Again the pellets were calcined at 1373 K (1100°C) for 2 hr. Four of the pellets were selected at random for compression testing and 12 were selected for a multicycle sulfidation test. For this test 12 pellets were placed in a single holder

and suspended in the TGA reactor where they were treated to three cycles of sulfidation and regeneration. Each sulfidation was conducted for 55 min. at 1153 K (880°C) using 1.6 vol.% H_2S, 24 vol.% H_2, and the balance nitrogen. Regeneration was again conducted at 1323 K (1050°C) by treating the material alternately with 13 vol.% O_2 and then with 9 vol.% H_2 in N_2. After the three cycles were completed, the pellets were divided and six of the pellets were returned to the reactor and subjected to three more cycles of sulfidation and regeneration conducted as before. Four of the treated pellets were then used for compression testing. The results of the compression tests are reported in Table 9 where the calcined by otherwise untreated pellets are designated as batch 9A and the sulfided and regenerated pellets as batch 9B. The results show that the compressive strength of the reacted and calcined pellets was almost identical to that of the pellets which had only been calcined, i.e., 8.9 N/mm. Therefore, sulfidation and regeneration seemed to have no effect on pellet compressive strength which disagrees with the tentative conclusion derived from the results of batches 7 and 8. Furthermore, the results of batches 9A and 9B seemed more reliable than those of batches 7 and 8 because the former were achieved with pellets selected at random from the same initial batch of pellets whereas the latter were not. But since there was little justification for completely disregarding either set of results, the most general conclusion is that sulfidation and regeneration does not reduce pellet strength and may actually enhance it.

While seeking a way to strengthen the shell material, it was discovered that stronger shells could be made by substituting –44 μm particles of limestone for the 44 to 210 μm particles which had been used in the standard shell mixture. To determine the effect of limestone concentration, several batches of core-in-shell pellets were made with different concentrations of –44 μm particles of Iowa limestone in the shell material which also contained T-64 tabular

alumina and A-16 SG alumina powder in a 3:2 ratio. These ingredients were mixed in the dry state and then used for coating pellet cores, most of which were made of 44 to 210 μm particles of Iowa limestone. One batch of pellet cores was made of Ohio dolomite of a similar size. A dilute lignin solution was applied during the pelletizing and coating process. The resulting core-in-shell pellets were then calcined at 1373 K (1100°C) for 2 hr and tested which produced the results shown in Table 10. For pellets of a similar size and with a similar shell thickness, the compressive strength varied greatly depending on the initial limestone concentration. It was found that a concentration of 5 wt.% in the initial dry mixture with alumina produced the strongest pellets.

The compressive strength of core-in-shell pellets made with 5 wt.% limestone (-44 μm) in the shell was also found to vary directly with shell thickness as shown by Figure 35 where the data points represent the compressive strength of individual pellets in batch 17A. For comparison the compressive strength is also shown for core-in-shell pellets made with 20 wt.%

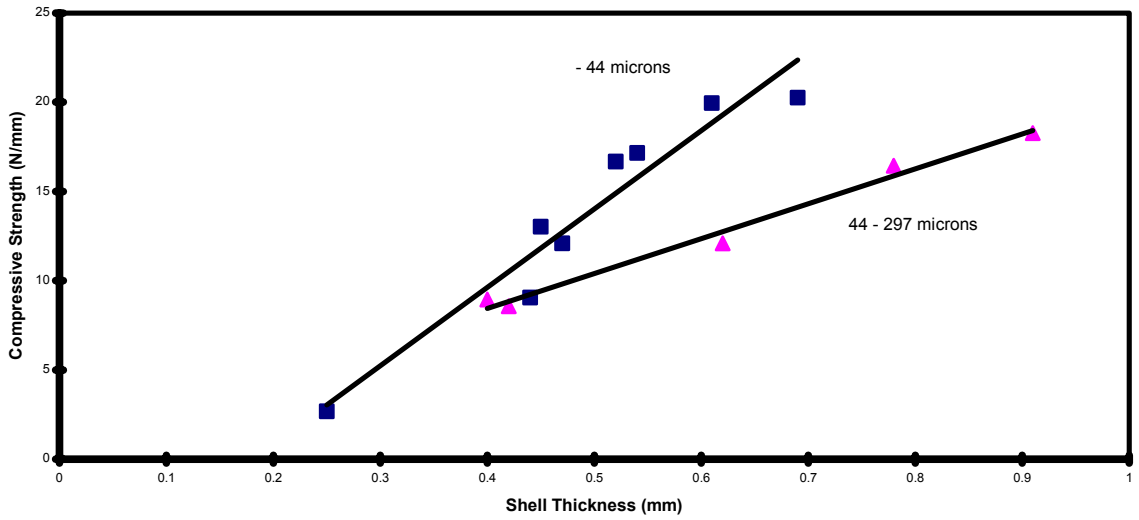

Figure 35. Effects of shell composition and thickness on compressive strength of core-in-shell pellets.

Table 10. Average compressive strength of calcined core-in-shell pellets with different shell concentrations of –44 μm limestone particles.

Pellet batch no.	10	11	12	13	14	15
[a]Lime concentration	0	5	5	10	20	20
Core material	limestone	dolomite	limestone	limestone	limestone	limestone
No. pellets tested	8	10	10	10	10	10
Pellet diameter (mm)	4.39 ± 0.23	4.34 ± 0.20	4.33 ± 0.20	4.40 ± 0.15	4.50 ± 0.19	4.34 ± 0.13
Shell thickness (mm)	0.46 ± 0.08	0.47 ± 0.04	0.49 ± 0.10	0.47 ± 0.07	0.42 ± 0.10	0.43 ± 0.11
Breaking force (N)	6.88 ± 1.36	66.50 ± 14.50	69.0 ± 44.0	42.0 ± 11.3	24.0 ± 13.5	22.0 ± 10.6
Compressive strength (N/mm)	1.56 ± 0.27	15.0 ± 3.5	16.0 ± 10.0	10.0 ± 2.4	5.0 ± 2.9	5.0 ± 2.4

[a]Concentration of –44 μm particles of Iowa limestone in initial dry shell mixture.

limestone (44 – 297 μm) in the shell. In this case the individual data points represent the compressive strength of the different batches of pellets listed in Table 4. In both cases straight lines were fitted to the data by applying linear regression analysis which produced the following relationships:

$$\text{5\% limestone:} \qquad S = 43.9\ t - 7.94 \tag{13}$$

$$\text{20\% limestone:} \qquad S = 19.5\ t + 0.645 \tag{9}$$

For equation 13 the correlation coefficient r was equal to 0.963 and for equation 9 it was 0.993. These results indicate that for any shell thickness t greater than 0.35 mm, the compressive strength of pellets made with 5 wt.% limestone (-44 μm) in the shell mixture will be greater than that of pellets made with 20 wt.% limestone (44 - 297 mm) in the mixture.

To see whether core-in-shell pellets made with 5 wt.% limestone (-44 μm) in the shell would be as reactive as those made with 20 wt.% limestone (44 – 210 μm), two batches of pellets were prepared corresponding to the different mixtures and then the batches were tested for compressive strength and reactivity. After the batches had been calcined at 1373 K (1100°C) for 2 hr, samples were taken and subjected to a multicycle absorption and regeneration test. However, instead of using thermogravimetric analysis for this test, eight pellets were placed in a ceramic boat and then treated in a horizontal tubular reactor at 1023 K (750°C). Furthermore instead of using H_2S as the absorbate, CO_2 was used. During the absorption phase of each cycle the pellets were treated for 20 min. with a gas mixture composed of 40 vol.% CO_2 and 60 vol.% N_2. The pellets were subsequently removed from the reactor and weighed to determine the amount of CO_2 absorbed. Then the pellets were returned to the reactor and regenerated by passing only N_2 through the reactor. After reweighing the pellets, they were returned to the reactor and the cycle was repeated so that eventually the pellets were subjected to a total of six

cycles. The crushing strength of pellets which had been treated was determined and compared to that of pellets which had only been calcined. The results are reported in Table 11 for the two different batches (16 and 17) before and after treatment (A and B). It can be seen that the average pellet dimensions including shell thickness were nearly the same for the two batched. On the other hand, the average compressive strength of pellets made with the –44 μm particles of limestone was much greater than that of pellets made with 44 to 210 μm particles. Also it is apparent that the multicycle absorption test with CO_2 had little if any effect on the compressive strength, although the compressive strength of the CO_2 treated pellets may have been slightly higher than those which had not been treated.

The gain in weight of the pellets during the CO_2 absorption phase of each cycle is shown in Table 12. Although the weight gained from cycle to cycle varied slightly, it did not trend either upward or downward. Therefore the reactivity of the sorbent did not appear significantly affected by the treatment. Furthermore, the average gain in weight of the sorbent for the six cycles was nearly the same for the two batches, since it was 5.56% for batch 16 and 5.40% for batch 17. Since this did not appear to be a significant difference, the resistance of the shell material to gas diffusion appeared nearly the same for the two materials. However, this finding requires confirmation to show that the overall rate of absorption was not controlled by gas phase diffusion resistance.

An alternate shell material which received serious consideration is kaolin because of its refractory nature, ready availability, and low cost. Preliminary attempts to make pellet shells entirely of kaolin were not successful. Although a method was demonstrated for coating pellet cores with kaolin, the resulting core-in-shell pellets were not strong even after being calcined at 1100°C for 2 hr. Next an experimental shell material was formulated in which limestone was

Table 11. Average compressive strength of core-in-shell pellets which had been calcined or calcined and then recarbonated and regenerated six times.

Pellet batch no.	16A	16B	17A	17B	18
Shell material	alumina & limestone (44 – 210 μm)	alumina & limestone (44 – 210 μm)	alumina & limestone (-44 μm)	alumina & limestone (-44 μm)	alumina & kaolin
Shell mixing method	dry	dry	dry	dry	wet
Core material	limestone	limestone	limestone	limestone	OK plaster
No. pellets tested	8	8	8	8	10
Final state	calcined	regenerated[a]	calcined	regenerated[a]	calcined
Pellet diameter (mm)	4.37 ± 0.12	4.66 ± 0.15	4.38 ± 0.17	4.55 ± 0.16	5.5 ± 0.2
Shell thickness (mm)	0.47 ± 0.12	0.50	0.49 ± 0.13	0.51 ± 0.11	0.81 ± 0.17
Breaking force (N)	35 ± 12	36.8 ± 8.5	61.4 ± 27.4	66.8 ± 25.6	86 ± 35
Comp. strength (N/mm)	8.05 ± 2.72	7.89 ± 1.85	13.9 ± 6.0	14.6 ± 5.3	15.6 ± 7.0
Failure rate (%)	---	---	---	---	20

[a]After 6 cycles of carbonation and regeneration at 1023 K (750°C).

Table 12. Results of multicycle absorption and regeneration tests conducted with CO_2 at 1023 K (750°C).

Cycle No.	Batch No. 16			Batch No. 17		
	Initial wt., mg	Final wt., mg	Gain, %	Initial wt., mg	Final wt., mg	Gain, %
1	1.169	1.219	4.22	1.183	1.246	5.35
2	1.120	1.218	8.77	1.162	1.227	5.59
3	1.166	1.215	4.14	1.188	1.233	3.79
4	1.167	1.231	5.48	1.163	1.233	6.04
5	1.170	1.230	5.14	1.171	1.233	5.30
6	1.172	1.238	5.62	1.163	1.236	6.303
7	1.168	---	---	1.160	---	---
Average	---	---	5.56	---	---	5.40

replaced with kaolin in the standard mixture. Consequently, the resulting mixture was composed of 48 wt.% T-64 tabular alumina, 32 wt.% A-16 SG alumina powder, and 20 wt.% kaolin. In the first attempt to utilize the mixture, the dry powders were mixed and then applied to pellet cores by the usual coating process. However, the resulting coating was not homogeneous, and after being calcined, the core-in-shell pellets had a very low crushing strength. Therefore, to make the coating more homogeneous, the materials were suspended in an aqueous solution containing 1.0 wt.% sodium hexametaphosphate and thoroughly mixed. The particle mixture was subsequently dried and repulverized as previously described. The improved mixture was then used in the making of core-in-shell pellets. While the coating was being applied, the surface of the pellets was sprayed intermittently with a dilute lignin solution having a pH of ~10 which was higher than previously used. The process was modified further by limiting the final coating consolidation step to 1 hr instead of 2 hr. The coated pellets were subsequently calcined at 1373 K (1100°C) for 2 hr and then tested to determine their crushing strength. The results of this test are reported for batch 18 in Table 11 where it can be seen that the average crushing strength was 15.6 N/mm for a batch of approximately 10 pellets. Although this value is greater than the average crushing strength of 14.1 N/mm reported for batch 7 prepared under similar conditions except for shell composition, it can not be concluded with certainty that the substitution of kaolin for limestone in the shell material produces stronger pellets because the standard deviation of the average crushing strength was relatively high for batch 18. Furthermore, batch 18 had a failure rate of 20% in contrast to a failure rate of 0% for batch 7. However, the results do provide a strong indication that pellet shells made with the alumina and kaolin mixture are probably as strong if not stronger than those made with the alumina and limestone mixture. Furthermore, the probability of improving the kaolin formulation is relatively high.

DEVELOPMENT OF A MODEL FOR THE ABSORPTION PROCESS

The preceding work showed that in some cases the results were difficult to interpret because the mechanism controlling the rate of absorption was unknown. To overcome this deficiency and provide a rational approach for further development of a core-in-shell pelletized sorbent, consideration was given to the rate controlling mechanism. The approach taken was to search for a mathematical model which would adequately represent the kinetics of sulfidation of the material. Such a model would not only support sorbent development, it would also facilitate the design and analysis of systems employing the material.

The experimental results reported below clearly show that a spherical pellet of CaO reacts with H_2S by a type of shrinking unreacted core process whereby the reaction proceeds inward from the surface of the pellet leaving behind an increasingly thick shell of CaS. Although a review of the technical literature showed that a number of mathematical models have been proposed to represent such a process, the present study found that a modified form of the classical shrinking core model first proposed by Yagi and Kunii[14] provides a good representation of the reaction process. The experimental work and steps leading up to the selection and verification of the model follow.

Experimental Results

Sorbent pellets both with and without supporting shells were prepared and their absorption characteristics were determined and analyzed to provide the data required for model selection and verification. The pellet cores were prepared from OK plaster of Paris and the shells were made of sintered alumina and lime in optimum proportions. In other words, the pellet cores were coated with a mixture consisting of 48 wt.% T-64 alumina, 32 wt.% A-16 SG alumina, and 20 wt.% Iowa limestone. The –210/+44 μm size fraction of limestone was used for

the shells. The cores and shells were prepared by the previously described two-stage pelletization method. The finished core-in-shell pellets were calcined in air 1373 K (1100°C) for 2 hr to sinter the shell material. The absorption and regeneration characteristics of single pellets were determined by employing the previously described TGA system and experimental procedure. First the $CaSO_4$ core of a new pellet was converted to CaO by the cyclic reduction and oxidation method which employed 9 vol.% H_2 for reduction and 13 vol.% O_2 for oxidation at 1323 K (1050°C). Then the temperature of the system was lowered to 1153 K (880°C) while passing nitrogen through the system. When this temperature was reached, the gas composition was changed to include appropriate concentrations of H_2S and H_2, and sulfidation of the sorbent was carried out under isothermal conditions. Sulfidation was continued until the rate of change of pellet weight was very small, whereupon the test was either discontinued or the sorbent was regenerated by alternately oxidizing and reducing the material at 1323 K (1050°C). Several treatment cycles involving oxidation with 13 vol.% O_2 followed by reduction with 9 vol.% H_2 were required to completely convert CaS to CaO.

The results of a typical extended sulfidation test of a single pellet core are shown in Figure 36. When the indicated cycle of sulfidation and regeneration was conducted, the sorbent had already been sulfided and regenerated once, although the initial sulfidation had been discontinued after 15 min. so the sorbent was only 30% converted to CaS. For both the first and second cycles of sulfidation the sorbent was treated with a gas mixture comprised of 1.0 vol.% H_2S, 24 vol.% H_2, and 75 vol.% N_2. As indicated the second sulfidation was continued for 100 min. which converted 90% of the CaO to CaS. However, the rate of conversion became very slow after the first 45 min., and during the following 55 min. the conversion only increased

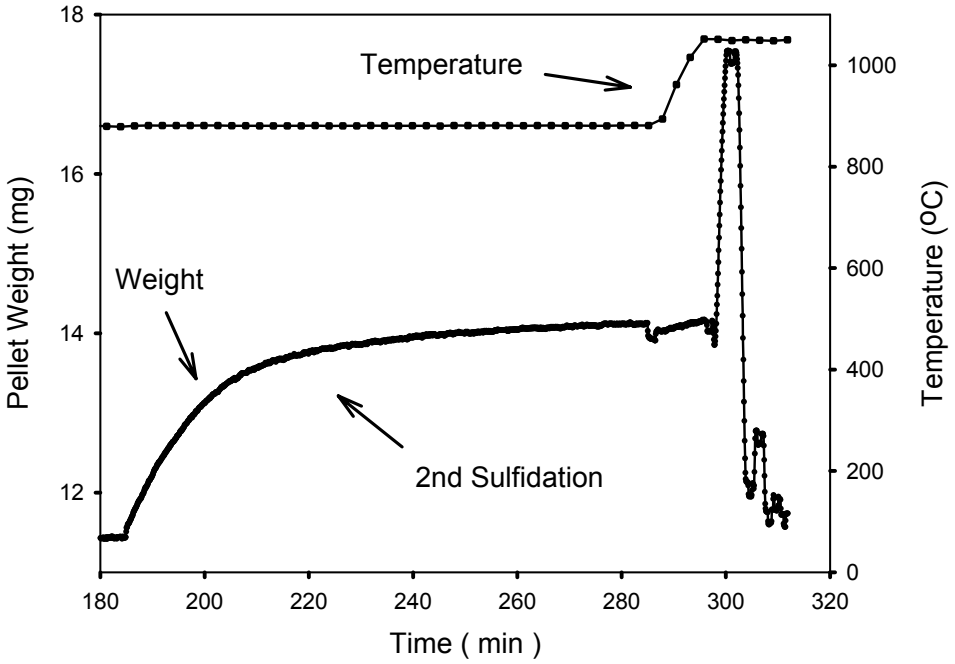

Figure 36. Results of a typical sulfidation and regeneration test of a pellet core using 1.0 vol.% H_2S and 24 vol.% H_2 for sulfidation.

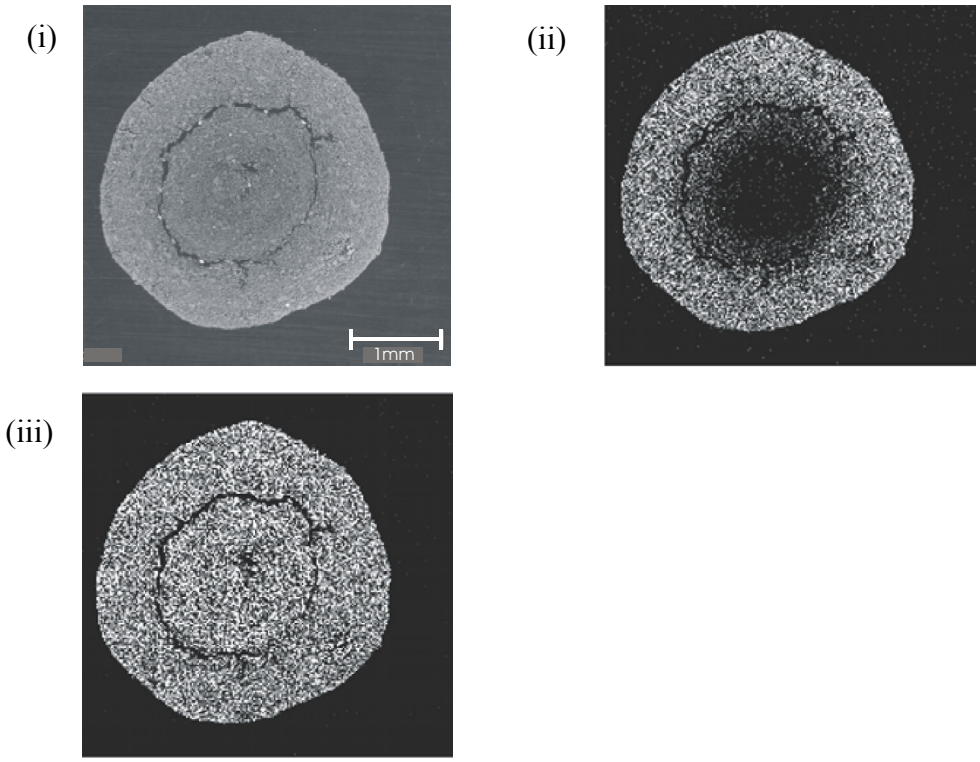

Figure 37. Micrograph of an incompletely sulfided, 3.2 mm diameter pellet core: (i) SEM view, (ii) sulfur map, and (iii) calcium map.

from 80% to 90%. Another pellet which was sulfided for 155 min. under similar conditions was still only 96% sulfided.

Several pellets which had been sulfided for different lengths of time were cross-sectioned and examined by scanning electron microscopy (SEM) to observe the physical structure and by the associated energy dispersive spectroscopy (EDS) to observe the distribution of sulfur, calcium, and aluminum. Typical results are presented in Figure 37 for a CaO core which had been 70% converted to CaS. It can be seen that the structure is granular with several major cracks, the principal one being a concentric circular crack midway between the center and outer edge. There are also several minor cracks which radiate outward from the circular crack. While the calcium is distributed uniformly throughout the pellet, the sulfur is nonuniformly distributed suggesting the results of a modified shrinking core process. Although sulfur appears to be uniformly distributed in a wide outer band or rim of the pellet and the dark inner core appears largely free of sulfur, there is not a sharp boundary between these two regions. Instead there is an intermediate region where the concentration of sulfur declines gradually from the outer uniformly sulfided region to the inner almost barren region. The results suggest that the rate of conversion is controlled by diffusion both between grains and within grains.

A core-in-shell pellet which had been reacted more completely and then cross-sectioned presented a different appearance (see Figure 38). The plaster-based core had shrunk and pulled away from the shell which seemed to have partly detached a thin layer of core material. Again there was a concentric circular crack within the core, but there were very few radial cracks. Both calcium and sulfur appeared to be uniformly distributed throughout the core. The sulfur distribution confirmed that the core was almost completely reacted. Also, both calcium and sulfur appeared to be present in the shell with calcium being much more in evidence than sulfur.

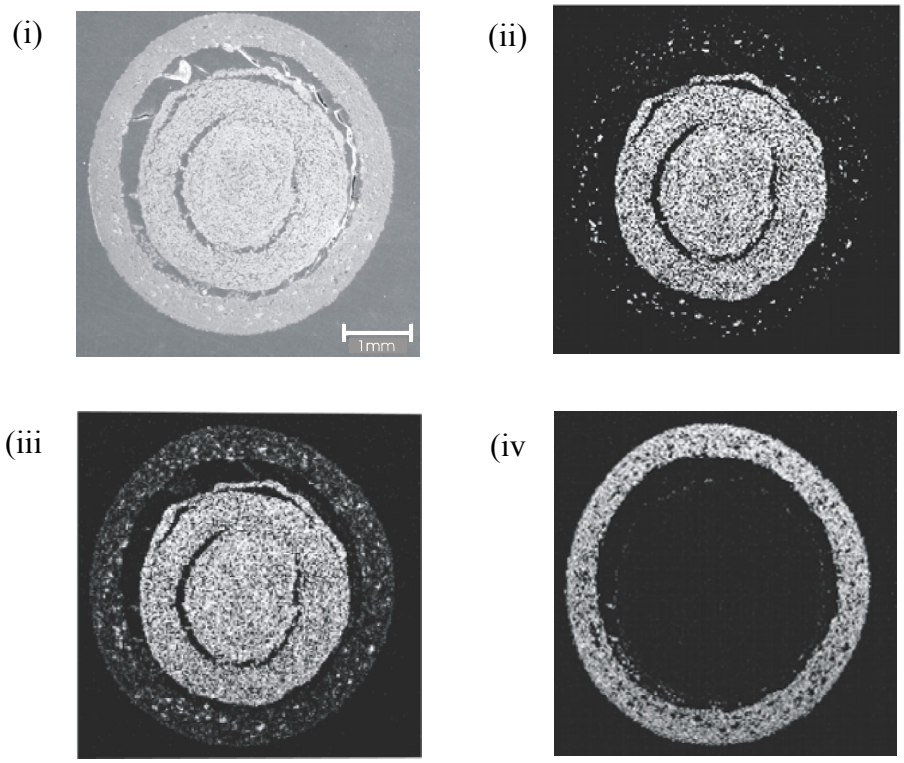

Figure 38. Micrograph of a highly sulfided, 4.4 mm diameter core-in-shell pellet: (i) SEM view, (ii) sulfur map, (iii) calcium map, and (iv) aluminum map.

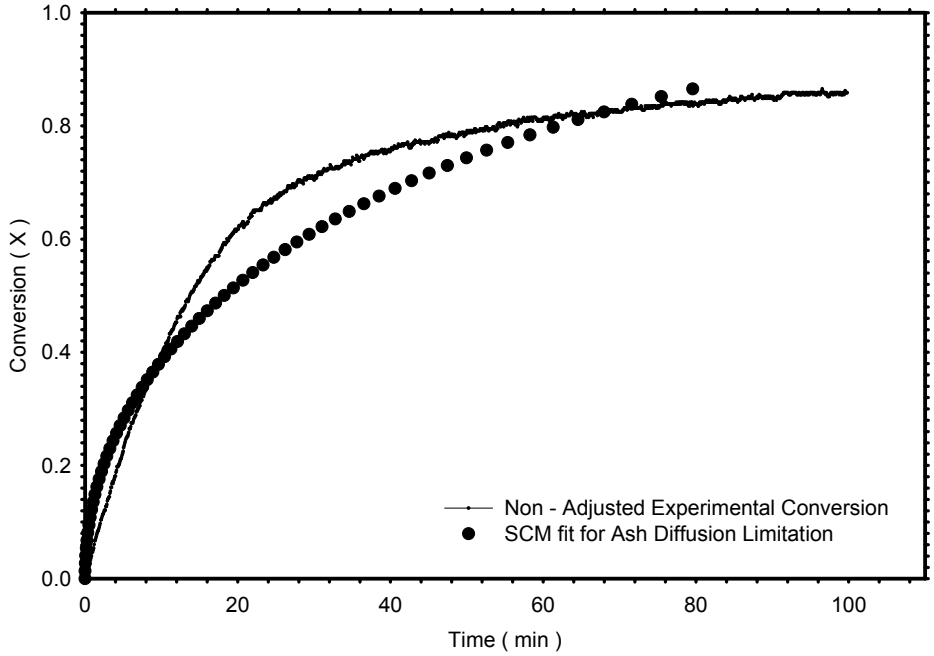

Figure 39. Results of fitting the shrinking core model to the unadjusted conversion data for a pellet core sulfided with 1.0 vol.% H_2S and 24 vol.% H_2 at 1153 K (880°C).

The presence of sulfur in the shell showed that at least some of the calcium in the shell was available for reaction. Of course, the predominant shell material was alumina which created the bright image for aluminum.

The appearance of the core-in-shell pellet cross-section differed markedly from that of a similar pellet in which the core had been derived from limestone. It had been found and reported previously that for such a pellet the calcined core was free of obvious cracks, and it had not shrunk away from the shell (see Akiti et al.[46]). Hence, the shrinking and cracking so apparent in Figure 38 was the result of the volume change which accompanied the dehydration of the core that was largely gypsum after pelletization.

In selecting an appropriate model to represent the CaO sulfidation process consideration was given to previous studies of the reaction kinetics and to models which were likely to apply. Among the noteworthy experimental studies, two in particular seem most applicable. The first by Borgwardt[47] showed that for micrometer size particles of CaO the rate of CaS formation is most probably limited by diffusion through the product layer surrounding individual CaO grains. Also it was observed that the activation energy of 31.0 kcal/mol seemed more indicative of solid state ionic diffusion than of gaseous diffusion through a porous layer. These observations were corroborated more recently by Agnihotri et al.[48] who concluded that the reaction of CaO with H_2S is limited by the diffusion of S^{2-} and O^{2-} ions through the CaS layer. In addition, they showed that for micrometer size particles not limited by external film diffusion, the process is well represented by the shrinking core model with diffusion of the gaseous reactant through the product (ash) layer as the controlling step.

While the preceding results should also apply to the individual grains of CaO which made up the pellet cores of the present sorbent, they do not account for other potential diffusion

resistances offered by the core-in-shell pellets. These resistances include the resistance of the gas film surrounding the pellet, the resistance of the porous supporting shell, and the resistance of the pores between the CaO grains. It seems likely that a combination of the last resistance and the resistance of the product layer surrounding individual grains accounted for the zone of partially converted material between the outer band of fully reacted material and the core of unreacted material so apparent in Figure 37. Also either or both of these resistances could have accounted for the very slow rate of reaction which occurred after a pellet was approximately 80% sulfided.

A review of existing models showed that none were likely to fit the core-in-shell pellet very well because of the widely different properties of the core and shell. While the grainy pellet model seemed to offer the greatest likelihood of representing the behavior of the pellet core by itself, and possibly that of the shell by itself, the model required extensive modification to fit the combined core and shell. Therefore, a simpler, semiempirical approach was taken which gave reasonable results. This was accomplished by fitting the classical, shrinking core model over the initial and subsequent portions of the sulfidation process which proceed rapidly but not the final, much slower portion which would not be used in most practical applications. For the bare pellet cores the transition from the rapid to the slow rate of conversion generally took place at approximately 78% conversion. Therefore, model fitting was limited to the range of 0 to 78%.

For the bare pellet cores it was found that the effect of external gas film diffusion could not be ignored. Consequently, it was necessary to consider the effect of both film diffusion and ash layer diffusion in selecting an appropriate model for a pellet core. The two effects are accounted for in the following expressions provided by Levenspiel:[49]

$$t_{total} = t_{film\ alone} + t_{ash\ alone} \tag{14}$$

$$t_{total} = \tau_{film} X + \tau_{ash} [1 - 3(1 - X)^{2/3} + 2(1 - X)] \quad (15)$$

The two coefficients which appear in this equation are defined as follows:

$$\tau_{film} = \frac{\rho_{CaO} R}{3 k_g C_{H_2S}} \quad (16)$$

$$\tau_{ash} = \frac{\rho_{CaO} R^2}{6 D_e C_{H_2S}} \quad (17)$$

When equation 15 was fitted to the results of the second sulfidation test shown in Figure 36 by applying nonlinear regression analysis, the best fit indicated by a relatively large correlation coefficient (r = 0.965) resulted in a negative value of τ_{film}. Since a negative value is unacceptable, the equation was refitted assuming this coefficient to be zero, and the results are compared with the experimental results in Figure 39. The visual appearance suggests a poor fit even though the correlation coefficient of 0.933 was still relatively high.

To achieve a better fit, the conversion versus time data were transformed by assuming that the pellet conversion was 100% for an actual conversion of 78%. In other words, for a given reaction time the adjusted conversion X_A was related to the actual conversion X by the following expression:

$$X_A = \frac{X}{X_{limit}} = \frac{X}{0.780} = 1.282 X \quad (18)$$

Refitting equation 15 to the adjusted conversion data produced the final result:

$$t = 7.91 X_A + 40.8\left[1 - 3(1 - X_A)^{2/3} + 2(1 - X_A)\right] \quad (19)$$

This equation fit the experimental data quite well as can be seen in Figure 40 and from the very high correlation coefficient (0.997). Both τ_{film} and τ_{ash} proved to be statistically significant. During the initial period of sulfidation, the rate of conversion was controlled by film diffusion,

Table 13. Results of fitting equation 15 to adjusted conversion data for pellet cores sulfided with 1.0 vol.% H_2S, 24 vol.% H_2, at 1153 K (880°C).

Pellet No.	[a]Wt., mg	R, mm	X_{limit}	τ_{film}, min.	τ_{ash}, min.
1	10.8	1.40	0.78	7.91	40.8
2	10.6	1.36	0.78	5.94	46.0
3	12.7	1.47	0.78	11.15	38.4
Ave.	11.37	1.41		8.33	41.7

[a]Initial weight of pellet just prior to sulfidation.

and as conversion increased, diffusion through the ash layer became more rate limiting. Of course, equation 19 could not represent the constant rate period of sulfidation above 78% actual conversion where the rate was probably controlled by a combination of diffusion between and within the pellet grains.

The results of sulfiding two other pellet cores were analyzed by the same procedure. In each case the data collected during the second sulfiding cycle were utilized, and equation 15 was fitted to the adjusted conversion data over the range of 0 to 78% actual conversion. For each pellet tested, the model fitted the adjusted conversion data very well resulting in a correlation coefficient of 0.997 or higher. The results of this analysis presented in Table 13 indicate some variation in the τ coefficients of similar size. The variation in τ_{film} was larger than the variation in τ_{ash} and seemed to correlate with pellet size. The variation in τ_{film} may also have been partly due to some variation in the sphericity and/or smoothness of the pellets, whereas the variation in τ_{ash} may have been the result of differences in the structural integrity of different pellets which displayed small cracks and other imperfections.

The usefulness of the model was demonstrated by using equation 15 together with the average τ values listed in Table 13 to predict the results of two different sulfidation tests. In one

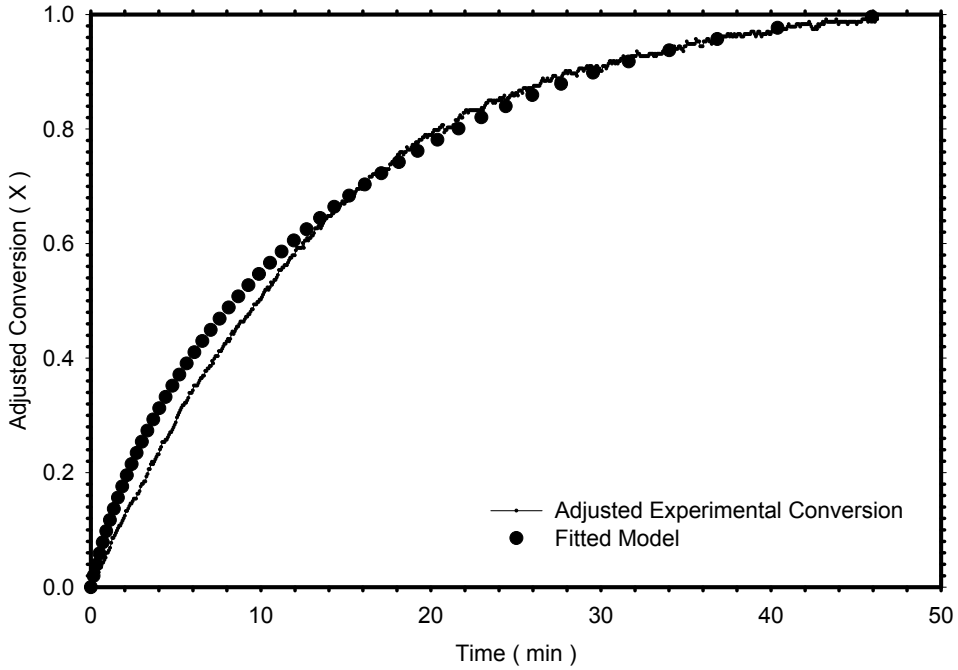

Figure 40. Comparison of adjusted experimental conversion and the fitted model conversion for pellet no. 2 sulfided with 1.0 vol.% H_2S and 24 vol.% H_2 at 1153 K (880°C).

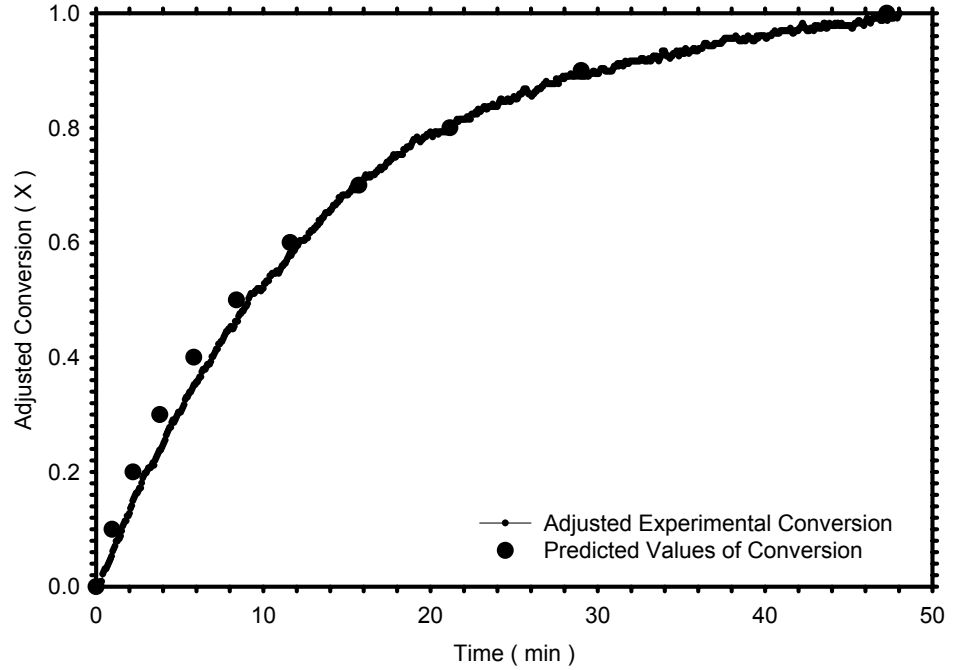

Figure 41. Comparison of adjusted experimental conversion and predicted conversion for pellet no. 2 sulfided with 1.0 vol.% H_2S and 24 vol.% H_2 at 1153 K (880°C).

case the results of the sulfidation test conducted with pellet no. 2, listed in Table 13, were predicted by using the average value of each coefficient listed in the table adjusted to account for the difference between the radius of pellet no. 2 and the average pellet radius. The adjustment was made to reflect the effect of pellet radius on the two coefficients as indicated by equations 16 and 17. Figure 41 shows that for this case the predicted values of adjusted conversion compare well with experimental values.

In another case, the average τ values were adjusted to match the conditions of a different sulfidation test which had been conducted with 0.50 vol.% H_2S instead of 1.0 vol.%. Again the predicted conversion compared well with the adjusted experimental conversion (see Figure 42). Therefore, the model appears to lend itself to account for some variation in pellet size or H_2S concentration.

A similar procedure was used to extend the semiempirical model to core-in-shell pellets. For these pellets the diffusion resistance of the porous shell had to be considered. For a homogeneous shell Akiti[50] had shown previously that if it were the only controlling resistance, the time required to react a core-in-shell pellet would be determined by the following relation:

$$t_{shell} = \frac{\rho_{CaO} R_2^3}{3 D_{es} C_{H_2S}} \left[\frac{1}{R_2} - \frac{1}{R_1} \right] X = \tau_{shell} X \qquad (20)$$

where R_1 is the outer shell radius and R_2 is the inner shell radius. Therefore, this term can be added to equation 15 to account for shell diffusion resistance. As it turned out τ_{shell} was so much greater than τ_{film} that the external film resistance could be neglected for a core-in-shell pellet. Therefore, equation 15 was adapted to a core-in-shell pellet by substituting τ_{shell} for τ_{film}. Although the shell contained some reactive CaO, its effect was not accounted for separately which seemed to make little difference when the model was applied to a core-in-shell pellet with

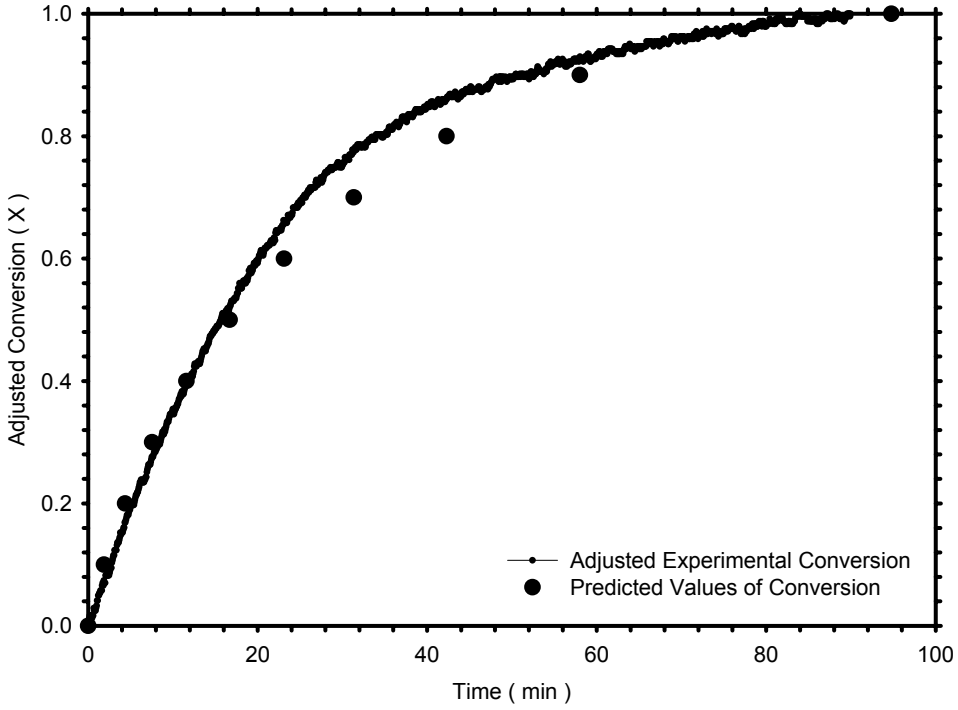

Figure 42. Comparison of adjusted experimental conversion and predicted conversion for a pellet sulfided with 0.5 vol.% H_2S and 24 vol.% H_2 at 1153 K (880°C).

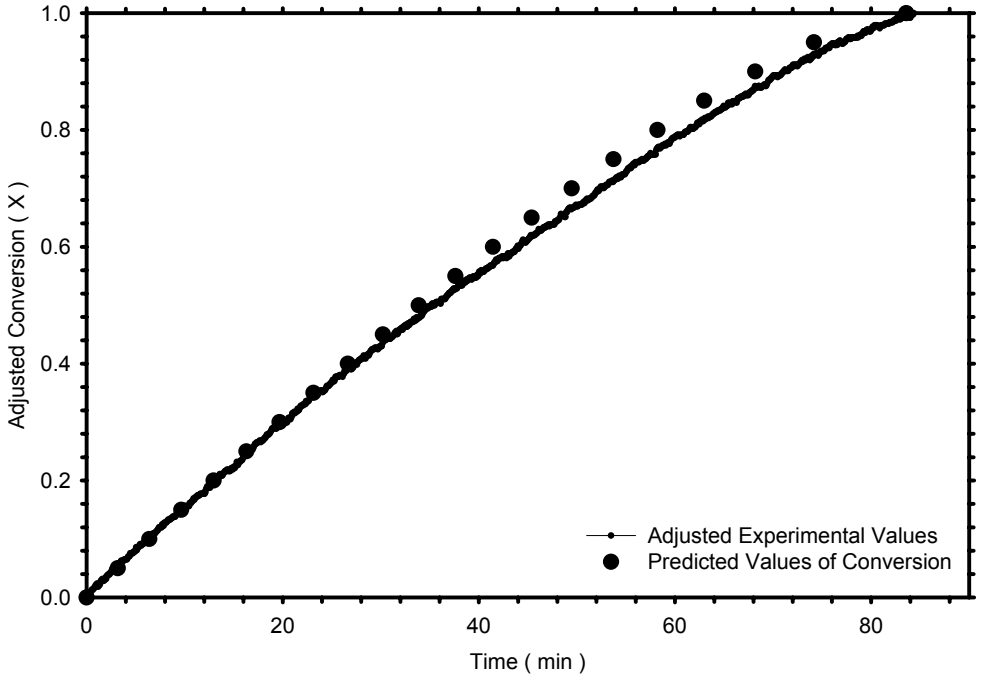

Figure 43. Comparison of predicted and experimental values of adjusted conversion for core-in-shell pellet no. 3 sulfided with 1.0 vol.% H_2S and 24 vol.% H_2 at 1153 K (880°C).

a relatively thin shell. The actual conversion for a core-in-shell pellet was estimated by employing

$$X = \frac{3.5(W_f - W_i)}{M_{CaO}} \tag{21}$$

The mass of reactive CaO in the denominator, M_{CaO}, is the sum of the CaO in the core and the reactive portion of the CaO in the shell. This portion was determined by conducting an actual sulfidation test on some of the shell material by itself, and it amounted to about 4% of the shell mass. As before the model was fitted to the adjusted conversion for a limited range of actual conversion. The upper limit of this range was marked by the transition from an increasing rate of conversion to a much slower, constant rate of conversion.

The results of fitting the model to the data collected in three separate sulfidation tests with core-in-shell pellets are presented in Table 14. Again the data collected during the second sulfidation cycle of each test were utilized. For each pellet the model was fitted to the adjusted conversion which was determined by equation 18 with the appropriate value of X_{limit} which was higher for a core-in-shell pellet than for a bare pellet core, i.e., X_{limit} ranged from 0.80 to 0.87 for

Table 14. Results of fitting equation 15 (modified) to adjusted conversion data for core-in-shell pellets sulfided with 1.0 vol.% H_2S, 24 vol.% H_2, at 1153 K (880°C).

Pellet No.	[b]Wt., mg	R_1, mm	R_2, mm	T, mm	X_{limit}	τ_{shell}, min.	τ_{ash}, min.
1	62.3	2.22	1.86	0.36	0.80	58.9	20.7
2	54.3	2.17	1.87	0.30	0.87	61.8	16.4
3	63.0	2.27	1.96	0.31	0.85	67.2	19.2
Ave.	59.9	2.22	1.90	0.32		62.6	18.8

[b]Initial weight of pellet just prior to sulfidation.

the core-in-shell pellets, whereas it was 0.78 for the pellet cores. In each case the model fitted the adjusted data for a core-in-shell pellet so closely that the correlation coefficient was essentially unity. Therefore, the fit was better and over a wider range than the fit for the bare cores. Although there was some variation in τ_{shell} and τ_{ash} among pellets, the differences were not unreasonable considering the cracks and imperfections which are so apparent in Figure 38. The relative values of τ_{shell} and τ_{ash} indicate that the shell provides a much greater resistance to diffusion than the ash layer provides over the entire range of adjusted conversion. Therefore, increasing the porosity of the shell would have a greater effect on the rate of conversion than increasing the porosity of the ash layer.

The model was used to predict the results of the sulfidation test with core-in-shell pellet no. 3 by employing average values of τ_{shell} and τ_{ash} which had been adjusted to reflect the difference in shell dimensions between pellet no. 3 and the average pellet. The adjustments for pellet radius were based on equations 17 and 20. It can be seen that predicted values of adjusted conversion compare well with experimental values in Figure 43.

Additional insight is gained by combining the average τ values over the fitted range of conversion (i.e., $X_A = 1.00$) for the two cases as shown below.

For pellet cores: $t_{total} = \tau_{film} + \tau_{ash} = 8.3 + 41.7 = 50.0$ min.

For core-in-shell pellets: $t_{total} = \tau_{shell} + \tau_{ash} = 62.6 + 18.8 = 81.4$ min.

In the first case, since the ash layer is the controlling resistance for diffusion, τ_{ash} is relatively large, whereas in the second case since the resistance of the ash layer is not as important as the resistance of the shell, τ_{ash} is relatively small.

The results of this work indicate that the sulfidation of a calcium-based, core-in-shell sorbent can be represented over a wide range of conversion by a semiempirical model which accounts for the resistance to gas diffusion presented by the porous shell and by a layer of reaction product or "ash." The model is basically an extension of the well-known SCM which has been widely used for gas-solid reactions. Although the model does not apply to high levels of conversion where the rate of reaction seems to be controlled by a combination of diffusion between and within grains, it provides a means for analyzing and predicting sorbent performance over a practical and, most likely, economical range of application.

CONCLUSIONS

The overall objective of developing an economical, reusable, and practical sorbent material for desulfurizing hot coal gas was largely achieved. The material is easily prepared by pelletizing powdered limestone or other calcium-bearing material and then coating the small pellets with a mixture of alumina and limestone particles. Subsequent calcination converts the limestone to highly reactive CaO and sinters the coating to produce a strong but porous shell. The resulting core-in-shell pellets are strong and abrasion resistant suitable for fixed bed and very possibly moving bed applications.

The sorbent material can be used to desulfurize coal gas at temperatures in the range of 1113 to 1193 K (840 to 920°C), and it is readily regenerated by a cyclic oxidation and reduction process which is conducted at approximately 1325 K (1050°C). At these temperatures there is a tendency for CaO to sinter and become less reactive. However, the results of multicycle absorption and regeneration tests showed that while the reactivity of the sorbent declines with usage, it seems to approach a constant value that will prove useful. Also the reactivity of the

sorbent can be stabilized by incorporating MgO in the material which can be accomplished by starting with dolomite or a dolomitic limestone in place of limestone.

An alternative use for the sorbent is the separation of carbon dioxide from fuel combustion products at somewhat lower temperatures (e.g., 873 – 1023 K or 600 - 750°C). Since the material can be regenerated at only slightly higher temperatures, there is less tendency for the CaO to sinter and suffer a decline in reactivity.

In either application the sorbent can be readily regenerated. The sulfided material can be regenerated by treating it alternately with oxidizing and reducing gases. The complete conversion of CaS to CaO can be achieved in as few as three cycles of oxidation and reduction. If the sorbent is used for capturing carbon dioxide, regeneration is accomplished by either raising the temperature or reducing the carbon dioxide partial pressure. Therefore, the sorbent lends itself readily to the pressure swing absorption method of application.

The compressive strength of the core-in-shell sorbent is directly proportional to shell thickness, and it depends on the composition and particle size distribution of the shell mixture. Strong, porous shells can be prepared by combining different sizes of ultrafine alumina particles with somewhat coarser limestone particles in specific proportions. Similar shells can be prepared by utilizing kaolin in place of limestone.

The results of this work showed that the rate of reaction of H_2S with CaO in the core-in-shell pellets is controlled by both the rate of diffusion of H_2S through the shell and by the rate of diffusion of H_2S through the reacted portion of the core material. The shell material offers the greater resistance to diffusion for small pellets.

REFERENCES

(1) Wheelock, T. D.; Doraiswamy, L. K.; Constant, K.; Akiti, Jr., T. T.; and Zhu, J. Development of a Calcium-Based Sorbent for Hot Gas Cleanup, Final Technical Progress Report, October 1, 1996 – September 30, 1999, DOE Grant No. DE-FG22-96PC96203, Chemical Engineering Dept., Materials Science and Engineering Dept., and Center for Sustainable Environmental Technologies, Iowa State University, Ames, Iowa.

(2) Baker, W. J. W.; van Rossen, J. C. P.; Janssens, J. P.; Moulijn, J. A. Hot Gas Cleaning, Sulfiding Mechanisms in Absorption of H_2S by Solids. In *Desulfurization of Hot Coal Gas;* Atimtay, A. T., Harrison, D. P., Eds.; Springer-Verlag, Berlin, 1998.

(3) Westmoreland, P. R.; Harrison, D. P. Evaluation of Candidate Solids for High-Temperature Desulfurization of Low-Btu Gases. *Environmental Science & Technology*, **1976**, *10*(7), 659.

(4) Gasper-Galvin, L. D.; Atimtay, A. T.; Gupta, R. P. Zeolite-Supported Metal Oxide Sorbents for Hot-Gas Desulfurization. *Ind. Eng. Chem. Res.*, **1998**, *37*, 4157.

(5) van der Ham, A. G. J.; Venderbosch, R. H.; Prins, W.; van Swaaij, W. P. M. Survey of Desulfurization Processes for Coal Gas. In *Desulfurization of Hot Coal Gas;* Atimtay, A. T., Harrison, D. P., Eds.; Springer-Verlag, Berlin, 1998.

(6) Westmoreland, P. R.; Gibson, J. B.; Harrison, D. P. Comparative Kinetics of High-Temperature Reaction between H_2S and Selected Metal Oxides. *Environmental Science and Technology*, **1977**, *11*(5), 488.

(7) van der Ham, A. G. J.; Heesink, A. B. M.; Prins, W.; van Swaaij, W. P. M. Proposal for a Regenerative High-Temperature Process for Coal Gas Cleanup with Calcined Limestone. *Ind. Eng. Chem. Res.,* **1996**, *35*, 1487.

(8) Abbasian, J. *In-situ* Desulfurization of Coal Gas with CaO-based Sorbents. In *Desulfurization of Hot Coal Gas*; Atimtay, A. T., Harrison, D. P., Eds.; Springer-Verlag, Berlin, 1998.

(9) Schwerdtfeger, K.; Barin, I. Problems in Hot Desulfurization of Coal Gas with Lime. *Erdöl und Kohle – Erdgas – Petrochemie vereinigt mit Brennstoff – Chemie,* **1993**, *46*(3), 103.

(10) Jagtap, S. B.; Wheelock, T. D. Regeneration of Sulfided Calcium-Based Sorbents by a Cyclic Process. *Energy & Fuels*, **1996**, *10*, 821.

(11) Voss, K. E. Limestone-based Sorbent Agglomerates for Removal of Sulfur Compounds in Hot Gases and Method of Making. U.S. Patent 4,316,813, 1982.

(12) Kamphius, B.; Potma, A. W.; Spitsbergen, U. Regenerative Sorbents for High Temperature Desulfurization of Coal Combustion Gases, *Proceedings of the 6th Annual International Pittsburgh Coal Conference*, Pittsburgh, PA, Sept. 25-29, 1989, Vol. 2, pp. 994-1003.

(13) Wheelock, T.D. Cyclic Process for Oxidation of Calcium Sulfide. U.S. Patent 6,083,862, July 4, 2000.

(14) Yagi, S.; Kunii, D. 5th Symposium (International) on Combustion. Reinhold: New York, 1955, p. 231. *Chem. Eng. (Japan)*, **1955**, *19*, 500.

(15) Sahimi, M.; Gavalas, G.R.; Tsotsis, T.T. Statistical and Continuum Models of Fluid-Solid Reactions in Porous Media. *Chem. Eng. Sci.* **1990**, *45*, 1443-1502.

(16) Szekely, J.; Evans, J.W.; Sohn, H.Y. *Gas-Solid Reactions;* Academic Press: New York, 1976.

(17) Ramachandran, P.A.; Doraiswamy, L.K. Modeling of Noncatalytic Gas-Solid Reactions. *AIChE J.* **1982**, *28*, 881-900.

(18) Doraiswamy, L.K.; Sharma, M.M. *Heterogeneous Reactions: Analysis, Examples and Reactor Design*; Vol. 1, Wiley Intersci.: New York, 1984.

(19) Doraiswamy, L.K.; Kulkarni, B.D. Gas-Solid Noncatalytic Reactions. In *Chemical Reaction and Reactor Analysis;* Carberry, J.J.; Varma, A. Eds.; Marcel Dekker: New York, 1986.

(20) Mazet, N. Modeling of Gas-Solid Reactions. 1. Nonporous Solids. *Intl. Chem. Eng.* **1992**, *32*, 271-284.

(21) Mazet, N. Modeling of Gas-Solid Reactions. 2. Porous Solids. *Intl. Chem. Eng.* **1992**, *32*, 295-408.

(22) Bhatia, S.K.; Gupta, J.S. Mathematical Modelling of Gas-Solid Reactions: Effect of Pore Structure. *Rev. Chem. Eng.* **1993**, *8*, 177.

(23) Bowen, J.H.; Cheng, C.K. A Diffuse Interface Model for Fluid-Solid Reaction. *Chem. Eng. Sci.* **1969**, *24*, 1829-1831.

(24) Mantri, V.B.; Gokarn, A.N.; Doraiswamy, L.K. Analysis of Gas-Solid Reactions: Formulation of a General Model. *Chem. Eng. Sci.* **1976**, *31*, 779-785.

(25) Bowen, J.H.; Khan, A.R.; Mutasher, E.I. Noncatalytic Gas-Solid Reactions – A Diffuse Interface Model. *Chem. Eng. Res. Des.* **1989**, *67*, 58-65.

(26) Dudukovic, M.P.; Lamba, H.S. A Zone Model for Reactions of Solid Particles with Strongly Adsorbing Species. *Chem. Eng. Sci.* **1978**, *33*, 471-478.

(27) Prasannan, P.C.; Doraiswamy, L.K. Gas-Solid Reactions: Experimental Evaluation of the Zone Model. *Chem. Eng. Sci.* **1982**, *37*, 925-937.

(28) Szekely, J.; Evans, J.W. A Structural Model for Gas-Solid Reactions with a Moving Boundary. *Chem. Eng. Sci.* **1970**, *25*, 1091-1107.

(29) Heesink, A.B.M.; Prins, W.; van Swaaij, W.P.M. A Grain Size Distribution Model for Non-Catalytic Gas-Solid Reactions. *Chem. Eng. J.* **1993**, *53*, 25-37.

(30) Dam-Johanson, K.; Hansen, P.F.B.; Ostergaard, K. High-Temperature Reaction Between Sulphur Dioxide and Limestone – III. A Grain-Micrograin Model and its Verification. *Chem. Eng. Sci.* **1991**, *46*, 847-853.

(31) Prins, W.; Kamphuis, B.; van Swaaij, W.P.M. A Sub-Grain Model for the Sulfation of Agglomerated-Limestone Pellets. ICHEME Symp. Ser. No. 131, 1993, pp. 211-227.

(32) Ramachandran, P.A.; Smith, J.M. A Single-Pore Model for Gas-Solid Noncatalytic Reactions. *AIChE J.* **1977**, *23*, 353-361.

(33) Bhatia, S.K.; Perlmutter, D.D. A Random Pore Model for Fluid-Solid Reactions. I. Isothermal Kinetic Control. *AIChE J.* **1980**, *26*, 379-385.

(34) Bhatia, S.K.; Perlmutter, D.D. The Effect of Pore Structure on Fluid-Solid Reactions: Application of the SO_2-Lime Reaction. *AIChE J.* **1981**, *27*, 226-234.

(35) Bhatia, S.K., Perlmutter, D.D. A Random Pore Model for Fluid-Solid Reactions. II. Diffusion and Transport Effects. *AIChE J.* **1981**, *27*, 247-254.

(36) Bhatia, S.K.; Perlmutter, D.D. Unified Treatment of Structural Effects in Fluid-Solid Reactions. *AIChE J.* **1983**, *29*, 281-289.

(37) Delikouras, E.A.; Perlmutter, D.D. Inaccessible Porosity in Gasification Reactions under Kinetic Control. *AIChE J.* **1991**, *37*, 1607-1612.

(38) Gupta, R. Center for Engineering and Environmental Technology at Research Triangle Park, North Carolina, personal communication, 1999.

(39) ASTM Standard Test Method for Attrition and Abrasion of Catalysts and Catalyst Carriers, Designation: D 4058-96, *Annual Book of ASTM Standards*, **2000**, *5.05*, 360.

(40) Morris, C. E.; Wheelock, T. D.; Smith, L. L. Processing of Waste Gypsum in a Two-Zone Fluidized Bed Reactor. In *AIChE Symposium Series*; Yang, W.-C., Ed.; American Institute of Chemical Engineers: New York, **1987**, Vol. 83 (No. 255), p. 94.

(41) Wheelock, T. D.; Riel, T. Cyclic Operation of a Fluidized Bed Reactor for Decomposing Calcium Sulfate. *Chem. Eng. Communications,* **1991**, *109*, 155.

(42) Karan, K.; Mehrotra, A. K.; Behie, L. A. On Reaction Kinetics for the Thermal Decomposition of Hydrogen Sulfide. *AIChE J.*, **1999**, *45*, 383.

(43) Higashihara, T.; Saito, K.; Yamamura, H. S_2 Formation During the Pyrolysis of H_2S in Shock Waves. *Bull. Chem. Soc. Japan,* **1976**, *49*(4), 965.

(44) Bandi, A.; Specht, M.; Sichler, P.; Nicholoso, N. *In situ* Gas Conditioning in Fuel Reforming for Hydrogen Generation. *Proceedings of the 5th International Symposium on Gas Cleaning at High Temperature*, Morgantown, WV, Sept. 18-20, 2002.

(45) Brown, R. A. Sintering in Calcium Oxide and Calcium Oxide Containing Strontium. *Am. Ceram. Soc. Bull.*, **1965**, *44*, 693-695.

(46) Akiti, T. T.; Constant, K. P., Doraiswamy, L. K.; Wheelock, T. D. An improved core-in-shell sorbent for desulfurizing hot cal gas. *Advances in Environmental Research*, **2001**, *5*(1), 31.

(47) Borgwardt, R. H. Surface Area of Calcium Oxide and Kinetics of Calcium Sulfide Formation. *Environ. Prog.* **1984**, *3*(2), 129.

(48) Agnihotri, R.; Chauk, S. S.; Mahuli, S. K.; Fan, L.-S. Mechanism of CaO reaction with H_2S: Diffusion through CaS product layer. *Chem. Eng. Sci.* **1999**, *54*, 3443.

(49) Levenspiel, O. *Chemical Reaction Engineering*; Wiley: New York, 3rd ed., 1999.

(50) Akiti, T. T. Development of a regenerable calcium-based sorbent for hot gas cleanup. Ph.D. Thesis, Iowa State University, Ames, Iowa, 2001.

APPENDIX

The results of this research project were also reported in various technical presentations and publications which are listed below.

PUBLICATIONS

Tetteh Akiti, "Development of a regenerable calcium-based sorbent for hot gas cleanup," Ph.D. thesis, Iowa State University, Ames, IA, 2001.

T. Akiti, D. Hasler, T. D. Wheelock, and K. Constant, "Desulfurization of Hot Coal Gas with an Advanced Calcium-based Sorbent," Proceedings of the 11th International Conference on Coal Science," San Francisco, CA, September 30 – October 4, 2001.

T. T. Akiti, Jr., K. P. Constant, L. K. Doraiswamy, and T. D. Wheelock, "Development of an Advanced Calcium-based Sorbent for Desulfurizing Hot Coal Gas," *Advances in Environmental Research*, **5**, 31-38 (2001).

T. T. Akiti, K. P. Constant, L. K. Doraiswamy, and T. D. Wheelock, "An Improved Core-in-Shell Sorbent for Desulfurizing Hot Coal Gas," *Advances in Environmental Research,* **6**, 419-428 (2002).

T. T. Akiti, Jr., K. P. Constant, L. K. Doraiswamy, and T. D. Wheelock, "A Regenerable Calcium-based Sorbent for Desulfurizing Hot Coal Gas," *Industrial & Engineering Chemistry Research*, **41**, 587-597 (2002).

T. D. Wheelock and D. J. L. Hasler, "A Reusable Calcium-Based Sorbent for Desulfurizing Hot Coal Gas," Proceedings of the 5th International Symposium on Gas Cleaning at High Temperatures (DOE/NETL-2003/1185), Morgantown, WV, September 17-20, 2002.

D. J. L. Hasler, L. K. Doraiswamy, and T. D. Wheelock, "A Plausible Model for the Sulfidation of a Calcium-Based Core-in-Shell Sorbent," *Ind. Eng. Chem. Res.*, **42**, 2644-2653 (2003).

D. J. L. Hasler, "Analysis and design of a calcium-based sulfur sorbent for applications in Integrated Gasification Combined Cycle energy systems," Ph.D. thesis, Iowa State University, Ames, Iowa, 2003.

T. D. Wheelock and T. T. Akiti, "Core-in-Shell Sorbent for Hot Coal Gas Desulfurization," U.S. Patent pending.

PRESENTATIONS

T. T. Akiti, Jr. (speaker) and T. D. Wheelock, "Development of a core-in-shell sorbent for desulfurizing hot coal gas," 112th Annual Meeting, Iowa Academy of Science, Des Moines, IA, April 21, 2000.

T. D. Wheelock, L. K. Doraiswamy, and K. Constant (presenter), "Engineering a New Material for Hot Gas Cleanup," poster presentation, University Coal Research Contractors Review Meeting, U.S. Department of Energy, Pittsburgh, PA, June 6-7, 2000.

D. Hasler (speaker), K. Constant, and T. D. Wheelock, "A Calcium-Based Sorbent for High Temperature Desulfurization," 113th Annual Meeting, Iowa Academy of Science, Des Moines, IA, April 20, 2001.

T. D. Wheelock (speaker), L. K. Doraiswamy, and K. Constant, "Engineering a New Material for Hot Gas Cleanup," (DOE) University Coal Research Contractors' Review Conference, Pittsburgh, PA, June 5-6, 2001.

D. Hasler (speaker) and T. D. Wheelock, "A Pelletized Core-in-Shell Sorbent for Desulfurizing Coal Gas," 114th Annual Meeting, Iowa Academy of Science, Des Moines, IA, April 19, 2002.

T. D. Wheelock (presenter), L. K. Doraiswamy, and K. P. Constant, "Engineering a New Material for Hot Gas Cleanup," poster presentation (DOE) University Coal Research Contractors' Review Meeting, Pittsburgh, PA, June 4-5, 2002.

T. D. Wheelock (speaker) and D. J. L. Hasler, "A Reusable Calcium-Based Sorbent for Desulfurizing Hot Coal Gas," 5th International Symposium on Gas Cleaning at High Temperature, Morgantown, WV, September 17-20, 2002.

D. J. L. Hasler, B. J. Franck and T. D. Wheelock, "A Reusable Calcium-Based Sorbent for Hot Gas Cleaning," AIChE Spring National Meeting, New Orleans, LA, March 30 – April 3, 2003.